Systematic Methods for Reaction Solvent Design and Integrated Solvent and Process Design

Dissertation

for the award of the degree of

Doktoringenieurin/Doktoringenieur (Dr.-Ing.)

by: M.Sc. Teng Zhou

Date of birth: 31 January 1988

accepted by the Faculty of Process and Systems Engineering

of the Otto-von-Guericke-University of Magdeburg

Reviewers:

Prof. Dr. Kai Sundmacher

Prof. Dr. Rafiqul Gani

Prof. Dr. Zhiwen Qi

Submitted on: 24 August 2016

Graduation Colloquium on: 15 December 2016

Abstract

The chemical industry makes extensive use of solvents in reaction and separation processes in order to reduce process costs while simultaneously increasing product quality. Solvent selection is a key factor in process design due to their substantial effects on process performance. When considering the large number of existing solvents and the necessity for finding new solvents, systematic methods for optimal solvent design are very significant. Until now, there have been numerous contributions made towards the molecular design of solvents as mass separating agents for various separation processes. Despite the strong impact of solvents on chemical reactions by changing the reaction rate and/or shifting the chemical equilibrium, limited work on reaction solvent design has been reported.

In the first part of this dissertation, systematic methods for reaction solvent design are proposed. For designing solvents to increase reaction rates, a new kind of solvent theoretical descriptor is introduced and used to correlate the effect of solvents on the reaction rate constant. Based on the parameterized rate constant prediction model and a group contribution method developed to estimate these descriptors, optimal solvents with the highest predicted reaction rates are identified from the formulation and solution of an optimization-based computer-aided molecular design (CAMD) problem. For designing solvents to improve reaction equilibrium conversions, a genetic algorithm based CAMD method is proposed. The reliability and efficiency of the method have been demonstrated on a selected esterification reaction.

Taking into account the multiple effects that a solvent can have on a continuous production process involving reaction and separation sections, as well as the strong interdependence between the selection of solvents and the operation of processes, the simultaneous design of solvents and processes based on a single process-wide objective is essential.

The second part of this dissertation proposes methods for integrated solvent and process design. An integrated reaction solvent and process design problem is first addressed. The best reaction solvent and optimal process operating conditions are simultaneously identified from the formulation and solution of a mixed-integer nonlinear programming (MINLP) problem where the overall process performance is maximized. The problem is simplified by assuming ideal mixture behavior and employing shortcut process models, afterwards, it is solved by a standard MINLP algorithm. Finally, a hybrid optimization algorithm is proposed for solving complex integrated solvent and process design problems where rigorous thermodynamic and process models are employed. The reliability of the algorithm is demonstrated on a coupled absorption-desorption process.

Zusammenfassung

In der chemischen Industrie sind Lösungsmittel in vielen Reaktions- und Trennungsprozessen weit verbreitet, um eine Reduzierung der Prozesskosten bei gleichzeitiger Verbesserung der Produktqualität realisieren zu können. Die Auswahl des optimalen Lösungsmittels ist dabei ein Schlüsselfaktor, da dieses einen erheblichen Einfluss auf die Prozessperformance ausübt. Betrachtet man die große Anzahl bereits bekannter Lösungsmittel als auch die Notwendigkeit neue Lösungsmittel zu finden, wird die Wichtigkeit systematischer Methoden für die Identifizierung des optimalen Lösungsmittel-Designs ersichtlich. In der Literatur findet sich eine Vielzahl an Veröffentlichungen bezüglich des molekularen Designs von Lösungsmitteln zur Nutzung als Trennmittel in unterschiedlichsten Trennprozessen. Aufgrund des starken Einflusses der Lösungsmittel auf chemische Reaktionen bei veränderten Reaktionsraten und/oder verschobenem chemischen Gleichgewicht existieren allerdings nur wenige Arbeiten zu Lösungsmitteln für chemische Reaktionen.

Im ersten Teil dieser Dissertation werden systematische Methoden für das Designen von Reaktionslösungsmitteln vorgestellt. Für das Designen von Lösungsmitteln zur Steigerung der Reaktionsraten wird eine neue Art von theoretischen Lösungsmitteldeskriptoren eingeführt, die genutzt werden, um den Einfluss des Lösungsmittels auf die Geschwindigkeitskonstante zu beschreiben. Mithilfe eines parametrisierten Vorhersagemodells für Geschwindigkeitskonstanten und einer Gruppenbeitragsmethode zur Abschätzung der Deskriptoren werden optimale Lösungsmittel mit den höchsten vorhergesagten Reaktionsraten identifiziert. Dafür wird ein optimierungsbasiertes, computergestütztes Molekulardesign-Problem (engl. computer-aided molecular design, CAMD) gelöst. Für das Designen von Lösungsmitteln zur Verbesserung des Gleichgewichtsumsatzes wird anschließend eine auf einem genetischen Algorithmus basierende CAMD-Methode vorgestellt. Die Zuverlässigkeit und Effizienz dieser Methode wird an einer ausgewählten Veresterungsreaktion gezeigt.

Betrachtet man sowohl die unterschiedlichen Auswirkungen von Lösungsmitteln auf einen kontinuierlichen Produktionsprozess, der Reaktions- und Trennschritte aufweist, als auch die starke gegenseitige Abhängigkeit von Lösungsmittelwahl und Betrieb des Prozesses, wird die Bedeutung eines simultanen Lösungsmittel- und Prozessdesigns unter Berücksichtigung einer einzigen prozessweiten Zielfunktion ersichtlich.

Der zweite Teil dieser Dissertation beschäftigt sich mit Methoden zum integrierten Lösungsmittel- und Prozessdesign. Die simultane Identifizierung des optimalen Lösungsmittels für eine Reaktion und die Bestimmung der optimalen Prozessbedingungen

wird durch das Aufstellen und Lösen eines gemischt-ganzzahligen nichtlinearen Optimierungsproblems (engl. mixed-integer nonlinear programming, MINLP) unter Berücksichtigung der Maximierung der Gesamtprozessperformance erreicht. Das Problem wird dabei zunächst durch die Annahme von idealem Mischungsverhalten und mittels Verwendung von Shortcut-Prozessmodellen vereinfacht und anschließend mithilfe eines MINLP-Algorithmus gelöst. Des Weiteren wird ein hybrider Optimierungsalgorithmus zur Lösung von komplexen integrierten Lösungsmittel- und Prozessdesignproblemen vorgestellt, der rigorose Thermodynamik- und Prozessmodelle nutzt. Die Zuverlässigkeit dieses Algorithmus wird an einem gekoppelten Absorptions-Desorptionsprozess demonstriert.

献给我的父亲母亲

(To my parents)

Declaration

The work in this dissertation has been carried out at the Process Systems Engineering (PSE) group at Max Planck Institute for Dynamics of Complex Technical Systems, Magdeburg, Germany between July 2012 and July 2016. The financial support from the "International Max Planck Research School for Advanced Methods in Process and Systems Engineering" and the Deutsche Forschungsgemeinschaft (DFG) for the "Integrated Chemical Processes in Liquid Multiphase Systems (InPROMPT)" project are gratefully acknowledged.

The author confirms the originality of the work and declares that no part of this dissertation has been submitted for a degree at another university. The dissertation contains materials that have been published or accepted for publication. Details are provided as follows.

- Zhou T, McBride K, Zhang X, Qi Z, Sundmacher K. Integrated solvent and process design exemplified for a Diels-Alder reaction. AIChE Journal. 2015, 61, 147−158. (*Sections 3.1.2, 3.2.1, and 5.1; Appendix C*)

- Zhou T, Lyu Z, Qi Z, Sundmacher K. Robust design of optimal solvents for chemical reactions − A combined experimental and computational strategy. Chemical Engineering Science. 2015, 137, 613−625. (*Sections 3.1.3 and 3.2.2; Appendix A; Appendix B*)

- Zhou T, Wang J, McBride K, Sundmacher K. Optimal design of solvents for extractive reaction processes. AIChE Journal. 2016, 62, 3238−3249. (*Sections 4.1, 4.2, 4.3, and 4.4*)

- Zhou T, Zhou Y, Sundmacher K. A hybrid stochastic-deterministic optimization approach for integrated solvent and process design. Chemical Engineering Science. 2016, doi:10.1016/j.ces.2016.03.011. (*Sections 6.1 and 6.2*)

It is worth mentioning that the interest of this dissertation lies in the molecular design of solvents. The author also proposed a model-based method for fast screening of solvents. Interested readers are encouraged to refer to the publication: Zhou T, Qi Z, Sundmacher K. Chem. Eng. Sci. 2014, 115, 177−185.

Acknowledgements

First of all, I would like to thank my supervisor Prof. Dr.-Ing. Kai Sundmacher for his inspiration, consistent support, and great guidance throughout these years. His rigorous thinking methods and scientific working attitude will definitely influence my entire career. Thank you for setting the high standard of quality and level of innovation for my work from the very beginning. Thank you for also providing me with much freedom to develop new ideas. It is really a great privilege and wonderful experience to have worked with you!

I sincerely appreciate Prof. Zhiwen Qi, my master supervisor at East China University of Science and Technology, for his continuous support and encouragement during my PhD study in Magdeburg.

I would like to thank all the colleagues in the PSE group, particularly Benjamin Hentschel, Kevin McBride, and Zhen Song. Thank you for the valuable discussions and advice. Thank you also for sharing your invaluable time with me, which I will never forget. Many thanks to the master students I have supervised. Thank you for your diligent work, great support, and friendship.

It is important to acknowledge all the predecessors, especially Prof. Claire Adjiman (Imperial College London) and Prof. Rafiqul Gani (Technical University of Denmark). Thank you for the pioneering and inspiring work in solvent design. If I have seen further it is by standing on the shoulders of giants.

Finally, I want to express my deepest gratitude to my family, especially my dear grandparents and parents. Nothing would have been possible without your support, love, understanding, and encouragement. I love you all!

Contents

Abbreviations

AD	Absorption-Desorption
ANN	Artificial Neural Network
CAMD	Computer-Aided Molecular Design
CAMPD	Computer-Aided Molecular and Process Design
CI	Capital Investment
COSMO	Conductor-Like Screening Model
CSM	Continuum Solvation Model
CSTR	Continuous Stirred Tank Reactor
DA	Diels-Alder
DFT	Density Functional Theory
EP	Economic Potential
FDM	Finite Difference Method
GA	Genetic Algorithm
GC	Group Contribution
GDP	Generalized Disjunctive Programming
HB	Hydrogen Bond
IL	Ionic Liquid
LLE	Liquid-Liquid Equilibrium
LSER	Linear Solvation Energy Relationship
MAPE	Mean Absolute Percentage Error
MILP	Mixed-Integer Linear Programming
MINLP	Mixed-Integer Nonlinear Programming
NLP	Nonlinear Programming
ODE	Ordinary Differential Equation
PBT	Payback Time
PCP-SAFT	Perturbed Chain Polar Statistical Associating Fluid Theory
PSE	Process Systems Engineering
QC	Quantum Chemistry
QSPR	Quantitative Structure-Property Relationship
SCD	Screening Charge Density
SMD	Signature Molecular Descriptor
TAC	Total Annual Cost
TI	Topological Index
TS	Transition State
TST	Transition State Theory
UC	Utility Cost
VLE	Vapor-Liquid Equilibrium

1. Introduction

1.1 Research vision

The conventional objective in chemical engineering is to minimize the cost of manufacturing a product after its molecular architecture and synthesis methods have been developed by chemists. However, one should realize that there are intrinsic links between different stages in a product R&D, i.e., from the consumers/market survey, computer-aided design, experimental verification, to the final industrial production. This characteristic makes the conventional sequential design approach (i.e. product/molecular design followed by process design) likely to miss potential optimal configurations, which can be obtained only if engineers succeed to consider all stages involved in a product-process system simultaneously. Nowadays, the task of Process Systems Engineering (PSE) has been transitioned from the traditional analysis and design of macro-scale process systems into the improvement of decision-makings for the discovery, design, manufacture, and distribution of chemical products. In other words, PSE should tie fundamental research at the molecular or microscopic level with the manufacturing of products at the industrial level (Grossmann and Westerberg, 2000).
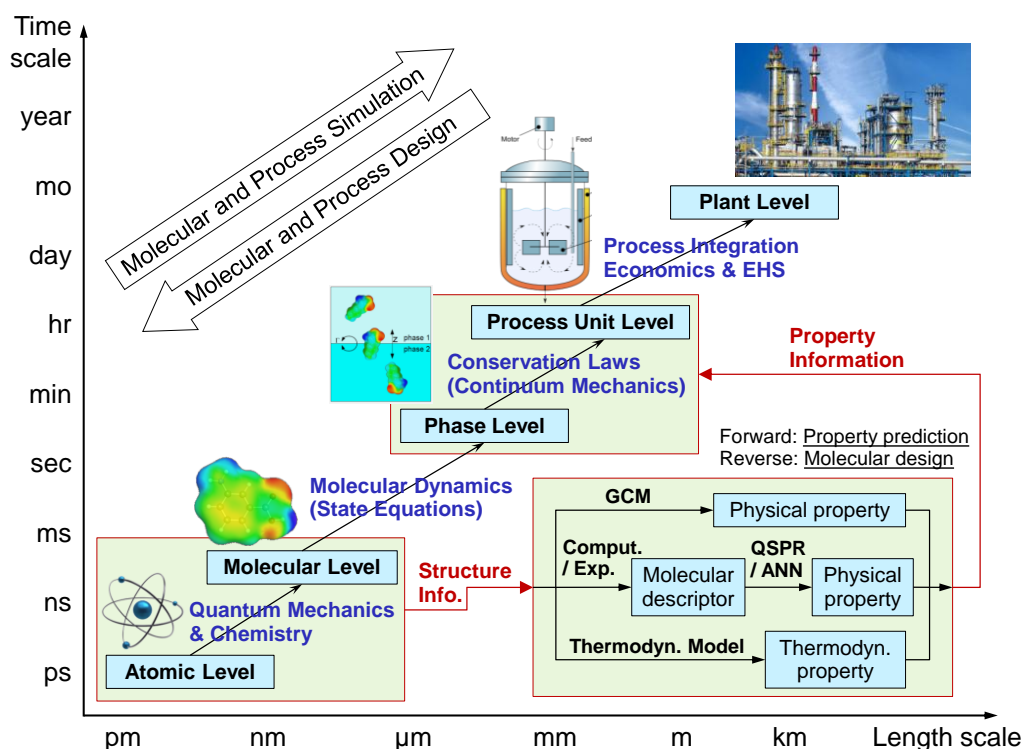
Figure 1.1: Strategic approach of multi-scale product and process design

Figure 1.1 briefly describes the methodology for multi-scale product and process design. Starting with a set of atoms, chemicals at the molecular level are synthesized. Subsequent steps aggregate the molecules into single or multiphase systems that finally present as macroscopic mixtures. Transitioning from chemistry into engineering, we move to the analysis and design of process units. The process units are finally integrated into a chemical plant under the consideration of economics and environmental, health, and safety regulations.

A successful multi-scale design requires the integration of models across different scales, where the utilization of atomic-level structural and functional models as well as molecular-level fluid phase equilibrium models is the most critical and challenging work. Instead of sending information stepwise through the length scale via rigorous quantum chemical calculations and molecular dynamics simulations, our approach is to bridge the gap between microscopic and macroscopic levels by using empirical or semi-empirical property models, such as group contribution models. These models allow for the prediction of physical and/or thermodynamic properties, as required in process development, from molecular structure information. This strategy can significantly reduce the computational cost and difficulty in solving multi-scale product and process design problems.

The chemical industry makes extensive use of solvents in reaction and separation processes in order to achieve a reduction of process costs while increasing the quality of products. In view of the huge number of existing solvents and the necessity for exploring new alternative solvents, systematic methods for the optimal design of solvents is very significant for efficient and sustainable industrial manufacturing. For considering the strong interaction between the selection of solvents and process operations, reliable and efficient methods for integrated solvent and process design are also required. As important example of "multi-scale product and process design", the molecular design of solvents as well as the integrated solvent and process design are primarily studied in this dissertation. The developed methodologies lay a solid foundation for the study on a wide range of chemical product design and integrated molecular and process design problems.

1.2   Research motivation and mission

The liquid state is so far the most important state for both chemistry and chemical engineering. For reaction and separation purposes it provides the advantage of intensive molecular contacting with ever-changing partners. Molecules of different species can be mixed and brought into contact in the liquid phase if solvents are appropriately chosen (Klamt et al., 2010).

Nowadays, millions of tons of solvents are used in industrial processes annually and the usage of and demand for solvents are still increasing. In addition to the capital and operational economic pressures, stricter safety, environmental, and health regulations have driven the search for

efficient alternative solvents. The optimal selection of solvents and the exploration for alternative solvents have been identified by the ACS Green Chemistry Institute as one of the top five priorities for green engineering research (Jiménez-González et al., 2011).

Since the late 15th century when chemists searched for universal solvents, work on understanding the role of solvents and their reasonable selection in chemical manufacturing processes has never stopped. Solvents play important roles in both reactions and separations (highlighted in Section 2.1). Due to the large number of existing solvents and the necessity for finding new solvents, one has to make use of computational design or search methods to guide the solvent selection. During the past few decades, the Computer-Aided Molecular Design (CAMD) method has been proposed and widely used for solvent screening and molecular design (Achenie et al., 2002). Until now, there have been numerous contributions to the CAMD of solvents as mass separating agents for various separation processes (Ng et al., 2015). Despite the strong impact of solvents on reaction performance by changing the reaction rate and/or by shifting the chemical equilibrium, limited work on reaction solvent design has been reported.

On the other hand, it should be noted that efficient processes can be designed only if engineers succeed to consider all levels involved in the process system simultaneously (see Figure 1.1), i.e., to bring molecular-level decisions into process design. A solvent can have multiple effects on a process it is used for. Considering these multiple influences as well as the strong interdependence between the selection of solvents and the operation of processes, the simultaneous design of solvents and process based on a single process-wide objective is essential. Integrated solvent and process design usually leads to complex mixed-integer nonlinear programming (MINLP) problems, especially when rigorous thermodynamic and process models are considered. To find the optimal solution of such problems using standard MINLP algorithms is very challenging without well-adjusted initial estimates.

In view of the above limitations, the objectives of this work are (1) to propose systematic methods for CAMD of solvents for chemical reactions with respect to solvent effects on reaction kinetics and chemical thermodynamics and (2) to propose reliable and efficient optimization approaches for solving complex integrated solvent and process design problems.

1.3   Organization of the dissertation

This dissertation consists of 7 chapters, including one introductory chapter, one fundamentals chapter, two chapters for reaction solvent design (Part I), two chapters for integrated solvent and process design (Part II), and finally a conclusion chapter.

Chapter 2 provides necessary fundamental knowledge. The usage and classification of solvents, solvent effects on reactions and separations, as well as the basic methods for predicting solvent effects are firstly discussed. The Conductor-like Screening Model (COSMO) based on which we

derive solvent molecular descriptors is then introduced. Finally, the CAMD approach is elaborated and previous work on the CAMD of solvents as well as computer-aided molecular and process design (CAMPD) is reviewed. The significance and key challenges in developing efficient methods for reaction solvent design and integrated solvent and process design are emphasized.

Part I of the dissertation introduces work on the CAMD of solvents for chemical reactions. Chapter 3 proposes a CAMD method for the optimal design of solvents to accelerate reaction rates for nonreversible reactions. The method is demonstrated on two example reactions, one simple and one complex. Chapter 4 introduces a method for the optimal design of solvents to improve the equilibrium conversion of reversible reactions. The method is illustrated on a selected esterification reaction.

Part II of the dissertation focuses on integrated solvent and process design. Chapter 5 deals with reaction solvents and Chapter 6 handles separation solvents. In Chapter 5, the reaction solvent as well as the reactor and downstream separation units are simultaneously designed to maximize the overall process performance. Chapter 6 proposes a novel optimization approach for solving complex integrated solvent and process design problems. The reliability and robustness of the approach are demonstrated on a coupled absorption-desorption (AD) process where the absorption solvent structure and the AD process are simultaneously optimized.

Chapter 7 closes the dissertation by summarizing the major achievements and limitations. A discussion on remaining challenges and future directions is also given.

2. Fundamentals

2.1 Solvents in process engineering

2.1.1 Definition, usage, and classification of solvents

A solvent, according to Wikipedia, is a substance that dissolves a solute (a chemically different liquid, solid or gas), resulting in a solution where all the ingredients are uniformly distributed at a molecular level. Solvents are used in almost everywhere in process industries, such as chemical, petrochemical, biotechnology, food, pharmaceutical, and microelectronic engineering. Their applications include the dissolution of solid materials, dilution of liquids, extraction, crystallization, facilitating reactions, etc. According to the Ceresana solvent market research, in 2013 about US$25 billion were generated from the sale of solvents worldwide and the global solvent sale will keep increasing by 4% per year until 2021.

Solvents can be classified according to their physical or chemical properties. Reichardt and Welton (2011) have reviewed five common classification systems based on physical constants, chemical constitutions, solute-solvent interactions, acid-base behaviors, and multivariate statistical methods. In the beginning, solvents were classified based on their physical properties, such as density, viscosity, melting and boiling points. For example, they can be broadly classified into low-, middle-, and high-boiling solvents with constraints of the normal boiling point < 100 °C, 100 ~ 150 °C, and > 150 °C, respectively. Later, solvents were classified into four categories: molecular liquids, switchable solvents, ionic liquids, and atomic liquids based on their chemical constitutions.

Molecular liquids (also known as molecular solvents) consist of water and non-aqueous organic compounds. Water has been used as a solvent since the early days of human civilization, and remains as a common solvent in modern industry. Organic compounds such as alcohols, esters, ethers, ketones, amines, nitriles are regarded as traditional solvents widely used in chemical and process industry. According to their polarities, usually indicated by the dielectric constant, molecular solvents can be classified into polar and nonpolar solvents. Normally, when the dielectric constant is larger than 15, the solvent is regarded as polar, otherwise, it is nonpolar. Heptane and benzene are typical examples of nonpolar solvents. Polar solvents can be further classified into polar protic solvents such as methanol and water, and polar nonprotic solvents such as dimethylsulfoxide and acetonitrile.

Switchable solvents are defined as solvents whose properties can be reversibly changed by means of an external stimulus such as a temperature change. This possibility of reversibly "switching" the physical characteristics and/or the polarity of the solvent largely facilitates both reaction and subsequent product separation (Pollet et al., 2011). Supercritical fluids with supercritical CO2 as the most important example are one kind of switchable solvents. Another

group of switchable solvents are gas-expanded liquids. Similarly, the most common gas-expanded liquids are CO2-expanded liquids. For more information on the properties and applications of supercritical fluids and gas-expanded liquids, please refer to Clifford and Clifford (1999) and Jessop and Subramaniam (2007), respectively.

Ionic liquids (ILs) are molten salts at room or near-room temperature. They are composed of ions, i.e., one cation and one anion. Walden (1914) synthesized one of the earliest ILs ethyl-ammonium nitrate. After that, the development of ILs has been relatively slow for a long time. In 1970s, ILs consisting of imidazolium or pyridinium cations and halide or tetrahalogenoaluminate anions were first synthesized and used as electrolytes in battery applications (Chum et al., 1975). Since then, ILs started to attract widespread attentions. Nowadays, they are widely used as separation solvents and reaction media. Interested readers can refer to Welton (1999) for a comprehensive introduction on the properties and applications of ILs.

Atomic liquids are metals with low melting points, such as mercury and liquid sodium. Until now, they have received very little attention as solvents.

2.1.2   Solvent effects

Chipperfield (1999) summarized the major four applications of solvents in process industry as reactants, reaction media, separation and transportation agents. As reaction media, solvents can facilitate reactions by increasing the reaction rate and/or improving the reaction equilibrium conversion. As separation agents, solvents are used in processes including gas absorption, liquid-liquid extraction, and extractive distillation. In order to find out the role of solvents in reaction and separation processes, the understanding of solvent effects on reaction kinetics as well as chemical and phase equilibrium is important.

a) Solvent effects on reaction kinetics

The influence of solvents on chemical reaction rates was first noticed by Berthelot and Pean de Saint-Gilles in 1862 when they studied the esterification reaction between acetic acid and ethanol. In 1890, Menschutkin thoroughly investigated the effect of 23 solvents on the reaction between trialkylamines and haloalkanes. He found that the reaction rate varied significantly in different solvents. In 1948, Grunwald and Winstein proved the strong solvent-dependence of the rate of the alkyl halide solvolysis reaction. Starting from these early works, solvent effects on reaction kinetics have been extensively studied. Table 2.1 summarizes the relative rate constants of the solvolysis of 2-chloro-2-methylpropane in different solvents. The reaction was found 335000 times faster in water than in ethanol (Fainberg and Winstein, 1956; Winstein and Fainberg, 1957). Table 2.2 shows the solvent-dependence of the rate constant of the reaction between cyclohexene and chloro-2,4-dinitrophenylsulfane, measured by Campbell and Hogg (1967). It was found that the rate constant is 2800 times larger in nitrobenzene than in carbon

tetrachloride. Solvent-dependent rate constants of many other reactions can be found in Reichardt and Welton (2011).

Table 2.1: Relative rate constants of the 2-chloro-2-methylpropane solvolysis reaction in different solvents

Solvent	C_2H_5OH	CH_3OH	$HCONH_2$	$HCOOH$	H_2O
Relative k	1	9	430	12200	335000

Table 2.2: Relative rate constants of the reaction between cyclohexene and chloro-2,4-dinitrophenylsulfane in different solvents

Solvent	CCl_4	$CHCl_3$	CH_3COOH	$(CH_2Cl)_2$	$C_6H_5NO_2$
Relative k	1	605	1370	1380	2800

Solvents influence reaction rates through the differential solvation of the reactants and transition state. According to the transition state theory (TST), reactants have to jump over an activated complex that lies at a saddle point of the potential energy surface before being transformed into the products. The complex with the highest energy is called the transition state (TS). The energy gap between the reactants and the TS is known as the activation energy. The Arrhenius equation defines the reaction rate constant $k = Aexp(-\Delta G^{\neq}/RT)$ where A is a pre-exponential factor, $\Delta G^{\neq}$ is the activation energy of the reaction, R is the universal gas constant and T is the absolute temperature. Now let us consider a simple $R \leftrightarrow P$ reaction carried out in two different solvents, Solvent I and Solvent II. The energetic paths of this reaction are sketched in Figure 2.1. Due to the different solvation abilities of the solvents on the reactant and the TS, Solvents I and II result in different levels of activation energy of the reaction ($\Delta G_I^{\neq} > \Delta G_{II}^{\neq}$). From the Arrhenius equation, it is clear that the reaction is faster in Solvent II than in Solvent I, i.e., $k_{II} > k_I$.
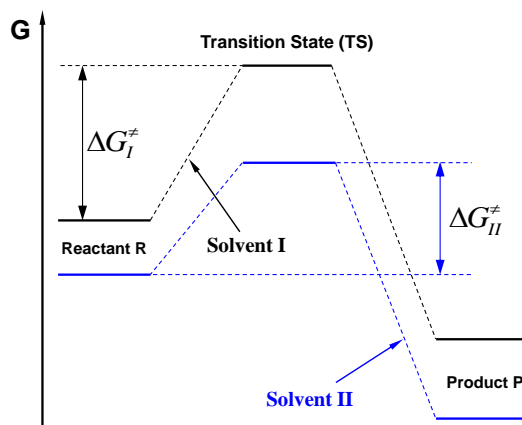

Figure 2.1: Gibbs free energy paths of an $R \leftrightarrow P$ reaction performed in two different solvents

b) Solvent effects on chemical and phase equilibrium

The influence of solvents on chemical equilibrium was initially discovered by Wislicenus (1896) when studying the keto-enol equilibrium of the ethyl formylphenylacetate tautomerization in eight solvents. Wislicenus found that the keto form dominates in alcohol solvents and the enol form dominates in chloroform as well as in benzene. It was concluded that the equilibrium keto-to-enol ratio depends much on the nature of solvent, more specifically, on solvent dissociating power, which can be indicated by the dielectric constant of the solvent. Table 2.3 summarizes the solvent-dependent chemical equilibrium of the tautomerization of 3-benzoyl camphor at 273.15 K (Dimroth, 1910).

Table 2.3: Keto-enol equilibrium of the 3-benzoyl camphor tautomerization in five solvents

Solvent	Diethyl ether	Ethyl acetate	Ethanol	Methanol	Acetone
Enol/keto	6.81	1.98	1.67	0.87	0.85

For the liquid $R \leftrightarrow P$ reaction taken place at a constant temperature and pressure, we have

$$\mu_R(T,P,x) = \mu_R(T,P) + RT \ln\left(\frac{f_R(T,P,x)}{f_R(T,P)}\right)$$

$$\mu_P(T,P,x) = \mu_P(T,P) + RT \ln\left(\frac{f_P(T,P,x)}{f_P(T,P)}\right)$$

where $\mu_i(T,P,x)$ and $f_i(T,P,x)$ are the chemical potential and fugacity of component i in the mixture, respectively. $\mu_i(T,P)$ and $f_i(T,P)$ are the chemical potential and fugacity of pure-component i, respectively. x is the composition vector, here $x = [x_R, x_P]$. When the reaction reaches equilibrium, we have $\mu_R(T,P,x^{eq}) = \mu_P(T,P,x^{eq})$.

$$\mu_R(T,P) + RT \ln\left(\frac{f_R(T,P,x^{eq})}{f_R(T,P)}\right) = \mu_P(T,P) + RT \ln\left(\frac{f_P(T,P,x^{eq})}{f_P(T,P)}\right)$$

After substituting activity coefficients into the above equation, we have

$$\mu_R(T,P) + RT \ln\left(x_R^{eq}\gamma_R^{eq}\right) = \mu_P(T,P) + RT \ln\left(x_P^{eq}\gamma_P^{eq}\right)$$

where x_R^{eq} and x_P^{eq} are the molar fractions of R and P at equilibrium, respectively. γ_R^{eq} and γ_P^{eq} represent the activity coefficients of R and P at equilibrium, respectively. The above equation can be reformulated as

$$\frac{x_P^{eq}}{x_R^{eq}}\frac{\gamma_P^{eq}}{\gamma_R^{eq}} = \exp\left(-\frac{\mu_P(T,P) - \mu_R(T,P)}{RT}\right)$$

For a liquid compound i, $\mu_i(T, P)$ is equal to $\mu_i(T, P^\theta)$ where P^θ denotes the standard pressure (usually 1 atm). In other words, $\mu_i(T, P)$ is only temperature-dependent. In fact, the right-hand term of the above equation is the temperature-dependent thermodynamic equilibrium constant of the reaction, which means the left-hand term $\left(x_P^{eq}\gamma_P^{eq}\right)/\left(x_R^{eq}\gamma_R^{eq}\right)$ is a constant under a specified temperature. It is now clear that solvents influence the equilibrium conversion of the reaction (indicated by x_P^{eq}/x_R^{eq}) through the variation of $\gamma_P^{eq}/\gamma_R^{eq}$ that can be estimated by activity coefficient models.

Solvents influence not only reaction equilibrium, but also phase equilibrium. For instance, when a solvent is used for gas separation, the vapor-liquid equilibrium equation under the assumption of ideal gases is given by

$$y_i P_{tot} = x_i \gamma_i P_i^{sat}(T) \quad \text{or} \quad y_i/x_i = \gamma_i P_i^{sat}(T)/P_{tot}$$

y_i and x_i represent the compositions of component i in the gas and liquid phases, respectively. γ_i is the activity coefficient of i in the liquid phase, P_i^{sat} is the temperature-dependent saturated vapor pressure of i and P_{tot} denotes the total pressure of the system. The selectivity of the solvent for separating gases i and j thus is determined by

$$S_{ij} = \frac{y_i/x_i}{y_j/x_j} = \frac{\gamma_i P_i^{sat}(T)}{\gamma_j P_j^{sat}(T)}$$

Similarly, when a solvent is used for liquid-liquid extraction, the liquid-liquid equilibrium condition of component i between phases α and β is written as

$$x_i^\alpha \gamma_i^\alpha = x_i^\beta \gamma_i^\beta$$

The extraction selectivity of the solvent

$$S_{ij} = \frac{x_i^\alpha/x_i^\beta}{x_j^\alpha/x_j^\beta} = \frac{\gamma_i^\beta/\gamma_i^\alpha}{\gamma_j^\beta/\gamma_j^\alpha}$$

The same with solvent effects on chemical equilibrium, the effect of solvents on phase equilibrium is finally attributed to solvent-dependent activity coefficients as well.

It should be noted that solvents can sometimes have influences on both chemical and phase equilibrium. In order to visualize these dual effects in ternary diagrams, a simple, hypothetical reaction $A \leftrightarrow B$ is considered. Figure 2.2 shows the effects of two solvents (S_1 and S_2) on the chemical and phase equilibrium of the reaction. UNIQUAC parameters of the virtual liquid compounds are listed in Table 2.4.
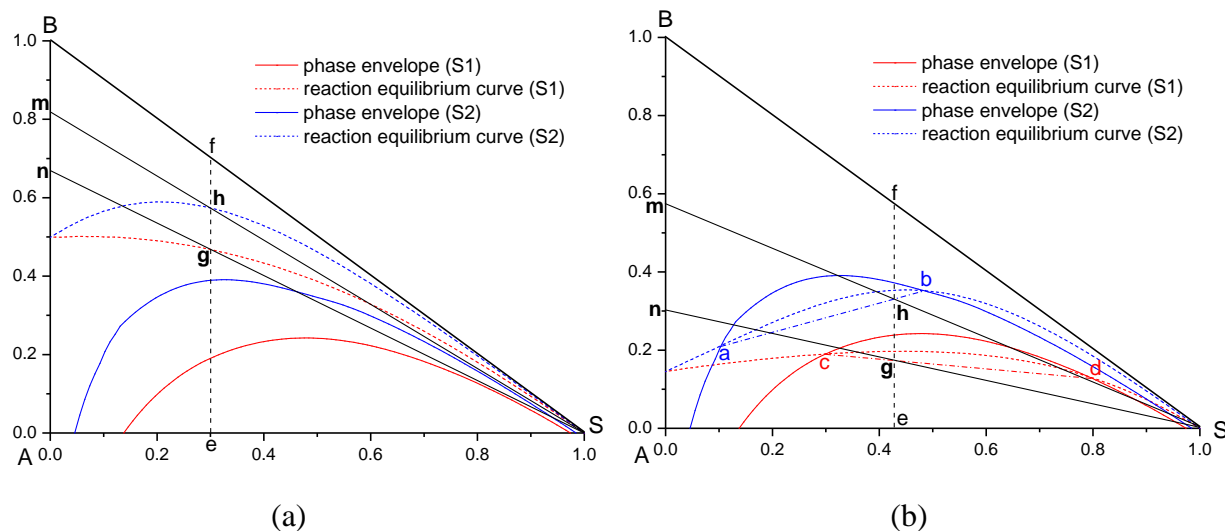
Figure 2.2: Phase diagrams for the A ↔ B reaction in the presence of inert solvents S_1 and S_2 at the thermodynamic equilibrium constant $K = 1$ (Figure 2.2a) and $K = 0.2$ (Figure 2.2b)

From the Gibbs phase rule it is known that for a three-component and one-reaction system at constant temperature and pressure, there are at most two liquid phases at equilibrium. Figure 2.2a shows the liquid-liquid phase envelope and reaction equilibrium curve of the ternary system where the thermodynamic equilibrium constant K is equal to unity. Here, the reaction equilibrium curve does not intersect with the phase envelope. This means that the final equilibrium state only has one liquid phase and the composition is completely constrained by the reaction equilibrium. The single degree of freedom is the composition of the solvent. Given an initial solvent composition, the equilibrium composition corresponds to the intersection of the stoichiometric line (vertical line for our A ↔ B reaction) through the initial composition and the reaction equilibrium curve. For example, when the initial amount of the solvent is at *e*, the equilibrium composition of the system will be located at *g* for solvent S_1 and *h* for solvent S_2 with the equilibrium conversions of the reaction being indicated by point *n* and point *m* for solvents S_1 and S_2, respectively.

Similarly, Figure 2.2b shows the phase envelope and reaction equilibrium curve at $K = 0.2$. For a mixture with an initial composition at *e*, two different liquid phases can be found at equilibrium. The compositions of the two phases are determined by the intersections of the reaction equilibrium curves and the phase envelopes since both reaction equilibrium and phase equilibrium conditions need to be satisfied. The total compositions of the two liquid phases correspond to point *g* for solvent S_1 and *h* for solvent S_2, and the reaction conversions are indicated by point *n* and point *m* for solvents S_1 and S_2, respectively.

From the above illustration, it is clear that solvent structure and its initial composition are the only degrees of freedom needed to define the equilibrium conversion of liquid phase reactions.

Table 2.4: UNIQUAC parameters (T = 298.15 K, P = 1 atm) used to generate Figure 2.2

Pure component parameters		
Component	r	q
B (1)	2.204	2.072
S_1 (2)	0.940	1.400
S_2 (2′)	1.200	1.700
A (3)	2.870	2.410
Binary interaction parameters (K)		
Ternary system of $\{A + B + S_1\}$		
a(1,1) = 0.00	a(1,2) = 10.20	a(1,3) = −10.57
a(2,1) = −13.94	a(2,2) = 0.00	a(2,3) = 100.80
a(3,1) = 37.80	a(3,2) = 333.89	a(3,3) = 0.00
Ternary system of $\{A + B + S_2\}$		
a(1,1) = 0.00	a(1,2′) = −20.20	a(1,3) = −10.57
a(2′,1) = −235.94	a(2′,2′) = 0.00	a(2′,3) = 150.80
a(3,1) = 37.80	a(3,2′) = 350.89	a(3,3) = 0.00

2.1.3 Solvent effect predictions

a) Prediction of solvent effects on reaction kinetics

Polar solvents normally have stronger interactions with more polar solutes than with less polar solutes. In other words, compared to less polar solutes, more polar solutes have lower energies in polar solvents. As explained in Section 2.1.2, it is the different solvation abilities of solvents on the reactants and the transition state that result in different levels of activation energy of the reaction, which finally lead to different reaction rate constants. Based on these considerations, Hughes and Ingold (1935) summarized the following heuristics on solvent kinetic effects.

(1) An increase in solvent polarity results in an increase in the rates of those reactions where the charge density (polarity) of the transition state is higher than that of the reactants.

(2) An increase in solvent polarity results in a decrease in the rates of those reactions where the charge density (polarity) of the transition state is lower than that of the reactants.

These heuristics can only provide a qualitative description of solvent kinetic effects. For quantitatively predicting these effects, either quantum chemical methods or empirical correlation methods can be employed.

The TST described in Section 2.1.2 is until now the most applicable theoretical method for determining reaction rate constants. The TST indicates that the quantification of solvent effects on reaction kinetics requires the prediction of solvent-dependent activation energy of the reaction. Despite the popularity of using quantum chemical methods to determine reaction activation energy, the computation procedure is at the moment still quite computationally complex and expensive, additionally, the predicted rate constants sometimes show substantial deviations from the experimentally determined ones (Struebing et al., 2013).

Given the difficulty in determining solvent kinetic effects by computational chemistry methods, empirical and semi-empirical methods have been proposed and widely used. A well-known semi-empirical approach is the quantitative structure-property relationship (QSPR) method (Jurs, 2008) where the physical or chemical property of a compound is related to certain parameters, properties, or molecular descriptors of the compound. Grunwald and Winstein (1948) correlated solvent-sensitive reaction rate constants with solvent ionizing power, an empirical measure of solvent polarity. With this correlation, they thoroughly studied the effect of solvents on S_N1 reactions and found that polar protic solvents are the most favorable solvents for accelerating the rates of S_N1 reactions. The Grunwald-Winstein correlation equation was later improved by adding another important factor, solvent nucleophilicity (Winstein et al., 1951), in addition to the ionizing power of solvent. The new equation shows an enhanced predictive power for S_N2 reactions.

In general, correlations taking into account more than two solvent parameters are regarded as multi-parameteric QSPR models. Fowler et al. (1971) first showed that by correlating with at least three solvent parameters or properties, the quality of prediction on solvent kinetic effects can be significantly improved. The Kamlet-Taft Linear Solvation Energy Relationship (LSER) model, also known as the solvatochromic equation, is one of the most successful multi-parameteric QSPR models on describing the effect of solvents on reaction rates. The equation first employed three solvent solvatochromic parameters. They are hydrogen-bond donor acidity α (Taft and Kamlet, 1976), hydrogen-bond acceptor basicity β (Kamlet and Taft, 1976), and polarity/polarizability π (Kamlet et al., 1977). Later, Kamlet et al. (1983) generalized the equation by including three more parameters. The generalized solvatochromic equation is expressed as:

$$\log k = \log k_0 + s\pi + d\delta + a\alpha + b\beta + h\delta_H^2 + e\xi$$

where log k is the logarithm of the rate constant. δ is a discontinuous polarizability correction term with $\delta = 0$ for nonhalogenated aliphatic solvents, $\delta = 0.5$ for polyhalogenated aliphatic solvents, and $\delta = 1$ for aromatic solvents. δ_H^2, the square of solvent Hildebrand solubility parameter (Hildebrand and Scott 1950), indicates the cohesive energy density of solvent molecules. ξ is the coordinate covalency parameter (Kamlet et al., 1983). log k_0, s, d, a, b, h, and e are fitting constants obtained from multi-linear regressions. To date, a large number of applications of the solvatochromic equation can be found in open literatures. For example, Folić et al. (2008) employed the solvatochromic equation to correlate the effect of solvents on the rate constant of a Menschutkin reaction.

b) Prediction of solvent effects on reaction thermodynamics

The effects of solvent structure and composition on the equilibrium conversion of liquid phase reactions are shown in Figure 2.2 by investigating a simple reversible A $\leftrightarrow$ B reaction. Now let us consider a more general A + B $\leftrightarrow$ C + D reaction taken place at a constant temperature T. The initial amount of the reactants and products as well as the amount of solvent added to the reaction mixture are given. If the final equilibrium state consists of only one liquid phase, the equilibrium conversion of the reaction can be directly determined from the solution of the chemical equilibrium equation $\left(x_C^{eq}\gamma_C^{eq}\right)\left(x_D^{eq}\gamma_D^{eq}\right)/\left(x_A^{eq}\gamma_A^{eq}\right)\left(x_B^{eq}\gamma_B^{eq}\right) = K(T)$ with a suitable activity coefficient model. When the equilibrium state has two liquid phases, a set of nonlinear equations including 4 mass balance equations, 1 chemical equilibrium equation, 5 phase equilibrium equations, and 2 summation equations can be derived. The final equilibrium state can be determined by solving this set of equations. It should be noted that due to the strong nonlinearities of these equations, a successful solution relies much on good initial estimates.

2.2 Conductor-like screening model

2.2.1 COSMO

Basic quantum chemistry (QC) methods describe isolated molecules at a temperature of 0 K, which allows a realistic description of molecules in vacuum or in the gas phase only. Continuum Solvation Models (CSMs) are extensions of the basic QC methods for treating liquid mixtures. In CSMs, the atomic structure of solvent is neglected and the electrostatic property of the solvent is represented by an infinitely extended dielectric continuum. The solute is treated as if embedded in the dielectric continuum where a molecular surface or "cavity" is constructed around the solute molecule. The electric field of the solute in the cavity is screened by the polarization of the solvent continuum. The effect of this polarization can be represented by the distribution of the screening charge density (SCD) produced on the cavity surface.

In 1993, Klamt and Schüürmann (1993) proposed a very popular CSM, known as conductor-like screening model (COSMO). In COSMO, the dielectric continuum that represents the solvent is

approximated by a conductor with a positive-infinity dielectric constant. The dielectric boundary condition thus is replaced by a much simpler conductor boundary condition, which substantially simplifies the calculation of the SCD distribution. Figure 2.3 concisely describes the basic steps of a COSMO calculation procedure. Firstly, the molecule of interest is built and optimized to its most stable configuration. A molecular cavity defining the boundary of conductor is constructed around the molecule. The conductor SCD distribution is then obtained from quantum chemical (usually Density Functional Theory, DFT) computation while the molecule is converged to its energetically optimal state in the conductor. Due to the wide popularity of the model, the COSMO calculation procedure has been standardized and implemented in many quantum chemical software packages, such as Turbomole (Schäfer et al., 2000) and Gaussian (Frisch et al., 2004). It is worth mentioning that even though the DFT calculation is time-consuming for large molecules, the calculation needs to be performed only once for a molecule and the result (mainly the SCD distribution) can be stored in a COSMO-file. The available COSMO database already covers a large number of common molecules. For more information on the COSMO theory and application, please refer to Klamt et al. (2010).
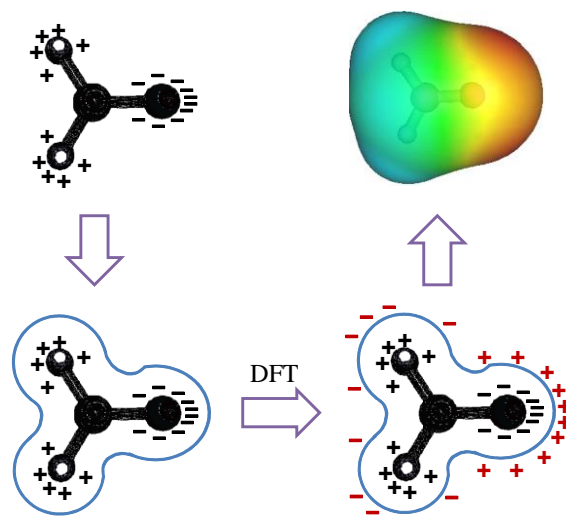
Figure 2.3: Schematic diagram of a COSMO calculation procedure

2.2.2 σ-profile

The COSMO calculation finally results in a spatial SCD distribution. This three-dimensional information can be converted into a histogram indicating the amount of molecular surface segments having a certain SCD value, σ. Figure 2.4 shows the SCD histogram of the water molecule. As shown, there is an accumulation of negative screening charges (blue) around the positively charged hydrogen atoms and positive screening charges (red) induced by the negatively charged oxygen atom. Through the continuation of the SCD histogram, we can finally obtain a very important composition function, so called σ-profile, $P(\sigma)$.
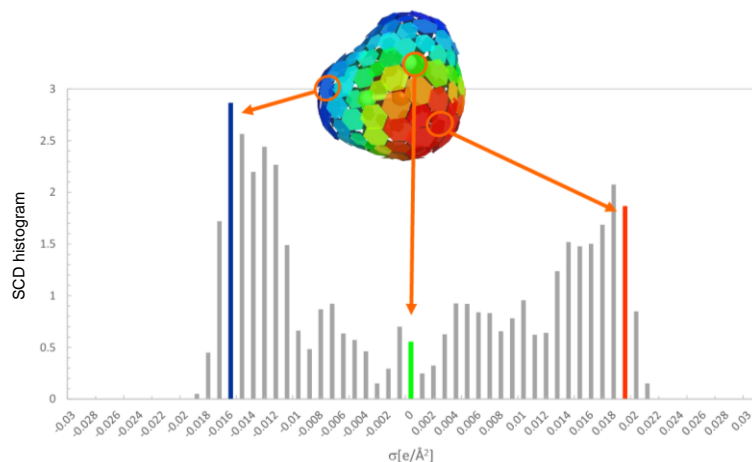
Figure 2.4: SCD histogram of the water molecule, taken from
http://www.cosmologic.de/files/downloads/theory/COSMO-RS-Theory-Basics.pdf

Figure 2.5 shows σ-profiles of four representative compounds: namely water (highly polar HB acceptor and HB donor), hexane (nonpolar), chloroform (HB donor) and acetone (HB acceptor). Qualitatively, a more polar molecule has a broader SCD distribution compared to a less polar molecule. When the SCD goes beyond ± 1.0 e/nm^2, the molecule is polar enough to form a hydrogen bond (HB). As depicted in Figure 2.5, water has a very broad σ-profile with two pronounced peaks around -1.6 e/nm^2 and $+1.8$ e/nm^2 resulting from the strongly polar hydrogen atoms and oxygen atom, respectively. Hexane is almost nonpolar, which can be reflected from its narrow distribution of the SCD around zero. The slightly negative SCD is assigned to the hexane hydrogen atoms and the slightly positive SCD denotes the carbon atoms. The σ-profiles of chloroform and acetone are very asymmetric. The peak at -1.4 e/nm^2 of the chloroform σ-profile arises from the acidic hydrogen atom and the peak around $+1.3$ e/nm^2 of the acetone σ-profile corresponds to its carbonyl group.

Figure 2.5: σ-profiles of water, hexane, chloroform, and acetone

Derived from uni-molecular quantum chemical calculation, σ-profile can well characterize the polarity and charge distribution of a molecule. Moreover, due to its molecule-specific nature, σ-profile can be regarded and used as a promising molecular fingerprint.
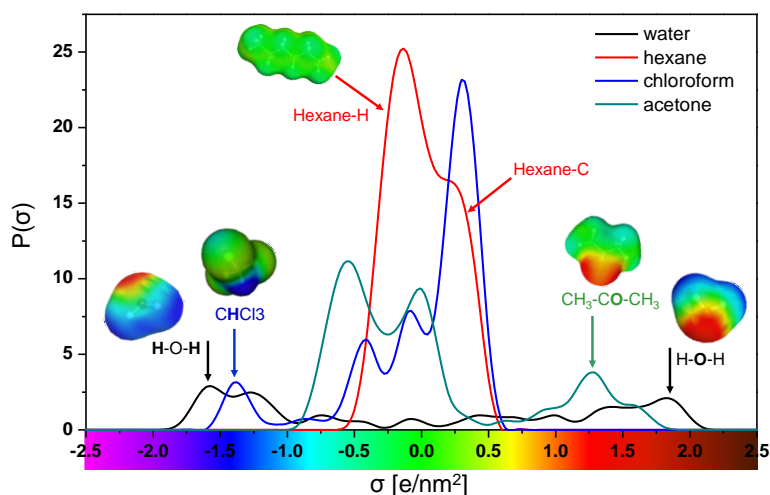
2.3   Computer-aided molecular design

From Section 2.1, we know that solvents can influence many process properties, such as reaction rate, chemical and phase equilibrium, etc. Therefore, the selection of a proper solvent is very important for developing highly efficient process systems. There are two main types of methods for making solvent selection decisions. The first is so called experience-and-experiment. Potential candidates are first selected from experiences or heuristics. Afterwards, specific experiments are carried out for each of the selected candidates, from which the best solvent is finally identified. Despite its wide applicability, the method is quite experience-limited and experimentally time-consuming. Recent advances in molecular property modeling, numerical algorithm, and computer power have brought the computer-aided molecular design (CAMD) method to the limelight. CAMD, introduced by Gani and Brignole (1983) as a new concept in the early 1980s, is a general term describing the procedure of rational selection or design of molecules that possess pre-specified, desirable properties using systems engineering principles. Since its emergence, the CAMD method has been widely used for designing solvents for specific applications.

2.3.1   The CAMD approach

The CAMD problem is described as: Given a set of molecular building blocks (usually structural groups), determine feasible molecular structures that possess pre-specified, desirable properties. Figure 2.6 concisely summarizes the basic procedures followed in solving a CAMD problem. Generally, each CAMD problem can be divided into a forward and a reverse subproblem. The task of the forward subproblem is to establish mathematical models for predicting molecular properties based on given molecular structures. In the reverse subproblem, molecular structures that possess desired properties are identified from either generate-and-test or mathematical optimization methods based on the established structure-property relationship models.
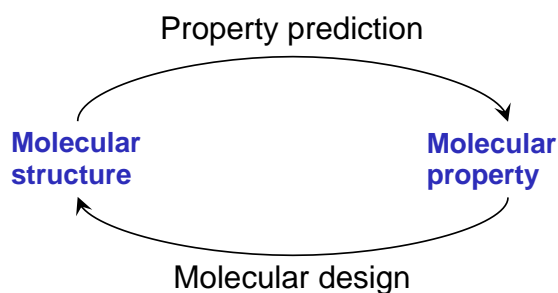

Property prediction

Molecular structure   **Molecular property**

Molecular design

Figure 2.6: The CAMD methodology

Due to the high complexity and computational load of first-principle models, in CAMD empirical or semi-empirical models are usually developed and used for predicting molecular properties (see Figure 2.7). Molecular properties generally include pure-component physical properties, such as heat capacity and boiling point, as well as mixture thermodynamic properties, such as activity coefficient and solubility. Pure-component physical properties are commonly estimated by group contribution (GC) methods where each structural group is assumed to contribute a specific amount to a certain property and the property is determined by the summation of group contributions multiplied by the number of groups present in the molecule. Another approach for predicting molecular physical properties is the semi-empirical QSPR modeling method. In this method, molecular properties are related to molecular structures via correlations with certain molecular descriptors. Linear correlations are typically used in QSPR modeling. The nonlinear relationship between molecular structure and property can be included by using advanced correlation methods such as artificial neural network (ANN). For estimating thermodynamic properties, predictive molecular thermodynamic models such as UNIFAC can be employed.
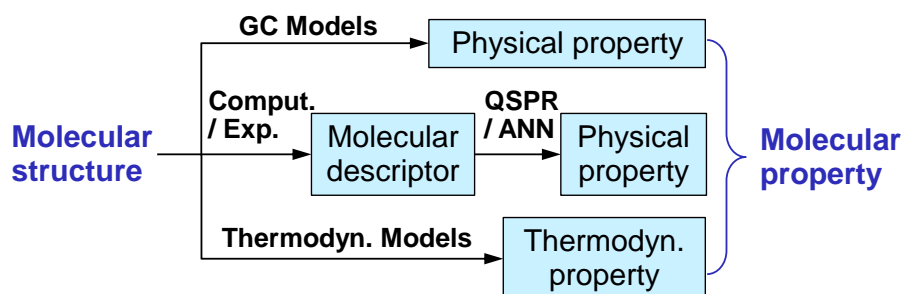
Figure 2.7: Methods for predicting molecular properties in CAMD

CAMD tasks can be solved as optimization problems where the number of building groups present in the molecule is the independent integer variable being optimized. Depending on the design task, molecular properties as dependent continuous variables are either constrained or posed as the objective function. Structural feasibility rules, used to ensure the chemical feasibility of generated molecules, are usually written as equality constraints. Structural complexity constraints, normally posed as inequality constraints, take into account the upper and lower limits on the number of each group as well as the limit on the total number of groups making up the molecule. Due to the inclusion of both discrete and continuous variables, the design task is intrinsically a Mixed-Integer Linear Programming (MILP) or Mixed-Integer Non-Linear Programming (MINLP) problem, depending on the form of the employed structure-property relationship models.

Methods for solving the MILP or MINLP formulated CAMD problem can be generally classified into two categories. They are the generate-and-test approach and the mathematical optimization approach.

a) CAMD via generate-and-test methods

Gani and Brignole (1983) and Brignole et al. (1986) first introduced the generate-and-test method. The key idea of this method is to generate all possible molecule candidates from a given set of building groups and test them one by one against all constraints, those unsatisfying the constraints are discarded and the left are evaluated and ranked according to their objective property values. Because all possible combinations of structural groups are generated and tested, the calculation can be quite computationally expensive as the number of building groups increases. Gani et al. (1991) improved the method by first using structural feasibility rules to ensure that only chemically feasible molecules are generated. These molecules are then filtered by multi-level property constraints. Molecules violating the preceding constraints are eliminated immediately without being assessed by the subsequent constraints.

Traditional generate-and-test methods cannot distinguish between structural isomers. Harper and Gani (2000) addressed this problem by proposing a multi-step CAMD framework. In this framework, the optimal combination of first-order structural groups is first identified via conventional generate-and-test methods where first-order group based GC models are employed. Later in a separate post-design step, all possible structural isomers that can be generated from the identified combination of first-order groups are further evaluated by using higher-order GC models, molecular modeling techniques, or experimental data if available. After that, a final selection of molecules can be made. The multi-step CAMD approach has been implemented into a computer program, ProCAMD (Gani, 2010). Apart from the aforementioned contributions, other CAMD works using the generate-and-test method or the ProCAMD program include Pretel et al. (1994); Constantinou et al. (1996); Harper et al. (1999); Chen et al. (2005); Karunanithi et al. (2005; 2006).

The generate-and-test method tests all the molecules in the design space. Therefore, the global optimality of the final identified molecule can be guaranteed. Despite this advantage, the limitation of the method is also obvious. Due to the full enumeration of solutions in the design space, the method can suffer greatly from the combinatorial explosion for design tasks with a large number of molecular building groups.

b) CAMD via mathematical optimization methods

Shortly after the first few applications of the generate-and-test method, Odele and Macchietto (1993) introduced the mathematical optimization method. This method is able to find promising molecules without testing all the candidates in the design space. This feature makes the method much less limited by the combinatorial complexity. Therefore, compared to the generate-and-test

method, mathematical optimization methods are more efficient for solving complex CAMD problems.

As is well known, deterministic and stochastic optimizations are the two categories of mathematical optimization techniques. CAMD using deterministic optimization seeks to find optimal molecules from the direct solution of the MILP or MINLP problem by derivative-based algorithms. When solving the MILP-formulated CAMD problem with deterministic optimization algorithms, global optimality of the solution is always ensured. However, for nonconvex MINLP-based CAMD problems, only local optimum can be guaranteed unless deterministic global algorithms are used. CAMD works employing deterministic optimization methods include Vaidyanathan and El-Halwagi (1994); Maranas (1997); Sahinidis and Tawarmalani (2000); Wang and Achenie (2002); Cheng and Wang (2007); Samudra and Sahinidis (2013). Stochastic optimization finds optimal solutions based on adaptive search strategies. Depending on the type of stochastic algorithm, different rules are defined to guide the movement from one solution towards another improved solution. Even though there is no theoretical guarantee on the optimality of solution, under properly adjusted algorithm parameters stochastic optimization can find global or near-global optimum for both convex and nonconvex problems. CAMD works using stochastic optimization methods include Venkatasubramanian et al. (1994; 1995); van Dyk and Nieuwoudt (2000); Marcoulaki and Kokossis (2000); Kim and Diwekar (2002).

2.3.2 CAMD of solvents

From Section 2.1, we know that solvents can have large influence on reactions and separations. Due to the large number of solvent candidates, theoretical methods for guiding the solvent selection are strongly required. The CAMD method allows for the optimal design of molecules for specific applications. Since its emergence, the method has been widely used for finding optimal solvents to improve the reaction and separation performance.

a) CAMD of separation solvents

Macchietto et al. (1990) first designed solvents for liquid-liquid extraction and gas absorption processes via the formulation and solution of CAMD problems. Marcoulaki and Kokossis (2000) proposed a CAMD method based on the simulated annealing algorithm to design solvents for liquid-liquid extraction, extractive distillation, and gas separation processes. Later, Kim and Diwekar (2002) developed another stochastic algorithm based CAMD method to design extraction solvents. Chen et al. (2005) applied the CAMD methodology to design solvents for separating hydrocarbons by extractive distillation. The generate-and-test approach was used to solve the design problem. Karunanithi et al. (2005) proposed a decomposition-based CAMD method to design solvents and solvent mixtures. In the method, the CAMD problem is decomposed into an ordered set of subproblems where each subproblem except the final one requires the consideration of only a subset of constraints from the original full set. Solvent

molecules generated by the ProCAMD program are tested one-by-one by the subproblems. Those unsatisfying constraints of the preceding subproblems are discarded without being evaluated by the subsequent subproblems. This decomposition strategy finally leads to a significantly reduced MILP or MINLP problem that can be comfortably solved. The efficiency of the method has been demonstrated on two case studies, one of which is to design solvents for separating acetic acid from water by liquid-liquid extraction. In Karunanithi et al. (2006), the method was applied to the optimal design of solvents for solution crystallization processes. Apart from the aforementioned contributions, numerous works on the CAMD of separation solvents can be found, such as Gani et al. (1991); Pretel et al. (1994); Harper and Gani (2000); van Dyk and Nieuwoudt (2000); Wang and Achenie (2002); Cheng and Wang (2007); Samudra and Sahinidis (2013).

b) CAMD of reaction solvents

In contrast to the numerous works on the CAMD of separation solvents, only a very few attempts have been made to tackle the reaction solvent design. Stanescu and Achenie (2006) studied the mechanism of the Kolbe-Schmitt reaction by quantum chemical DFT calculation and determined the best solvent to maximize the reaction rate. ProCAMD was first used to generate solvent candidates that fulfill all design constraints including inert to the reactants and products, non-toxic, and liquid under the reaction condition. It was assumed that a solvent with the same Hansen solubility parameters as the product will stabilize the product and therefore improve its yield. Based on this criterion, a few promising solvents were selected from the generated candidates and they were further evaluated by DFT calculations. The one with the largest reaction rate constant was finally selected as the optimal solvent. Despite the great success, limitations of the method are obvious. Firstly, the applicability of the method is quite limited because the solubility parameter assumption is no more reasonable for reactions involving polar compounds as reactants or transition states. Secondly, the generation of solvent candidates via ProCAMD can suffer from combinatorial explosion if a large number of molecular building groups are considered. Lastly, the DFT calculation of reaction rate constant is quite computationally expensive and the resulting rate constant values may have large deviations.

Gani et al. (2005; 2008) proposed a method for the optimal selection of solvents for organic reactions. Five steps are involved in the method and they are summarized as follows.

Step 1: Reactions are specified and the available reaction characteristics are defined. The desired solvent functionality is specified based on the operational needs of the reaction.

Step 2: Reaction (R) indices are defined based on knowledge of the reaction and desirable solvent properties. The solvent functions that fulfill the reaction operational requirements are assigned with R indices.

Step 3: Suitable solvents for the specified reaction are determined through the database search or CAMD method. Reaction-Solvent (RS) indices are assigned to the solvents based on their properties and R index values.

Step 4: Scores are assigned to the solvents based on their RS indices and a predefined scoring system. All the suitable solvents are ranked according to their scores.

Step 5: Solvents with high scores are selected. The performance of these solvents in the specified reaction is further analyzed through more rigorous calculations, for example, liquid-liquid phase equilibrium calculation. Those showing the highest reaction performance can be targeted for experimental verifications.

The method takes into account multiple considerations that impact the selection of solvents, which makes it applicable for a wide range of reactions and situations. The drawback of the method is that it requires a large amount of knowledge, experience, and insight on both the reaction and solvents. Additionally, the method cannot give any quantitative prediction on solvent effects because no real reaction kinetics is considered.

Folić et al. (2007) proposed an optimization-based CAMD method for the optimal design of solvents to accelerate reaction rates. An empirical solvent-sensitive rate expression (the solvatochromic equation) is established by linearly correlating the experimentally determined reaction rate constants in a small number of solvents with the corresponding solvent solvatochromic parameters. Based on the parameterized solvatochromic equation and a GC method to estimate solvent solvatochromic parameters from solvent molecular structures, a MILP-based CAMD problem is formulated and solved to identify the optimal solvent structure that provides a maximum rate constant. The method has been successfully applied to a S_N1 reaction (Folić et al., 2007) and a S_N2 reaction (Folić et al., 2008).

The method introduced in Folić et al. (2007) requires experimental reaction rate constants measured in a few solvents. In theory, DFT calculations can be used to predict rate constants for liquid phase reactions when experimental kinetic data are not available. Struebing et al. (2013) developed a framework combining DFT calculations and the CAMD method proposed in Folić et al. (2007) to design solvents to increase reaction rates. In order to minimize the DFT computational effort, an iterative strategy was employed. The main steps in the framework are summarized as follows. Firstly, an initial set of 6-7 diverse solvents are chosen. The reaction rate constants in these solvents are determined by DFT calculations combined with a continuum solvation model. The determined rate constants are then used to parameterize the solvatochromic equation, which is used in a subsequent optimization-based CAMD problem. An optimal solvent with the highest reaction rate constant is identified from the solution of the CAMD problem. If a solvent that is not included in the initial solvent set is designed, this solvent is added into the solvent set and the solvatochromic equation is re-parameterized based on the extended rate

constant database. A new CAMD problem based on the updated solvatochromic equation is then solved and consequently, a new optimal solvent can be found. The procedure is repeated until the solvatochromic equation is self-consistent, i.e., an optimal solvent is identified for a second time. Although in principle no experimental data is required, Struebing et al. claimed that the method is flexible as experimental rate constants can be used to complement the DFT prediction if they are available and accurate.

2.3.3   Computer-aided molecular and process design

The selection of solvents, catalysts, or other functional chemicals is very crucial for achieving processes with better economics and lower environmental impacts (Pistikopoulos et al., 2010). The important role of molecular-level decisions in developing highly efficient processes has led process engineers to recognize that the tool box of process development should include molecular design aspects, in addition to the conventional process design and optimization. For a computer-aided molecular and process design (CAMPD) problem, there are two main solution strategies, i.e., the decomposed design strategy and the integrated design strategy.

Figure 2.8 depicts the decomposed molecular and process design method where two steps are involved. The first is to find suitable molecular structures from a given set of building groups to match a set of molecular property targets. This is usually done by solving a MILP or simple MINLP based molecular design problem. In the second step, for each molecule identified from the first step, process optimization is performed to find the best process operating conditions to meet predefined process performance targets. This process optimization task is normally solved as a nonlinear programming (NLP) problem. In general, the two-step method decomposes the CAMPD problem into a molecular design and a process design problem, both of which can be efficiently solved via commercial solvers. Despite the high efficiency, one should note that to use the decomposed design method can lead to suboptimal solutions due to the following two reasons. (1) Usually, molecules have multiple effects on a process they are designed for. It is often difficult to know in advance which molecular property dominates the determination of process performance. For instance, Kossack et al. (2008) used the separation selectivity as the objective property to design entrainers for an extractive distillation process. The designed entrainer was later found not very desirable in terms of process economics. (2) The specification of process conditions strongly influences the selection of a suitable molecule and on the other hand, the selected molecule reversely determines the optimal operating conditions of the process. Decomposed molecular and process design cannot reasonably capture this interdependent relationship.
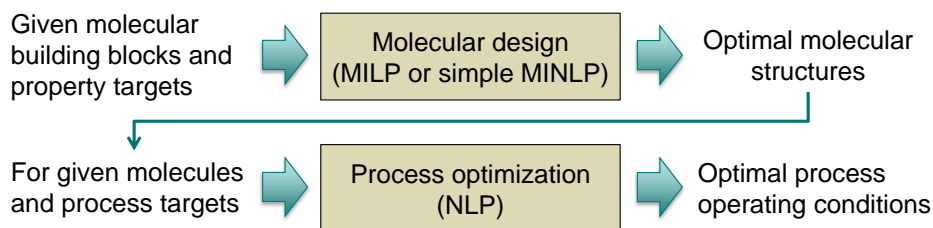
Figure 2.8: The decomposed molecular and process design method

Unlike the decomposition-based design method, integrated molecular and process design (see Figure 2.9) attempts to find the optimal molecular structure and process conditions simultaneously. A process performance index such as the process cost and energy consumption is defined and optimized subject to molecular structural constraints, pure-component and mixture property constraints, process and cost models, etc. Due to the large mixed discrete-continuous design space as well as the high nonlinearities of the process and cost models, integrated molecular and process design normally results in very complex MINLP problems. For solving these problems, reliable and efficient algorithms are strongly required.
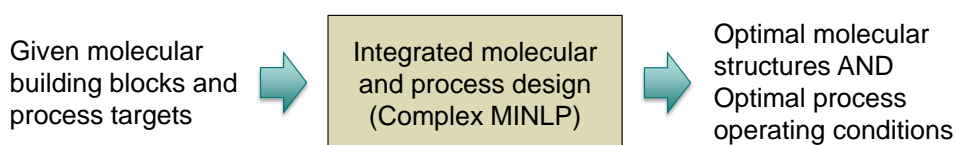
Figure 2.9: The integrated molecular and process design method

A sizable number of CAMPD works can be found in literature. Below are a few selected examples.

Eden et al. (2004) and Eljack et al. (2007) proposed a two-step method for general molecular and process design based on a visualization tool developed by Shelley and El-Halwagi (2000). The first step of the method solves a reverse simulation problem to determine target molecular properties for maximizing the process performance. In the second step, molecular structures are designed to match the property targets by solving a separate CAMD problem.

Papadopoulos and Linke (2005; 2006; 2009) suggested another two-step approach for the optimal design of solvents for separation processes. In the first step, multiobjective optimization is used to identify Pareto-optimal solvents for a set of important solvent properties impacting the process performance. In the second step, a molecular clustering technique is employed to integrate solvent selection and process design based on the obtained set of Pareto-optimal solvents. The approach has been extended to the optimal design of working fluids for organic rankine cycles (Papadopoulos et al., 2010).

Bardow et al. (2010) proposed a two-stage method CoMT-CAMD to address complex CAMPD problems. In their work, the perturbed-chain-polar-statistical-associating-fluid-theory (PCP-SAFT) equation of state is used as the thermodynamic model. Each molecule is described and represented by a set of continuous PCP-SAFT parameters rather than a combination of structural groups. In the first stage of CoMT-CAMD, the PCP-SAFT parameters characterizing molecules and the process operating conditions are simultaneously optimized. The results include the optimal process conditions as well as an optimal set of PCP-SAFT parameters describing a hypothetical target molecule. In the second stage, a real, existing molecule that has the closest parameters as the target molecule is identified as the final optimal molecule. The method was applied to a CO_2 capture process where the absorption solvent and the process were simultaneously designed.

Pereira et al. (2011) proposed a method for the optimal design of n-alkane solvents to separate CO_2 from methane through physical absorption. By treating the chain length (number of carbon atoms) of n-alkanes as a continuous variable and optimizing it together with process variables, the MINLP-based integrated solvent and process design problem was successfully converted into a much simpler NLP problem. The solution of this NLP problem includes the optimal process conditions and the optimal chain length, based on which the best n-alkane solvent was identified.

Lek-utaiwan et al. (2011) developed a four-step method for the optimal design of extractive distillation processes considering solvent selection and column optimization. In the first step, the generate-and-test approach is used to solve a CAMD problem to suggest a ranked list of promising solvents. In the second and third steps, a small number of top solvents resulting from the first step are selected for experimental verification where the vapor-liquid equilibrium (VLE) data of the ternary system consisting of a solvent and two azeotropes are experimentally determined. The VLE data are used to parameterize the thermodynamic model used for process optimization. In the final step, the extractive distillation process is optimized for three to five experimentally verified solvents, respectively. The one with the lowest annual manufacturing cost is selected as the optimal process.

Roughton et al. (2012) proposed a method for the simultaneous design of ionic liquid entrainer and energy efficient extractive distillation process. For a given azeotropic mixture, the CAMD method is used to identify the optimal ionic liquid entrainer with the objective to minimize the amount of entrainer that can break the azeotrope. Once the optimal entrainer has been found, the extractive distillation process for separating the azeotropic mixture is designed using the driving force method. The authors found that to use an optimally designed ionic liquid entrainer can reduce a lot of energy consumption, compared to the case when an ionic liquid that is known to break the azeotrope but not designed by CAMD methods is used.

Since it is difficult to directly solve the integrated molecular and process design problem via standard MINLP algorithms, until now most of the CAMPD work relies on various decomposition-based solution strategies. Burger et al. (2015) is one of the first attempts to solve the integrated design problem by local MINLP solvers without any assumption and model simplification. In their work, a multiobjective optimization problem where only reduced process models are considered is first solved to generate a set of Pareto-optimal solutions. These solutions are then used as initial guesses for solving a second MINLP problem where full process models are applied. Due to the nonconvexity of the MINLP problem and the utilization of local solvers, suboptimal solutions can be obtained. However, the probability of finding high-quality suboptimum is increased by solving the problem multiple times starting from different initial estimates.

Part I

Reaction Solvent Design

Solvents are widely used as reaction media in liquid phase reactions. It has been indicated in Section 2.1.2 that the variation of the type of solvent can dramatically change the reaction rate and equilibrium conversion. Despite that, there are still very few works addressing the optimal selection or design of solvents for chemical reactions. Since solvents can influence both reaction kinetics and reaction thermodynamics, Chapter 3 proposes a method for the molecular design of solvents to increase reaction rates for nonreversible reactions and Chapter 4 focuses on the optimal design of solvents to improve equilibrium conversions of reversible reactions.

3. Optimal design of solvents to increase reaction rates

In order to develop a CAMD method for rationally selecting or designing solvents to increase reaction rates, a solvent structure based model for predicting solvent kinetic effects is indispensable. Figure 3.1 depicts the concept for the CAMD of solvents to maximize the reaction rate. For a given set of building groups, the optimal solvent structure is determined from the solution of a CAMD problem where the solvent-dependent reaction kinetic model is parameterized with experimental kinetic data measured in a small number of known solvents.
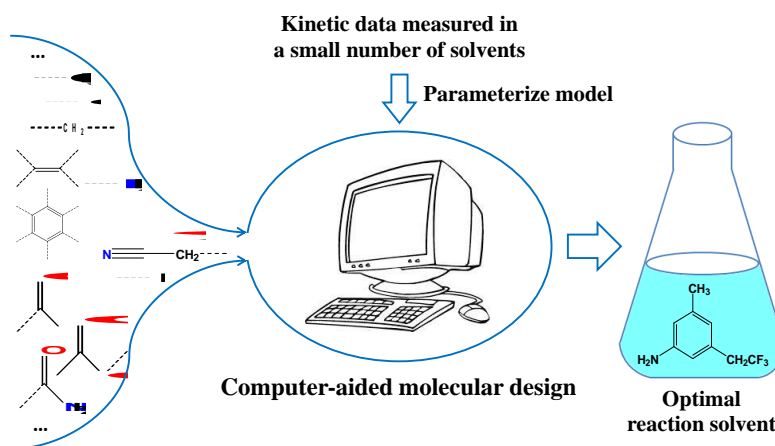
Figure 3.1: Schematic diagram of the CAMD of solvents for maximizing reaction rates

The semi-empirical QSPR model is widely used for predicting solvent kinetic effects where experimentally measured solvent parameters, such as the solvatochromic parameters, are usually used to correlate the effect of solvents on reaction rate constants (Abraham et al., 1987; Folić et al., 2007; Chiappe et al., 2010). Over the last few decades, theoretical and computational chemistry have been developed very fast and the computer power nowadays has reached a relatively high level. This opens the possibility to make use of solvent theoretical descriptors (Zhou et al., 2014; Karelson, 2000; Lowrey et al., 1995; Shang et al., 2013; Katritzky et al., 2010) for correlating solvent effects on reactions. Theoretical descriptors are normally derived from molecular structural or electronic information. They are easy-to-generate and do not require any experiments. More importantly, compared to the experimentally determined parameters, theoretical descriptors are molecular structure related thus they can be more accurately estimated by group contribution methods (Sheldon et al., 2005; Zhou et al., 2015a). This advantage ensures the high reliability of solvent molecular design results.

In this chapter, we introduce a new kind of solvent theoretical descriptor and determine the contributions of common structural groups to these descriptors. Based on a pre-built solvent-sensitive reaction rate model and the developed group contribution method, optimal solvents that

possess the best reaction performance are identified through the formulation and solution of an optimization-based CAMD problem. The methodology is elaborated in Section 3.1 and illustrated with two application examples in Section 3.2.

3.1 Methodology

As described in Section 2.3.1, a standard CAMD procedure consists of two subproblems. The forward problem relates molecular structures to molecular properties through certain property prediction models. The reverse problem determines the best molecular structure that possesses the optimal property via either generate-and-test methods or mathematical optimization methods. For CAMD of reaction solvents, we introduce a new type of solvent molecular descriptor and use these descriptors to correlate the effect of solvents on chemical reaction rates. As illustrated in Figure 3.2, starting from a given set of building groups, different solvent molecular structures are generated. Through DFT calculations based on the COSMO solvation model, we obtain the screening charge density distribution, σ-profile, of each solvent molecule. Then, we partition the σ-profile into six sections and use the areas underneath the curve sections as solvent descriptors. By correlating experimental reaction rate constants measured in a few known solvents with their descriptors, we parameterize a QSPR model (i.e., rate constant expression) which describes the solvent effect on the rate of the investigated reaction. Based on this model and an additionally developed group contribution method, COSMO-GC, for estimating the descriptors from solvent molecular structures, one can reversely optimize solvent structures in terms of the combination of groups for identifying an optimal solvent featuring a highest reaction rate or rate-related reaction property, such as the reaction selectivity.
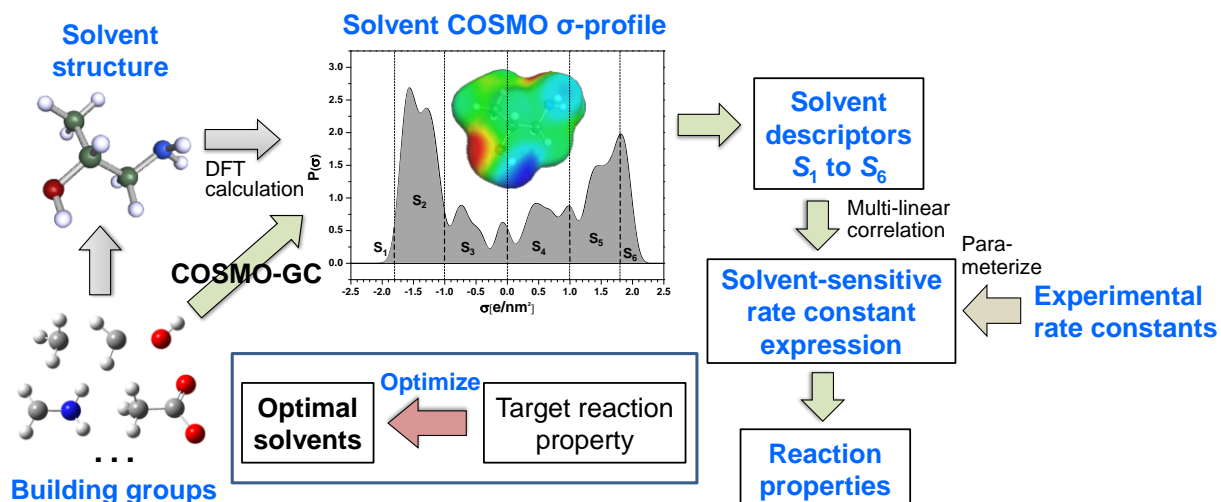

Figure 3.2: Overview of the proposed solvent design methodology

The methodology is described in the following sections in a more detailed way. The new type of solvent descriptor is introduced in Section 3.1.1. The COSMO-GC method for estimating solvent descriptors is explained in Section 3.1.2 and the mathematical formulation of the optimization-based CAMD problem is presented in Section 3.1.3.

3.1.1   COSMO-based solvent descriptors

Derived from uni-molecular quantum chemical calculation, σ-profile can well characterize the polarity and charge distribution of a molecule. More importantly, the molecule-specific nature of σ-profile makes it very suitable fingerprint for quantitatively correlating molecular properties and behaviors. In this work, solvent σ-profile curves are divided into six segments in the entire [–2.5 e/nm^2, +2.5 e/nm^2] σ-region. Six areas (S_1 to S_6) are obtained for each solvent by integrating those segments over the screening charge density, as depicted in Figure 3.2. Afterwards, the six area parameters are used as solvent molecular descriptors to correlate solvent-sensitive reaction rate constants.

3.1.2   GC methods for predicting solvent descriptors

With the solvent-sensitive rate constant expression, we successfully connect solvent descriptors to reaction properties in a quantitative way. However, for CAMD of solvents (see Figure 3.2), we still lack a relation linking the molecular structure and the descriptors. Group contribution (GC) methods, such as Rihani and Doraiswamy (1965); Constantinou et al. (1995); Marrero and Gani (2001), are widely used for estimating solvent physical properties based on their molecular structures. From Figure 2.5 we can see that the σ-profile of a molecule is closely related to the atoms or groups of the molecule. In other words, a certain group should contribute a specific part of the σ-profile. This inspires us to develop a GC method, COSMO-GC, for estimating the solvent descriptors. The expression of the GC model is given by Eq. (3.1) where S_i ($i = 1, 2, \ldots,$ 6) are the six solvent descriptors, s_{ij} is the contribution of the j-th group to the i-th descriptor, and s_{i0} are fitting constants. n_j denotes the number of group j present in the molecule while N is the total number of different groups. The fitting constants and contributions of 48 structural groups and 12 single-group solvents (some solvent molecules cannot be divided into sub-groups thus are treated as whole structures) to the six descriptors are obtained from the multi-linear regression of $S_1 \sim S_6$ of 168 common solvents, whose σ-profiles are taken from the latest COSMO database (C30-1201). All the selected groups are UNIFAC structural groups (http://www.aim.env. uea.ac.uk/aim/info/UNIFACgroups.html). The regressed s_{10} is −0.00202, s_{20} is −0.15091, s_{30} is 3.58025, s_{40} is −0.91960, s_{50} is 0.38711, and s_{60} is 0.07294. The contribution of each group to the six descriptors is given in Table A1 in Appendix A.

$$S_i = s_{i0} + \sum_{j=1}^{N} n_j s_{ij} \quad (i = 1, 2, \ldots, 6; j = 1, 2, \ldots, N) \tag{3.1}$$

For verifying the quality of the regression, the six descriptors of the 168 solvents estimated from COSMO-GC are plotted versus the original six σ-profile areas of the solvents in Figure 3.3. The overall Mean Absolute Percentage Error (MAPE) between the GC-predicted and the original solvent descriptors is 7.28%. It is concluded that the solvent descriptors can be estimated from the proposed COSMO-GC method at a relatively high accuracy.
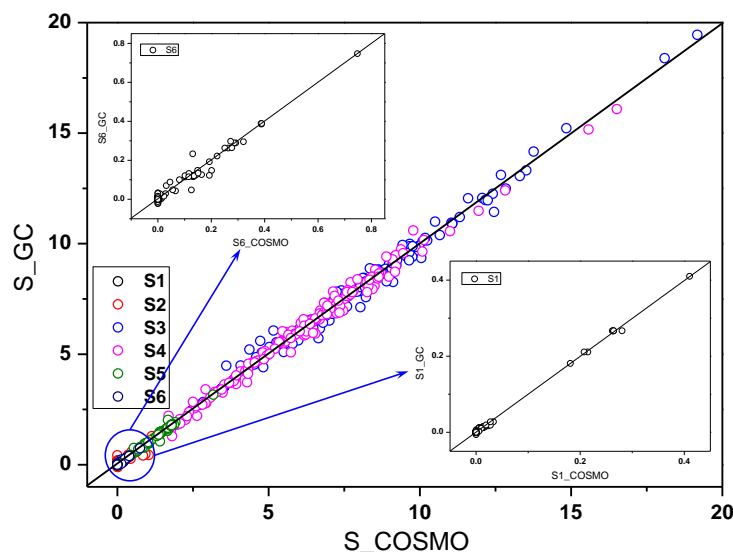
Figure 3.3: The six GC-predicted solvent descriptors plotted with the original six σ-profile areas for the 168 solvents

3.1.3   Mathematical formulation of the CAMD problem

With the solvent-sensitive rate constant expression and the COSMO-GC model, we successfully connect solvent molecular structures to solvent-dependent reaction properties (see Figure 3.2). The optimal solvent structure can now be determined from the solution of a CAMD problem. In optimization-based CAMD problems, each molecule is represented by a composition vector $\mathbf{n}$ = $[n_1, \ldots, n_j, \ldots, n_N]$ with the element integer variable n_j denoting the number of group j present in the molecule. The composition vector is optimized to give an optimal solvent molecule that possesses a maximum (or minimum) objective property value and meanwhile satisfies certain structural and property constraints. The structural constraints normally include chemical feasibility rules that ensure the generation of structurally feasible molecules and chemical complexity constraints that make sure the designed solvent molecules are not very big and complex. Besides the structural constraints, a number of solvent property constraints are also required. For instance, solvents should be chemically inert under the reaction condition, solvents must have a high miscibility with the reactants, solvents should be liquid at room temperature, etc. The formulated optimization problem for the CAMD of reaction solvents is given below.

$$\max_{n_j\,(j=1,\,2,\,...,\,N)} obj$$

Subject to:

(1) Objective function (reaction rate or rate-related reaction property) calculation

(2) Structural constraints

a) Chemical feasibility

Three binary variables (y_1, y_2, y_3) are introduced to represent the type of designed molecules. Specifically, $y_1 = 1$ gives acyclic compounds, $y_2 = 1$ gives bicyclic compounds, and $y_3 = 1$ gives monocyclic molecules. The constraint

$$y_1 + y_2 + y_3 = 1 \tag{3.2}$$

is used to limit that only one type of molecule can be generated. A new variable m is expressed in terms of the binary variables.

$$m - (y_1 - y_2) = 0 \tag{3.3}$$

whereas $m = +1, 0, -1$ indicate acyclic, monocyclic, and bicyclic structures, respectively.

The octet rule (Eq. (3.4)) is employed to ensure that the molecule has zero valence and the modified bonding rule (Eq. (3.5)) is used to ensure that two adjacent groups in a molecule are not linked by more than one bond. v_j stands for the valence of group j.

$$\sum_{j=1}^{N}(2 - v_j)\, n_j - 2m = 0 \tag{3.4}$$

$$n_j(v_j - 1) + 2\left(m - \sum_{i \in Sg} n_i\right) - \sum_{k=1}^{N} n_k \leq 0 \quad (\forall j = 1...N) \tag{3.5}$$

The following constraint ensures no more than one single-group solvent is generated.

$$\sum_{j \in Sg} n_j \leq 1 \tag{3.6}$$

The sixty structural groups and single-group solvents are listed in Table A1 in Appendix A. Group classes and ID numbers, abbreviation names of the subset groups are summarized in Table 3.1. For aromatic molecules, the number of aromatic groups (Ag) must be equal to 6 if the molecule is monocyclic or 10 if it is bicyclic. Eq. (3.8) provides the possibility to separately arrange the hydroxyl groups (i.e., not connected to the same group).

$$\sum_{j \in Ag} n_j = 6 y_3 + 10 y_2 \tag{3.7}$$

$$\sum_{j=1}^{N} n_j \geq 2n_{OH} \tag{3.8}$$

Table 3.1: Group classes, ID numbers, and abbreviation names of the subset groups

Group class	Group ID number	Abbreviation
Main groups	1-9	Mg
Double and triple bond groups	5-9	Dtbg
Aromatic groups	10-14, 16, 29, 36-39, 45	Ag
Non-chain-ending functional groups	6, 7, 8, 18, 21, 24, 25, 28, 33, 34, 41, 48	Nceg
Chain-ending functional groups	5, 9, 15, 17, 19, 20, 22, 23, 26, 27, 30, 31, 32, 35, 40, 42, 43, 44, 46, 47	Ceg
Single-group solvents	49-60	Sg

b) Chemical complexity

Considering the size and structural complexity of typical solvent molecules, the total number of groups making up a molecule is limited (Eq. (3.9)) and the maximum number of each group is also specified, as given in Eq. (3.10). The allowed maximum number of each group $n^{upp}(j)$ is listed in Table A1 in Appendix A, together with the group ID and valence.

$$n_{\min} \leq \sum_{j=1}^{N} n_j \leq n_{\max} \tag{3.9}$$

$$0 \leq n_j \leq n^{upp}(j), (j = 1, 2, \ldots N) \tag{3.10}$$

In addition, the total numbers of main groups and functional groups are also limited.

$$\sum_{j \in Mg} n_j \leq 2y_3 + n_{\max} y_1 \tag{3.11}$$

$$\sum_{j \in (Ceg \cup Nceg \cup Sg) \setminus Dtbg} \frac{n_j}{n_j^{upp}} \leq y_1 + y_3 \tag{3.12}$$

In aromatic molecules, the existence of ACCH, AC, and $ACCH_2$ groups is represented by the binary variables y_4, y_5, and y_6, respectively. y_7 is another binary variable that is active when both y_5 and y_3 are active.

$$n_{ACCH}/100 \leq y_4 \leq n_{ACCH} \tag{3.13}$$

$$n_{AC}/100 \leq y_5 \leq n_{AC} \tag{3.14}$$

$$n_{\text{ACCH2}}/100 \leq y_6 \leq n_{\text{ACCH2}} \tag{3.15}$$

$$100\, y_7 \geq y_3 + y_5 - 1 \tag{3.16}$$

$$100\, (y_7 - 1) - y_3 - y_5 + 2 \leq 0 \tag{3.17}$$

The AC group can appear up to once in monocyclic molecules and should appear twice in bicyclic molecules so that:

$$2y_2 + y_7 - n_{\text{AC}} = 0 \tag{3.18}$$

The complexity of designed molecules is reduced by allowing at most one AC, ACCH or ACCH$_2$ group to be active in monocyclic molecules by:

$$y_4 + y_6 + y_7 \leq 1 \tag{3.19}$$

The ACCH group must be connected with two side chains. One of them is limited to the CH$_3$ group.

$$y_4 \leq n_{\text{CH3}} \tag{3.20}$$

Other constraints used to reduce the complexity of the molecule include limitations on the total number of chain-ending and non-chain-ending functional groups:

$$\sum_{j \in Ceg} n_j \leq 3y_1 + y_4 + y_6 + y_7 \tag{3.21}$$

$$\sum_{j \in Nceg} n_j \leq 3y_1 + y_6 + y_7 \tag{3.22}$$

(3) Property constraints

a) Inertness to reaction

Two Diels-Alder reactions are studied in this dissertation. For such reactions, we assume that solvent molecules without double and triple bonds will not react with the reactants and products. Aromatic solvents are allowed because they normally do not take part in cycloaddition reactions.

$$\sum_{j \in Dtbg} n_j = 0 \tag{3.23}$$

b) Miscibility

Our experimental experiences suggest that for the investigated Diels-Alder reactions, except water, organic solvents generally would not cause phase splitting under the reaction condition. In order to avoid any immiscibility problem, water is excluded from the design space.

c) Melting point and boiling point

Melting and boiling point constraints are used to ensure that the generated solvents are liquid at room temperature. Taking into account the deviation in the employed group contribution methods, we specify an upper bound for T_m of 315 K and lower bound for T_b of 293 K.

$$\sum_{j=1}^{N} n_j t_{m,j} \leq \exp\left(\frac{T_m^{upp}}{T_{m0}}\right) \tag{3.24}$$

$$\sum_{j=1}^{N} n_j t_{b,j} \geq \exp\left(\frac{T_b^{low}}{T_{b0}}\right) \tag{3.25}$$

where T_m^{upp} = 315 K, T_b^{low} = 293 K, the constants T_{m0} = 147.450 K and T_{b0} = 222.543 K. The contributions of structural groups to the melting point ($t_{m,j}$) and boiling point ($t_{b,j}$) can be found in Marrero and Gani (2001).

3.2 Applications

The Diels-Alder (DA) reaction is widely used in organic synthesis for forming cyclic structures. One of the most interesting aspects of this reaction is its pronounced solvent dependence, which has received considerable attentions in the last few decades (Chiappe et al., 2010; Nobuoka et al., 2013; Cativiela et al., 1996; Ruiz-Lopez et al., 1993). In Section 3.2.1, the proposed method is applied to the optimal design of solvents to maximize the rate of a simple DA reaction. In order to verify the wide applicability of the design approach, in Section 3.2.2, the method is applied on a competitive DA reaction with the objective of maximizing the production of the desired product relative to that of the byproduct.

3.2.1 Simple Diels-Alder reaction

Blankenburg et al. (1974) systematically studied the effect of solvents on DA reactions between 1,3-cyclopentadiene and various dienophiles. In this work, the reaction between 1,3-cyclopentadiene and acrolein at 303 K (see Figure 3.4) is considered as the example reaction where 15 solvents with a wide variation of physical and chemical properties were experimentally investigated. Table 3.2 presents the six molecular descriptors of the 15 solvents and their corresponding experimental reaction rate constants, taken from Blankenburg et al. (1974).
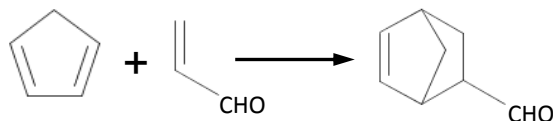

Figure 3.4: The DA reaction between 1,3-cyclopentadiene and acrolein producing
5-norbornane-2-carboxaldehyde

Table 3.2: The six descriptors of the 15 reaction solvents, together with their corresponding experimental reaction rate constants

Solvent	$\log k_{\mathrm{exp}}$	S_1	S_2	S_3	S_4	S_5	S_6
Acetic acid	−2.491	0.2805	0.5864	4.5564	1.9442	1.8717	0
Ethanol	−2.964	0.0135	0.6676	4.5887	2.3670	1.0127	0.1639
1-Propanol	−3.186	0.0163	0.6709	5.7535	3.2236	1.0294	0.1427
1-Butanol	−3.219	0.0122	0.6794	6.9118	4.0754	1.0128	0.1359
Methanol	−3.257	0.0190	0.7260	3.4825	1.3293	1.0064	0.1927
Chloroform	−3.383	0	0.8256	3.4240	7.5032	0	0
1,2-dichloroethane	−3.602	0	0.4368	4.7253	6.5480	0	0
Dimethylformamide	−3.640	0	0	8.0367	1.6913	1.7447	0.1161
Dichloromethane	−3.699	0	1.1114	2.8389	5.8986	0	0
Toluene	−3.745	0	0	7.1149	6.9400	0	0
Acetonitrile	−3.757	0	0.3018	4.5277	2.0646	1.3673	0
1,4-Dioxane	−3.827	0	0	8.2030	1.9772	1.8345	0.0311
Tetrachloromethane	−3.873	0	0	4.9773	8.4433	0	0
Acetone	−3.983	0	0	6.6600	1.9346	1.6555	0.0129
Ethyl acetate	−4.036	0	0	8.6090	2.9359	1.8029	0.0008

The following linear regression formula between the logarithm of the solvent-sensitive reaction rate constant and the six solvent descriptors is obtained:

$$\log k = -4.0113 + 4.7103\ S_1 + 0.3012\ S_2 + 0.0050\ S_3 + 0.0274\ S_4 - 0.0292\ S_5 + 3.1087\ S_6 \quad (3.26)$$

The MAPE between $\log k_{exp}$ and $\log k_{cal}$ is 2.58%. The evaluated coefficient of determination, R^2, is 0.9231. These two statistical indicators show that the six σ-profile area parameters are indeed good descriptors for quantifying the effect of solvents on reaction rates. For better demonstration, we compared the calculated $\log k_{\mathrm{cal}}$ values with the experimental $\log k_{\mathrm{exp}}$ values in Table 3.3. Despite some quantitative deviations, the regression model (Eq. (3.26)) can be used for solvent ranking with respect to reaction rates. The model predicts the same first five solvents as the top five experimentally ranked solvents, although the order is not exactly the same. These findings suggest that the regressed rate constant prediction model can be further used for solvent screening and molecular design.

Table 3.3: Experimental log k_{exp}, calculated log k_{cal} and associated solvent rankings of the 15
solvents used for the DA reaction (the unit of k is L/(mol×s))

Solvent	log k_{exp}	log k_{cal}	Predicted ranking
Acetic acid	−2.491	−2.492	1
Ethanol	−2.964	−3.179	3
1-Propanol	−3.186	−3.202	4
1-Butanol	−3.219	−3.210	5
Methanol	−3.257	−3.080	2
Chloroform	−3.383	−3.540	7
1,2-dichloroethane	−3.602	−3.677	9
Dimethylformamide	−3.640	−3.615	8
Dichloromethane	−3.699	−3.501	6
Toluene	−3.745	−3.786	11
Acetonitrile	−3.757	−3.881	13
1,4-Dioxane	−3.827	−3.873	12
Tetrachloromethane	−3.873	−3.755	10
Acetone	−3.983	−3.933	14
Ethyl acetate	−4.036	−3.938	15

Eq. (3.1) and Eq. (3.26) together allow for the prediction of the reaction rate constant for a given
solvent. Optimal solvents can be identified from the solution of an optimization-based CAMD
problem where the rate constant as the objective function is maximized. It is worth noting that in
Chapter 5 the reaction solvent will be simultaneously designed with the reactive process
including downstream separations. This integrated solvent and process design problem is very
computationally expensive. In order to simplify the problem, a reduced set of 15 common groups
(CH_3, CH_2, CH, C, OH, CH_3CO, CH_2CO, CHO, CH_3COO, CH_2COO, $HCOO$, OCH_3, OCH_2,
OCH, and $COOH$) selected from the full set of groups listed in Appendix A will be utilized. For
better comparing the results, the same group set is used in this section, which means in the
CAMD problem the total number of different groups N is 15. Due to the exclusion of cyclic
groups, only acyclic molecules can be designed. In this case, y_1 is 1 and all the other binary
variables are zero. The minimum and maximum number of groups making up a molecule n_{min}
and n_{max} are set to 2 and 5, respectively.

Under the above conditions, the optimization problem presented in Section 3.1.3 is simplified as follows.

$$\max_{n_j \,(j=1,\,2,\,...,\,N)} \{\log k\}$$

Subject to:

(1) Objective function calculation: Eq. (3.1) and Eq. (3.26)

(2) Structural constraints: Eq. $(3.3 - 3.5)$; Eq. $(3.9 - 3.12)$

(3) Property constraints: Eq. (3.24) and Eq. (3.25)

The solution of the above CAMD optimization problem is an optimal solvent structure having the highest reaction rate constant. Due to the convexity of the MILP problem, global optimality of the solution can be guaranteed. However, considering the model deviations, we generate a list of promising solvents by using the integer cut method instead of only presenting the very best one. Table 3.4 lists the top 10 solvents and their corresponding log k values. As indicated, carboxyl acids and alcohols are the most promising solvent types for accelerating the here investigated DA reaction. This is in good agreement with the reported kinetic solvent effects where acetic acid is found to be the best solvent and the second to the fifth solvents are all alcohols. The solvents listed in Table 3.4 are predicted to have higher rate constants than the best experimentally identified solvent acetic acid. They can be targeted for further experimental verifications.

Table 3.4: Predicted top 10 reaction solvents and their corresponding log k_{pred} values

Ranking	Group combination	Solvent	log k_{pred}
1	2 CH$_3$, 1 C, 1 OH, 1 COOH	(CH$_3$)$_2$C(OH)COOH	−1.875
2	3 CH$_2$, 1 OH, 1 COOH	OHCH$_2$CH$_2$CH$_2$COOH	−1.934
3	1 CH$_3$, 1 CH$_2$, 1 CH, 1 OH, 1 COOH	CH$_3$CH(OH)CH$_2$COOH	−1.942
4	2 CH$_2$, 1 OH, 1 COOH	OHCH$_2$CH$_2$COOH	−1.962
5	1 CH$_3$, 1 CH, 1 OH, 1 COOH	CH$_3$CH(OH)COOH	−1.971
6	1 CH$_2$, 1 OH, 1 COOH	OHCH$_2$COOH	−1.991
7	3 CH$_3$, 1 C, 1 COOH	(CH$_3$)$_3$CCOOH	−2.406
8	2 CH$_3$, 1 C, 1 CH$_3$CO, 1 COOH	CH$_3$COC(CH$_3$)$_2$COOH	−2.455
9	2 CH$_3$, 1 C, 1 HCOO, 1 COOH	HCOOC(CH$_3$)$_2$COOH	−2.462
10	1 CH$_3$, 3 CH$_2$, 1 COOH	CH$_3$(CH$_2$)$_3$COOH	−2.465

3.2.2 Complex Diels-Alder reaction

The CAMD method has been successfully applied to the optimal design of solvents for a simple DA reaction. However, it is well known that solvents can have very different effects on each single reaction in a multiple reaction system (Nobuoka et al., 2013; Dontsova et al., 2013; Selim et al., 2014). In this section, we investigate the applicability of the proposed method on a competitive DA reaction where optimal solvents are found to promote the main reaction while suppressing the side reaction. With this understanding, applications of the method to other complex reactions could be attainable.

Figure 3.5 shows the reaction scheme for the competitive DA reaction between methyl acrylate (A) and isoprene (B). C denotes the desirable product (methyl 4-methyl-3-cyclohexene-1-carboxylate) and D represents the byproduct (methyl 3-methyl-3-cyclohexene-1-carboxylate). Fourteen solvents with a broad range of physical and chemical properties were selected and kinetic experiments for the DA reaction were performed in the 14 solvents. Based on the experimental data, rate constants of the main and side reactions, k_1 and k_2, in each solvent were regressed. Appendix B gives more detailed information on the kinetic experiments and rate constant regression. Table 3.5 summarizes the six molecular descriptors of the 14 studied solvents and the corresponding experimental k_1 and k_2 values.
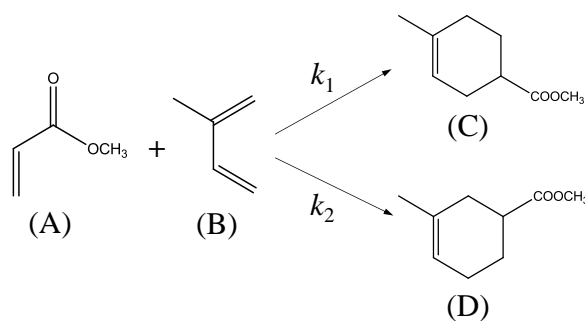
Figure 3.5: Reaction scheme of the competitive DA reaction

The rate constants of the two parallel reactions were correlated with the six solvent descriptors. The correlation models as well as the evaluated MAPE and R^2 values are given below.

$$k_1 = 0.1004 - 0.7797\, S_1 + 0.6274\, S_2 - 0.2831\, S_3 + 0.4533\, S_4 + 1.6771\, S_5 + 3.4491\, S_6 \qquad (3.27)$$

(MAPE = 0.0913, R^2 = 0.9573)

$$k_2 = 0.1984 - 0.6694\, S_1 + 0.0543\, S_2 - 0.1143\, S_3 + 0.1744\, S_4 + 0.6857\, S_5 + 1.5590\, S_6 \qquad (3.28)$$

(MAPE = 0.0921, R^2 = 0.9349)

Table 3.5: The six molecular descriptors of the 14 studied reaction solvents, together with the corresponding experimental rate constants of the two parallel DA reactions

Solvent	$k_{1,exp} \times 10^5$ /(L/(mol×s))	$k_{2,exp} \times 10^5$ /(L/(mol×s))	S_1	S_2	S_3	S_4	S_5	S_6
Hexane	0.845	0.414	0	0	8.3483	7.3412	0	0
Cyclohexane	1.086	0.527	0	0	6.9695	6.1789	0	0
Dibutylether	1.355	0.661	0	0	12.8398	7.1797	0.8779	0.0659
Butyl acetate	1.311	0.628	0	0.0018	11.7329	3.9766	1.6495	0
Toluene	1.444	0.694	0	0	7.1149	6.9400	0	0
Dioxane	1.699	0.803	0	0	8.2030	1.9772	1.8345	0.0311
Chlorobenzene	2.105	0.988	0	0.0296	5.7664	8.2986	0	0
DMF	2.245	1.046	0	0	8.0367	1.6913	1.7447	0.1161
Ethanol	2.152	0.917	0.0135	0.6676	4.5887	2.3670	1.0127	0.1639
Propanoic acid	2.922	1.191	0.2642	0.5932	5.5777	2.9083	1.7835	0
1-Butanol	2.865	1.252	0.0122	0.6794	6.9118	4.0754	1.0128	0.1359
Propylene carbonate	3.030	1.387	0	0.1298	7.4306	3.1351	2.1070	0
Trifluoroethanol	4.096	1.390	0.1811	0.9766	2.7081	6.2031	0.8103	0
DMSO	3.568	1.674	0	0.1822	7.3987	1.5409	1.2973	0.7474

For better evaluating the above solvent-sensitive rate constant correlations, we compare the calculated and experimental rate constants in Table 3.6. It is clear that despite some quantitative deviations, Eq. (3.27) and Eq. (3.28) generally yield reliable solvent performance rankings. In particular, Eq. (3.27) predicts exactly the same first five solvents as the top five experimentally ranked solvents for the main reaction. The same top three solvents are also predicted by Eq. (3.28) for the side reaction. These findings support the reliability of the two rate constant prediction models for further use in solvent molecular design.

Table 3.6: Experimental and calculated reaction rate constants, together with the predicted solvent performance rankings for the two parallel DA reactions

Solvent	$k_{1,exp} \times 10^5$ /(L/(mol×s))	$k_{1,cal} \times 10^5$ /(L/(mol×s))	Predicted ranking
Trifluoroethanol	4.096	3.976	1
DMSO	3.568	3.572	2
Propylene carbonate	3.030	3.033	3
Propanoic acid	2.922	2.997	4
1-Butanol	2.865	2.575	5
DMF	2.245	1.919	8
Ethanol	2.152	2.547	6
Chlorobenzene	2.105	2.249	7
Dioxane	1.699	1.859	9
Toluene	1.444	1.232	12
Dibutylether	1.355	1.420	10
Butyl acetate	1.311	1.349	11
Cyclohexane	1.086	0.929	14
Hexane	0.845	1.065	13

Solvent	$k_{2,exp} \times 10^5$ /(L/(mol×s))	$k_{2,cal} \times 10^5$ /(L/(mol×s))	Predicted ranking
DMSO	1.674	1.686	1
Trifluoroethanol	1.390	1.458	2
Propylene carbonate	1.387	1.347	3
1-Butanol	1.252	1.054	6
Propanoic acid	1.191	1.146	4
DMF	1.046	0.952	8
Chlorobenzene	0.988	0.988	7
Ethanol	0.917	1.064	5
Dioxane	0.803	0.912	9
Toluene	0.694	0.595	12
Dibutylether	0.661	0.687	10
Butyl acetate	0.628	0.681	11
Cyclohexane	0.527	0.479	14
Hexane	0.414	0.524	13

It is obvious that the two reactions show some similarities on their solvent dependences. Nevertheless, we can still find from Eq. (3.27) and Eq. (3.28) that the six solvent descriptors contribute differently to k_1 and k_2. This gives us the opportunity to design certain solvents to provide a maximum concentration of the desired product C relative to that of the byproduct D. In this case study, we choose to maximize the concentration gap between C and D after a moderate reaction time in an ideal batch reactor. All the groups listed in Table A1 in Appendix A are considered as candidate groups for generating solvent molecules, which means N is 60. The minimum and maximum number of groups making up a molecule, $n_{\min}$ and $n_{\max}$, are set to 1 and 7, respectively. The CAMD optimization problem is outlined as follows.

$$\max_{n_j\,(j=1,\,2,\,...,\,N)} \{C_C - C_D\}$$

Subject to:

(1) Objective function calculation

   a) Rate constant correlation models: Eq. (3.27) and Eq. (3.28)

   b) COSMO-GC models: Eq. (3.1)

   c) Determination of product concentrations:

$$\frac{dC_C}{dt} = k_1 C_A C_B \tag{3.29}$$

$$\frac{dC_D}{dt} = k_2 C_A C_B \tag{3.30}$$

$$C_A = C_{A0} - C_C - C_D \tag{3.31}$$

   The initial conditions at $t = 0$ s are $C_{A0} = C_{B0} = 1$ mol/L and $C_{C0} = C_{D0} = 0$ mol/L. The final product concentrations C_C and C_D are determined at $t = 10^5$ s.

(2) Structural constraints: Eq. (3.2 − 3.22)

(3) Property constraints: Eq. (3.23 − 3.25)

The above MINLP-based solvent design problem was solved by the SBB solver (Brooke et al., 1998) in the GAMS modelling environment (Rosenthal, 2006). Due to the non-convexity of the problem, we cannot guarantee that the resulting solvent represents the global optimum. However, many different initializations were used to increase the likelihood of finding the very best solution. Considering possible experimental errors and model deviations, instead of only presenting the very best solvent, we generate a list of top ranked solvents by using the integer cut method. The top 10 solvents and their corresponding rate constant and objective function values are presented in Table 3.7. Large structural similarities among the solvent molecules can be

found. Specifically, the top three solvents are all aromatics with $-NH_2$ and $-CH_2CF_3$ substituent groups on the aromatic ring. The remaining seven solvents are all saturated halogenated hydrocarbons containing two $-CF_3$ groups.

In order to better demonstrate the solvent design results, we calculated ($C_C - C_D$) values for all the experimentally investigated solvents. The best one we found is trifluoroethanol and its ($C_C - C_D$) value is 0.3914 mol/L. From this perspective, about 10.9% improvement in the reaction performance can be achieved via the optimal design of reaction solvents.

Table 3.7: The top 10 solvents identified for the competitive DA reaction, together with the calculated reaction rate constant and objective function values

Ranking	Solvent structure	$k_{1,cal} \times 10^5$ /(L/(mol×s))	$k_{2,cal} \times 10^5$ /(L/(mol×s))	$C_C - C_D$ /(mol/L)
1	3 ACH, 1 ACCH$_3$, 1 ACCH$_2$, 1 ACNH$_2$, 1 CF$_3$	4.382	1.426	0.4342
2	3 ACH, 1 ACCH$_2$, 1 ACNH$_2$, 1 ACF, 1 CF$_3$	4.689	1.551	0.4335
3	4 ACH, 1 ACCH$_2$, 1 ACNH$_2$, 1 CF$_3$	4.441	1.457	0.4325
4	2 CH$_3$, 1 CH$_2$, 2 CH, 2 CF$_3$	4.540	1.549	0.4220
5	1 CH$_3$, 3 CH$_2$, 1 CH, 2 CF$_3$	4.436	1.511	0.4211
6	3 CH$_3$, 1 CH, 1 C, 2 CF$_3$	4.439	1.514	0.4207
7	5 CH$_2$, 2 CF$_3$	4.333	1.474	0.4201
8	2 CH$_3$, 2 CH, 2 CF$_3$	4.426	1.512	0.4199
9	2 CH$_3$, 2 CH$_2$, 1 C, 2 CF$_3$	4.335	1.476	0.4197
10	1 CH$_3$, 2 CH$_2$, 1 CH, 2 CF$_3$	4.322	1.475	0.4189

3.3 Summary and outlook

This chapter introduces a CAMD method for the optimal design of solvents to maximize reaction rates or rate-related reaction properties. The method has been successfully applied to two case studies. The first designs solvents to maximize the rate of a simple DA reaction. The second case study considers a competitive DA reaction with the objective of maximizing the production of the desired product relative to that of the byproduct.

Because the latest COSMO database already covers σ-profiles of several hundred common solvents, one can easily obtain the six descriptors of these solvents. Therefore, the parameterized rate constant prediction models can be directly used for the fast screening of solvents based on extensive model predictions on the common solvents using the six descriptors. Unlike solvent

screening whose aim is to identify the best solvent from a given set of candidates, solvent molecular design can lead to unconventional but outstanding solvent structures. From this perspective, the proposed method can be a valuable tool for finding new promising solvents.

The introduced solvent descriptors have been proven to be very good parameters for quantifying solvent effects on reaction kinetics. Due to their molecule-specific nature, these descriptors in theory can be used to correlate various solvent properties, effects, or behaviors, which make the proposed CAMD method extendable to other solvent design problems.

Finally, it should be noted that since the solvent-sensitive rate constant prediction model is parameterized from limited experimental data, large uncertainties can be associated with the obtained model parameters. This dissertation only shows our work on deterministic solvent design where the parameter uncertainties are not considered. We have also proposed a robust solvent design framework in Zhou et al. (2015b) which incorporates the parameter uncertainties into the CAMD formulation. It was found that for the same reaction, the top solvents obtained from the robust solvent design are very similar to those identified by the deterministic design. This finding demonstrates the reliability of the design method in the presence of model uncertainties.

4. Optimal design of solvents to improve reaction equilibrium conversions

The previous chapter proposes a CAMD method for the optimal design of solvents to accelerate reaction rates. However, as outlined in Section 2.1.2, besides kinetic effects, solvents as reaction media can also change the chemical equilibrium of the reaction. Abildskov et al. (2013) proposed a method to help select solvents to improve equilibrium conversion of liquid phase reactions. The limitation of this method is that the effect of solvents on phase separations is not considered, which has been proven to be another significant factor on enhancing product yields due to the selective extraction of products into a separate phase (Samant and Ng, 1998; Wang and Achenie, 2002). In recent decades, coupled reaction and separation operations have shown significant benefits, with reactive distillation being one of the most significant examples. Another important integrated process is extractive reaction where a solvent is added to the reaction mixture to selectively extract products into a separate phase. This strategy can break the chemical equilibrium limitation and thus allows for higher product yields. Samant and Ng (1998) developed a systematic method to design extractive reaction processes. Despite these insights into process development, the large effect of solvents has not yet been studied.

To date, there is little work done on the optimal design of solvents to improve equilibrium conversion of liquid phase reactions via the extractive reaction strategy. One of the key hurdles is the lack of a reliable and fast numerical method to simultaneously determine chemical and phase equilibrium. Recently, a rate-based dynamic method has been proposed and applied to solve chemical equilibrium (Zinser et al., 2016) and multicomponent fluid phase equilibrium (Zinser et al., 2016; Steyer et al., 2005; Ye, 2014) problems. This method has been proven to be reliable, easily implementable, and computationally efficient. In this chapter, the method is extended to solve the combined chemical and phase equilibria of liquid phase reactions. Due to the difficulty in satisfying the liquid-liquid equilibrium (LLE) condition within an optimization environment, this condition is often solved externally from the optimization problem. Therefore, the CAMD of solvents for extractive reaction cannot be formulated as a conventional mixed-integer program and solved deterministically. However, it can be solved stochastically using a stochastic algorithm, such as the genetic algorithm (GA). The GA (Affenzeller et al., 2009) has been proven to be very efficient in solving problems with large combinatorial and/or discontinuous search spaces, such as complex molecular design (Venkatasubramanian et al., 1994; Nachbar, 2000; Xu and Diwekar, 2005; Herring and Eden, 2015). In this chapter, a GA-based CAMD methodology is developed to determine optimal solvents for liquid phase reactions where the equilibrium conversion determined by the rate-based dynamic method is maximized.

In the following sections, the design task is first proposed and the solution strategy is concisely outlined. After a brief review of the conventional methods for calculating thermodynamic equilibrium, the rate-based dynamic method for simultaneous determination of the chemical and

phase equilibrium is introduced. Finally, the GA-based solvent design methodology is proposed and applied to design solvents for a selected esterification reaction.

4.1 Problem statement and solution strategy

The significance of optimal selection of solvents for improving reaction equilibrium conversion has been demonstrated on the hypothetical A ↔ B reaction in Figure 2.2. Now a more common A + B ↔ C + D reaction is considered. The schematic diagram of using the extractive reaction strategy to enhance the product yield is shown in Figure 4.1. The design problem is described as: *Given a liquid reaction mixture composed of a known amount of reactants A and B under a specified temperature and pressure, determine which solvent and by which amount it should be added to the mixture in order to achieve a maximum equilibrium conversion of the reaction.*
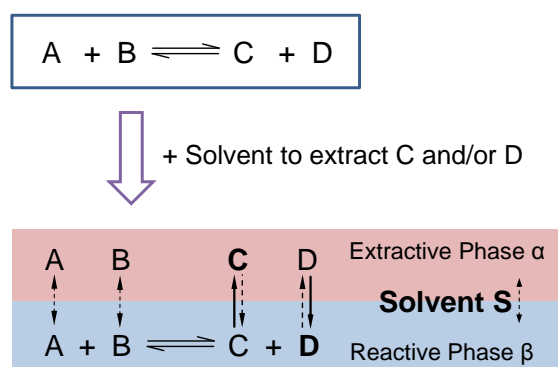

Figure 4.1: Schematic diagram of a solvent-aided extractive reaction

The design task is inherently an optimization problem whose solution strategy is depicted in Figure 4.2. For a given solvent structure and composition, the rate-based dynamic method is used to calculate the combined chemical and liquid-liquid phase equilibrium, through which the thermodynamic equilibrium state and the corresponding equilibrium conversion of the reaction are determined. The GA-based CAMD method is then used to optimize the solvent structure and composition for achieving a maximum reaction equilibrium conversion. The rate-based dynamic method and GA-based CAMD method are introduced in Sections 4.2 and 4.3, respectively. In Section 4.4, the solution strategy is applied to design solvents for an esterification reaction.
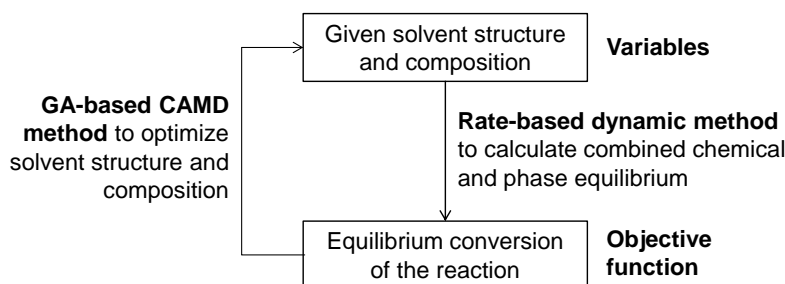

Figure 4.2: Solution strategy for the addressed solvent design problem

4.2 Chemical and phase equilibrium calculation

4.2.1 Conventional methods

The calculation of multicomponent phase equilibrium is a challenging task, especially for systems containing more than one liquid phase. Methods for solving liquid-liquid equilibrium are classified into two major categories, global and local methods. The necessary and sufficient condition for a multiphasic nonreactive or reactive system to achieve thermodynamic equilibrium under fixed temperature and pressure is that the total Gibbs free energy of the system is at the global minimum. Based on this consideration, global methods formulate and solve chemical and phase equilibrium problems by minimizing the total Gibbs free energy (McDonald and Floudas, 1997; Wasylkiewicz and Ung, 2000). The major limitation of global methods is that due to the large non-convexity and nonlinearity of thermodynamic models, the global minimization of the Gibbs free energy is computationally expensive. On the other hand, local methods (e.g., Pham and Doherty, 1990) formulate the equilibrium problem as a set of nonlinear equations based on the requirement that the chemical potentials of all components are equal in all phases. This set of nonlinear equations is normally solved using Newton or Quasi-Newton methods. Although the solution procedure is direct and computationally inexpensive, its convergence to a feasible solution relies heavily on good initial estimates. Often the calculation converges to trivial solutions (see e.g., Michelsen, 1982; Green et al., 1993).

Additionally, hybrid methods combining the certainty of global methods and the efficiency of local methods have been developed (Müller and Marquardt, 1997; Bausa and Marquardt, 2000). The state-of-the-art hybrid method for determining liquid-liquid phase equilibrium is the approach proposed in Bausa and Marquardt (2000). The idea behind this method is to provide good initial estimates using a homotopy continuation algorithm, which significantly reduces the calculation complexity. Although this method has been proven to be reliable and faster than previous approaches, it is unclear how it can be used in combined chemical and phase equilibrium calculations. This is the motivation for developing a new and efficient method that is able to accomplish such a task.

4.2.2 Rate-based dynamic methods

The idea of using a rate-based dynamic method to determine liquid-liquid phase equilibrium is first introduced in Steyer et al. (2005). Using four example cases, the method was proven to be highly reliable and faster than Bausa and Marquardt (2000)'s method by an average factor of more than two. Recently, the method has been generalized and applied to solve chemical equilibrium and fluid phase equilibrium problems (Ye, 2014; Zinser et al., 2016).

Solving chemical and phase equilibria via the rate-based dynamic method is based on the simulation of the dynamic evolution of a mixture from a randomly initialized, non-equilibrium composition towards the final equilibrium composition. The change of phase compositions is the

result of chemical reactions inside the phases and mass transfers between phases. Phase specific reactions are driven by the Gibbs free energy difference of reactants and products, and the mass transfer between phases is driven by component chemical potential differences. Based on these considerations, the evolution of phase compositions can be formulated as a set of ordinary differential equations (ODEs). The thermodynamic equilibrium of a system is finally attained when all driving forces become zero (i.e., all the ODEs reach steady states). Compared to conventional equilibrium calculation methods, the dynamic method is less dependent on initial estimates and not limited by problem size (Ye, 2014). In this work, the dynamic method is extended to calculate the combined chemical and phase equilibria of complex liquid systems.

Despite the much lower dependency of the dynamic method on initial estimates, a good initial condition is still preferable for an efficient thermodynamic equilibrium calculation. Steyer et al. (2005) recommend a starting point for the liquid-liquid phase equilibrium calculation where the initial two liquids have significantly different compositions. For binary mixtures, one can simply initialize the two liquids as pure compounds. However, it is not clear how to initialize phase compositions for multicomponent mixtures, such as the system studied here. Bausa and Marquardt (2000) use the homotopy continuation method to find solutions to difficult multicomponent phase equilibrium problems by starting at solving a simple binary mixing problem. Inspired by their work, two liquid phases (phase I and phase II) are initialized with the two compounds having the largest difference in polarity and all the other components are placed into a virtual environment, phase E (see Figure 4.3). The components are continuously transferred from phase E to phase I or phase II, depending on the sizes of component activities in the two phases. The thermodynamic equilibrium state of the system is finally obtained when no compound is left in phase E, reaction equilibria in phase I and phase II are attained, and phase equilibrium between the two phases is reached.
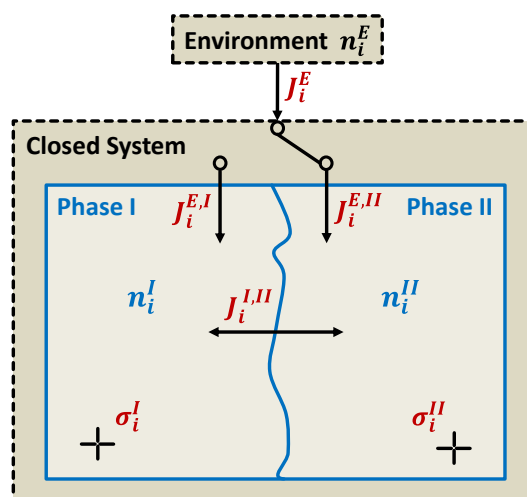

Figure 4.3: Schematic diagram on the modeling and simulation of the thermodynamic (chemical and phase) equilibrium of liquid reaction mixtures using the rate-based dynamic method

The mass transfer from phase E to the closed system containing phases I and II is:

$$J_i^E = \begin{cases} const & if \ n_i^E > \varepsilon \\ 0 & if \ n_i^E \leq \varepsilon \end{cases} \quad (i = A, B, C, D, S)$$

where *const* is a fixed mass transfer rate, *A* and *B* represent the reactants, *C* and *D* denote the products, *S* stands for the solvent (see Figure 4.1).

The mass transfer rate between phase I and phase II:

$$J_i^{I,II} = k_{trans} \left(x_i^I \gamma_i^I - x_i^{II} \gamma_i^{II} \right)$$

Reaction rates in phase I and phase II:

$$r^P = k_{reac} \left[\left(x_A^P \gamma_A^P \right)\left(x_B^P \gamma_B^P \right) - \frac{1}{K(T)} \left(x_C^P \gamma_C^P \right)\left(x_D^P \gamma_D^P \right) \right] \quad where \ P \in \{I, II\}$$

The equilibrium state does not depend on the sizes of the mass transfer rate constant k_{trans} and reaction rate constant k_{reac}. In principle, they can be set to any arbitrary positive values.

The sources/sinks of components:

$$\sigma_A^P = \sigma_B^P = -r^P, \ \sigma_C^P = \sigma_D^P = r^P, \ \sigma_S^P = 0$$

Finally, component mass balances in all the phases are given by the following ODEs:

$$\frac{dn_i^E}{dt} = -J_i^E$$

$$\frac{dn_i^I}{dt} = y_i J_i^E - J_i^{I,II} + \sigma_i^I$$

$$\frac{dn_i^{II}}{dt} = (1 - y_i) J_i^E + J_i^{I,II} + \sigma_i^{II}$$

where $y_i = \begin{cases} 0 & if \ \left(x_i^I \gamma_i^I - x_i^{II} \gamma_i^{II} \right) \geq 0 \\ 1 & if \ \left(x_i^I \gamma_i^I - x_i^{II} \gamma_i^{II} \right) < 0 \end{cases}$

The dynamic simulation is performed along the discretized time until all the ODEs reach steady states. It is at this point that the reaction equilibrium conversion can be determined.

It is worth noting that when using the rate-based dynamic method to calculate chemical and phase equilibria, homogeneous liquid reactions are simply a special case of heterogeneous liquid reactions where the finally obtained liquid phases (phases I and II) have the same composition. From this perspective, the method can be used to determine the combined chemical and liquid-liquid phase equilibrium for reactions where the number of phases present at equilibrium is unknown *a priori*.

4.3 GA-based solvent design

Starting from the first generation consisting of a population of randomly initialized potential solutions (individuals), the GA repeatedly modifies individual solutions by means of selection and variation. At each step, the GA randomly selects individuals from the current generation as parents to produce offspring (new individuals) for the next generation according to certain genetic variation rules. The probability of an individual to be selected as a parent is proportional to its fitness value, a non-negative measure of the individual's performance. Over a number of successive generations, the most promising individuals accumulate in the evolution and the best individual in a generation converges towards the optimal solution.

To implement the GA into a CAMD work, one needs to specify a suitable molecular encoding method, a fitness function that assigns merit to each encoded molecule-individual, a selection rule that favors the selection of fitter individuals as parents, genetic operators for producing new individuals, and finally a stopping criterion to terminate the GA computation.

4.3.1 Molecular encoding

In order to use the GA for molecular design, molecular structures must be expressed in a readable and operable form. This procedure is known as the molecular encoding. A good encoding method must facilitate the generation of new individuals via genetic operations and meanwhile favor the decoding procedure where individual fitness is evaluated. Venkatasubramanian et al. (1994) represent chemical structures as a string of symbols. By pre-defining two-valence groups as main chain building blocks and one-valence groups as side chain building blocks, the GA was successfully employed to design acyclic polymers with simple side chain structures. Later, Xu and Diwekar (2005) represent molecules as N-element vectors where N is the pre-defined maximum number of allowable building groups. Each element in the vector contains a group ID number representing a group or is set to zero when no group is present. This molecular encoding method is very simple and straightforward. However, it cannot guarantee the generation of structurally feasible molecules. Nachbar (2000) proposed another encoding method where atoms instead of structural groups are treated as the basic elements in molecular graphs. The hierarchical chemical topology is then represented by an adjacent matrix of atoms, facilitating the detailed representation of molecular structures. However, it makes the decoding procedure very complicated for some design problems.

This work proposes a new molecular encoding method where solvent molecules are represented as tree structures stored in the form of a dynamic list with UNIFAC groups (Fredenslund et al., 1977) as the tree nodes (building blocks). In computer science, a dynamic list (also known as linked list) is a data structure consisting of a group of nodes which together represent a sequence. It provides users much convenience in storing, reading, and manipulating data. In tree structures, nodes can be easily deleted, inserted, and modified using the dynamic list to store data.

Considering the dynamic tree structure of a molecule, each group node is a structural array with several fields (see Figure 4.4). The first two fields provide information on group identity and valence. The last two fields contain structural information of the molecular tree. "Size" denotes the size of the sub-tree, i.e., the number of group nodes in the sub-tree. "*Child" is the pointer that indicates the location of connected child nodes. The number of allowable child nodes for a group node depends on the valence of the group, e.g., the number of child nodes is two for three-valence groups and one for two-valence groups. For root and leaf nodes, only one-valence groups can be selected. Additionally, the number of child nodes is limited to one for root nodes and no child node is allowed for leaf nodes. The characteristics of the proposed dynamic tree structure always guarantee structurally feasible solvent molecules. Figure 4.5 exemplifies the molecular representation and encoding method using diisopropyl ether as an example.
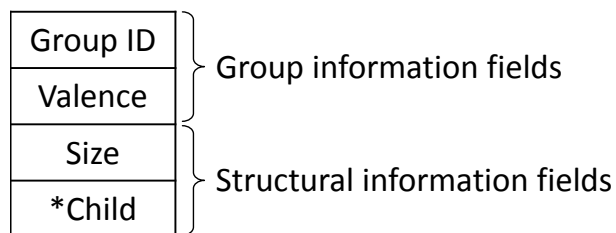

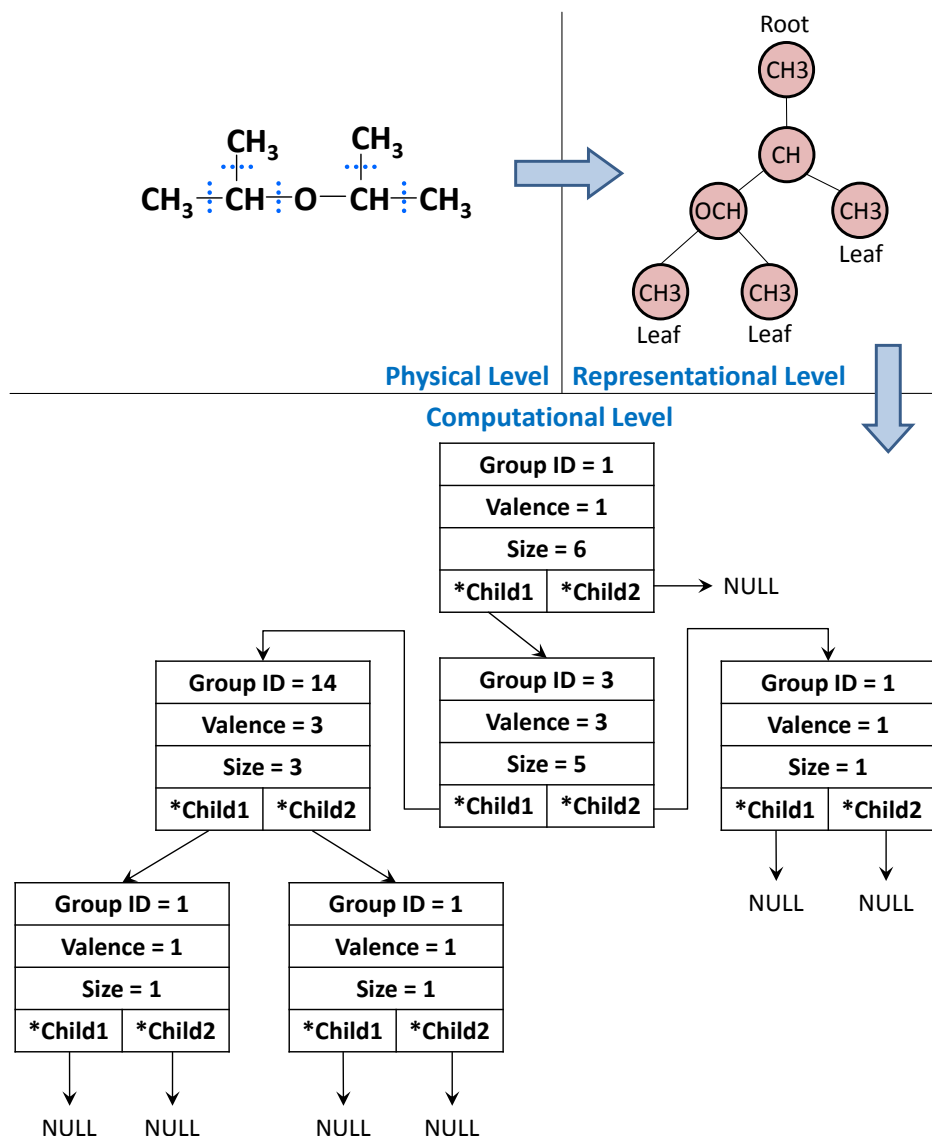**Figure 4.4:** Structure of a group node in the molecular tree

Figure 4.5: The dynamic tree structure of diisopropyl ether (Each group is assigned with an ID number. Here, ID = 1, 3, and 14 represent CH_3, CH, and OCH, respectively)

It has been demonstrated in Figure 2.2, Section 2.1.2 that apart from the type of solvent, the initial composition of the solvent is the other degree of freedom to define the equilibrium conversion of a liquid phase reaction. Therefore, the initial solvent composition should also be optimized. In the GA, continuous variables are normally represented by binary arrays and as such, the initial molar composition of the solvent is encoded as the binary array $b[k]$. The precision is determined by the length of the array string, k, with longer arrays ensuring higher precision, however, at the expense of computational effort. The following equation is used to decode the binary array into the solvent composition.

$$x_S = x_{S,\min} + \frac{x_{S,\max} - x_{S,\min}}{\sum\limits_{m=1}^{k} 2^{m-1}} \left(\sum_{m=1}^{k} 2^{m-1} \cdot b[m] \right)$$

where $x_{s,\min}$ and $x_{s,\max}$ are the lower and upper bounds of the solvent composition in mole fractions, set to 0.2 and 0.8, respectively. In this work, k is set equal to six in order to maintain a good balance between the result accuracy and computational cost.

4.3.2   Fitness function and fitness proportionate selection

In the GA, each individual solution is evaluated and assigned with a fitness value. The fitness function is a measure of merit that tells how desirable a candidate solution is. Normally, two terms are included in the fitness function: the first term is some type of objective value and the second is a measure of constraint violation. This measure of constraint violation is most efficiently handled by using penalty functions (Michalewicz and Schoenauer, 1996). Penalties are assigned to those design solutions which violate the defined constraints with the penalty size being proportional to the magnitude of the violation. The fitness function is then expressed as either a summation or product of the objective and penalty functions. The product form is employed in this work.

$$F = obj \times \prod_{i \in nc} Pen_i$$

where *obj* represents the objective function (reaction equilibrium conversion), Pen_i denotes the penalty function of the *i*-th constraint whose value is between 0 and 1, and *F* is the fitness value.

In the GA, new generations are successively produced from the current generation. A standard reproduction process usually consists of two steps: selecting individuals as parents from the current generation and generating new individuals for the next generation from genetic operations performed on the selected parents. In order to mimic the natural selection process, prominent individuals should have high probabilities to be selected as parents. The most popular and widely employed selection rule is "fitness proportionate selection" also known as "roulette wheel selection" (Holland, 1975). Using this rule, the selection of parents is random, but the probability of an individual being selected is proportional to its fitness value.

4.3.3   Genetic operations

New individuals are created from the selected parents of the last generation using modifications known as genetic operations. Analogous to the natural reproduction process, two genetic operators, mutation and crossover, are traditionally used for reproducing individuals in the GA. By definition, mutation creates new individuals by introducing random variations in certain genes of the parents. Crossover creates new individuals by randomly exchanging some genetic information between selected parents. Figure 4.6 illustrates the mutation and crossover

operations on binary arrays. These genetic operators are sufficient for binary coding. However, for manipulating molecular structures, one should include two more operators: insertion and deletion. These two operators are essential for generating molecules with different sizes (number of group nodes).
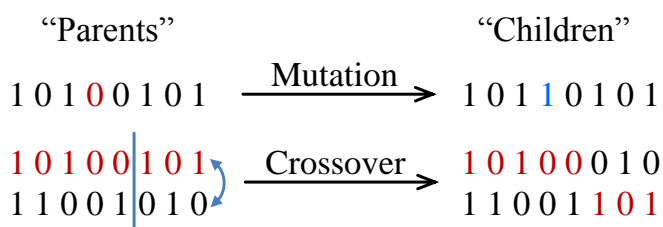
"Parents"   "Children"

1 0 1 0 0 1 0 1 $\xrightarrow{\text{Mutation}}$ 1 0 1 1 0 1 0 1

1 0 1 0 0 1 0 1
1 1 0 0 1 0 1 0 $\xrightarrow{\text{Crossover}}$ 1 0 1 0 0 0 1 0
1 1 0 0 1 1 0 1

Figure 4.6: Mutation and crossover operations on binary arrays

The handling of genetic operations for molecular design is very simple and straightforward using the dynamic tree structure. The four genetic operations applied on solvent molecular trees are depicted in Figure 4.7. Each operation is based on randomly choosing group nodes in the molecular tree and groups from the group set having a defined valence. In mutation, a group is only allowed to mutate with another group having the same valence. Crossover is performed by randomly choosing two non-leaf group nodes (one in each molecular tree) and exchanging their "*Child" pointer addresses. In insertion, only groups with a valence larger than one are allowed to be inserted. The insertion of two-valence groups is simple and straightforward. However, in order to maintain a feasible chemical structure, the insertion of three or four-valence groups must be accompanied by including one or two additional one-valence groups, respectively. Similar to insertion, only groups with a valence larger than one can be deleted. When deleting a three or a four-valence group one should respectively delete one or two additional one-valence groups in the molecular tree. If the deleted group node has more than one child node, the right-hand branch of the node is grafted to its left-hand branch. By following these genetic operation rules, structural feasibility of newly generated molecule is preserved.
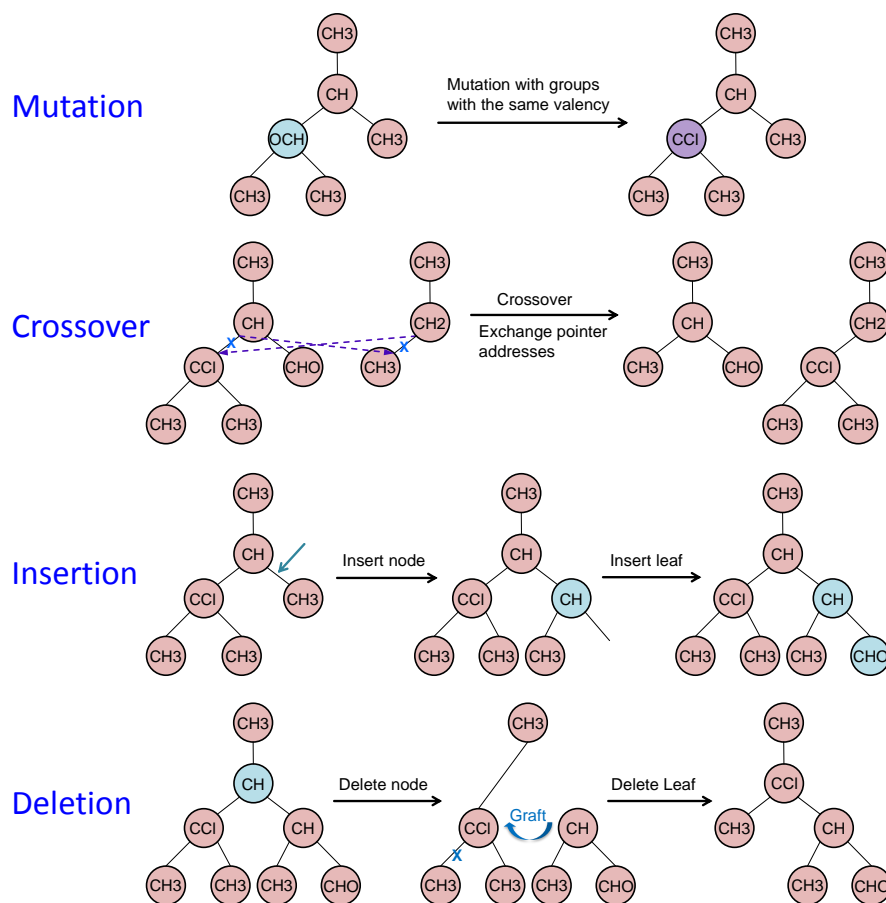
Figure 4.7: Genetic operations applied on solvent molecular trees

It is worth noting that each genetic operation is performed with a pre-defined probability. In other words, parents can remain unchanged even when they are selected for reproduction. Additionally, according to the *elitism* rule, a small fraction of top solutions from the current generation are carried over directly to the next generation without any modification. This strategy ensures that the best solution in a generation does not worsen from one generation to the next.

4.3.4 Stopping criterion

The best solution in a generation improves or remains unchanged as the generation number increases. In order to obtain a high-quality result in a reasonable computational time, a stopping criterion needs to be defined in advance. The GA calculation is then terminated when the criterion is satisfied. To set a maximum number of generations is a widely employed stopping criterion in GAs.

4.3.5 Solution framework

The overall solvent design framework is shown in Figure 4.8. The main steps are summarized as follows.

1. To start the program, first set the parameters for the genetic algorithm and specify a set of structural groups from which solvent molecules are generated.

2. Randomly initialize the first-generation individuals: this includes solvent molecules encoded using dynamic tree structures and initial solvent compositions using binary arrays.

3. Solvent physical properties are then evaluated via QSPR or GC models and the equilibrium conversion is determined by the rate-based dynamic method. The property estimation and reaction conversion calculation are performed on all the individuals in the generation.

4. Determine the fitness value of each individual in the generation.

5. The calculation is terminated if the stopping criterion is met. The optimal solvent structure and composition are obtained. If the criterion is not satisfied, go to Step 6.

6. Select parents from the current generation based on the fitness proportionate selection rule.

7. Create offspring for the next generation by performing genetic operations on the molecular tree and on the binary array of the selected parents.
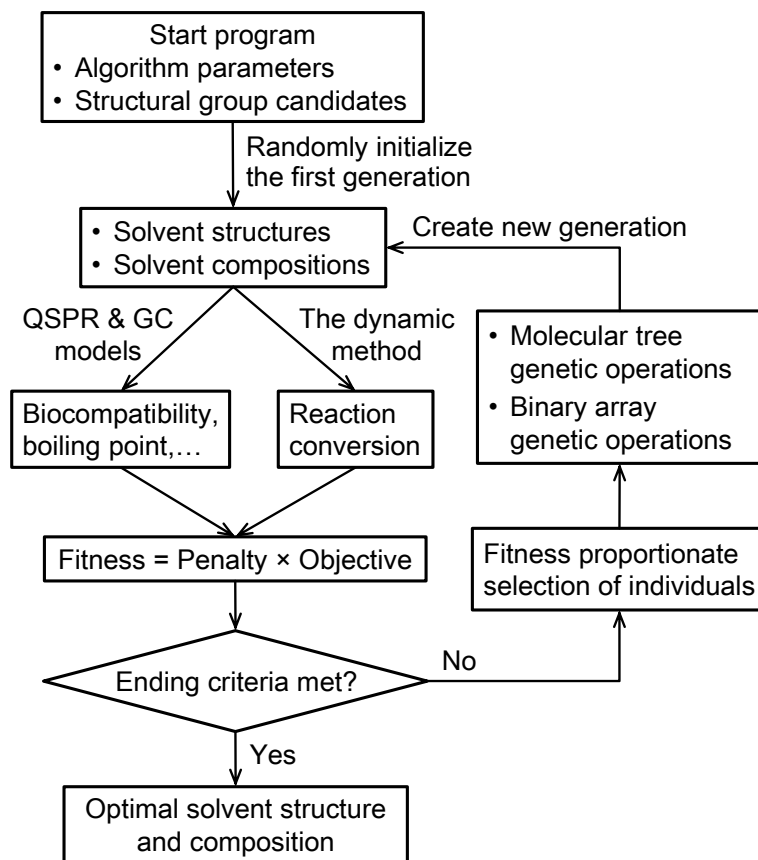

Figure 4.8: The overall solvent design framework

4.4   Application on an esterification reaction

The proposed methodology is applied to design solvents for an esterification reaction. The reaction scheme with abbreviations for each compound is given in Figure 4.9. This reaction is a good example because the large effect of solvents on the reaction equilibrium is well recognized (Voutsas et al., 2002).
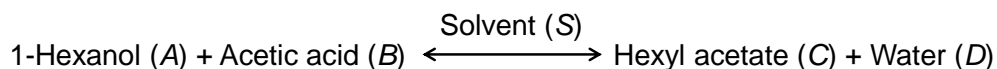
$$\text{1-Hexanol } (A) + \text{Acetic acid } (B) \xleftrightarrow{\text{Solvent } (S)} \text{Hexyl acetate } (C) + \text{Water } (D)$$

Figure 4.9: The reaction scheme with abbreviations for each compound

4.4.1   Initializations and parameter specifications

The total amount of the mixture is set to one mole. The initial molar composition of solvent x_S is a design variable to be optimized along with the solvent structure. A 50% reaction conversion is assumed before the simulation (see the "rate-based dynamic methods" section) starts, thus the initial compositions of all the reactants and products are set to $(1-x_S)/4$. This assumption facilitates the initialization of the system and importantly, it does not affect the final equilibrium state. The thermodynamic equilibrium constant K calculated from the standard molar Gibbs free energy of formation for all the reactants and products given in Voutsas et al. (2002) is 50.84. *const* is set to 0.1 mol/s and ε is 10^{-5} mol. k_{reac} is set to 50 with k_{trans} set to 0.5.

(Phase I)   (Phase II)

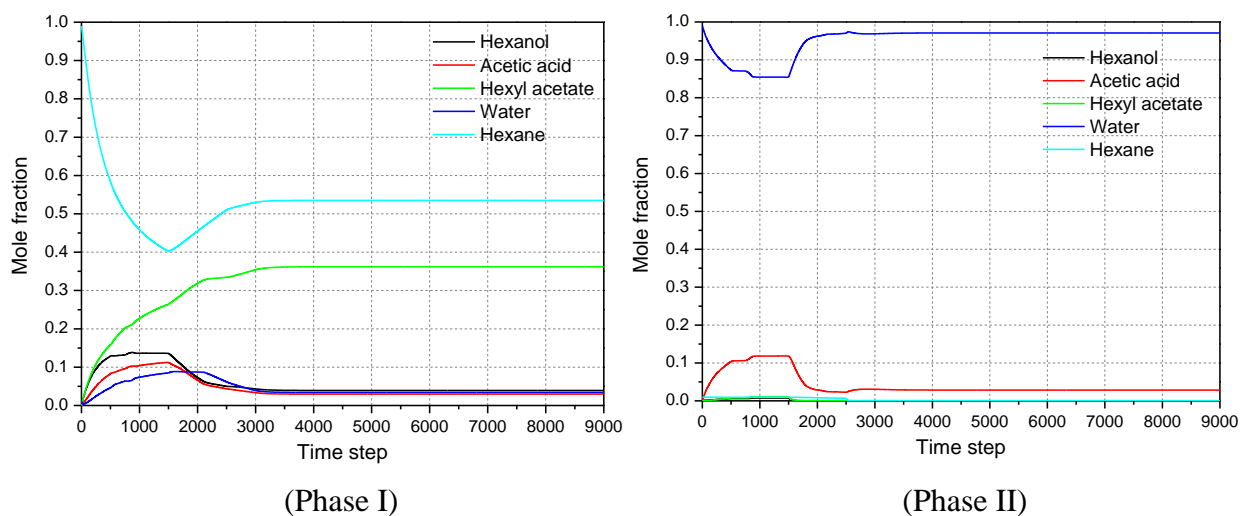**Figure 4.10:** The evolution of component molar compositions in phase I and phase II determined by the rate-based dynamic method

The reliability and efficiency of the rate-based dynamic method in determining combined chemical and phase equilibria are demonstrated with the esterification reaction where hexane is fixed as the solvent and its initial molar composition is set to 0.4. Phases I and II (see Figure 4.3)

are initialized as pure hexane and water, respectively, with all the other compounds placed into phase E. The evolution of component molar compositions in phase I and phase II is shown in Figure 4.10. The compositions in both phases change frequently in the beginning due to the occurrence of chemical reactions and large driving forces for the mass transfer between phases I and II. Afterwards, the system approaches the equilibrium state. The total CPU time for this computation is about 2.0 seconds.

Notably, the final equilibrium state can have one or two liquid phases, depending on which solvent and by which amount it is added to the reaction mixture. Nevertheless, both cases are acceptable and can be appropriately predicted by using the rate-based dynamic method. In other words, even though the benefit of introducing a second phase to extract the products is obvious, we have not set phase splitting as a necessary condition for solvent design. Instead, those solvents that do not result in a second liquid-phase have also been evaluated, although they may show lower equilibrium conversions when compared to those that lead to phase splitting.

With a reliable method to determine the equilibrium conversion of the esterification reaction, solvent structures and initial compositions can now be optimized via the GA-based CAMD method to maximize the equilibrium conversion. As described in Figure 4.8, to start the GA-based solvent design program, the values of algorithm parameters need to be assigned. The selection of GA parameters is fully task-specific, i.e., it depends on the nature of the design problem. Parameters involved in this work include the population size, maximum number of generations, and the probabilities that each of the genetic operations will occur. The population size and maximum number of generations are normally selected according to the size of the design space. When selecting genetic operation probabilities, it is important to consider the tradeoff between the solution quality and computational cost. Using large probabilities is helpful in introducing new individuals during evolution. This increases the possibility of finding the best solution. However, it significantly slows down the convergence of the calculation. All the parameters were tested and reasonably selected. In total, 31 individuals are included in a generation. The maximum number of generations is set to 100. The probabilities of performing crossover, mutation, deletion, and insertion operations are set to 0.2, 0.3, 0.3, and 0.3, respectively. To avoid any premature convergence, the probabilities of all the genetic operations are increased to 1 from the 14th to the 16th generation. In order to guarantee that the best solution in a generation does not deteriorate from one generation to the next, the best individual in one generation is directly passed into the next generation without any modifications.

In addition to the algorithm parameters, group candidates, from which solvent molecules are constructed, also need to be defined. The following are UNIFAC structural groups commonly used for molecular design, CH_3, CH_2, CH, $CH_2=CH$, $CH=CH$, OH, H_2O, CH_3CO, CH_2CO, CHO, CH_3COO, OCH_3, OCH_2, OCH, $COOH$, CH_2Cl, $CHCl$, CCl, $CHCl_2$, CCl_2, Br. Reaction

solvents should be chemically inert under the reaction condition and therefore OH, H_2O, CH_3COO, and COOH are excluded from our group set. After selecting algorithm parameters and group candidates, the first step is to initialize individuals for the first generation (see Figure 4.8). As clarified before, each individual consists of one solvent molecule in the form of a dynamic tree structure and one solvent molar composition expressed by a binary array. Solvent molecules in the first generation are randomly initialized with chain molecules whose sizes (number of groups) are between 3 and 8. The elements in the solvent composition array are randomly assigned with either 0 or 1.

The proposed dynamic tree structure only guarantees the generation of structurally feasible molecules. In order to obtain physically relevant solvents, a number of property constraints (such as biocompatibility) are required. In this work, the property constraints are handled with penalty functions. The penalty function of the kth property constraint is given by:

$$Pen_k^{upp} = \begin{cases} w \cdot b^{(P_k - P_{k,upp})} & P_k - P_{k,upp} > 0 \\ 1 & P_k - P_{k,upp} \leq 0 \end{cases}$$

$$Pen_k^{low} = \begin{cases} w \cdot b^{(P_{k,low} - P_k)} & P_{k,low} - P_k > 0 \\ 1 & P_{k,low} - P_k \leq 0 \end{cases}$$

Pen_k^{upp} denotes the penalty function for properties with an upper bound and Pen_k^{low} is the penalty function for properties with a lower bound. $P_{k,upp}$ represents the allowed upper limit of the kth property, and $P_{k,low}$ is the lower limit of the kth property. P_k is the kth solvent property estimated by QSPR or GC correlations. Individuals whose properties are outside of the allowed ranges are penalized. The sizes of the parameters w and b indicate the relative importance of different constraints. The GC models (Martin and Young, 2001; Constantinou and Gani, 1994) used to estimate solvent properties are:

Biocompatibility: $-\log(LC_{50}) = \sum_{i \in G} n_i \alpha_i$

Normalized melting point: $t_m = \exp(T_m/t_{m0}) = \sum_{i \in G} n_i t_{m,i}$

Normalized boiling point: $t_b = \exp(T_b/t_{b0}) = \sum_{i \in G} n_i t_{b,i}$

Where t_{m0} is 102.425 K and t_{b0} is 204.359 K. n_i is the number of group i present in the molecule. The contributions of structural groups to solvent biocompatibility α_i, melting point $t_{m,i}$, and boiling point $t_{b,i}$ can be found in Martin and Young (2001), Constantinou and Gani (1994), and Constantinou and Gani (1994), respectively. Taking into account the error in the GC models, an upper bound for the melting point T_m of 315 K and a lower bound for the boiling point T_b of 293

K are specified. Solvent property bounds and penalty function parameters for each property constraint are presented in Table 4.1. There is no theoretical guide on how to set parameters for the penalty function. Practically, they are chosen empirically or by test-and-set methods. In the simplest exponential penalty function, the coefficient w is set to 1.0 and the base b is normally adjusted to keep the penalty size in the same magnitude as the objective function. Based on this consideration, 0.97~0.99 was empirically found to be a suitable range for b. When testing, we found that compared to other constraints, most of the generated molecules can satisfy the boiling point constraint, and those unsatisfying ones generally deviate from the allowed boundary more lightly (i.e., the exponent of the penalty function is smaller). In order to make the boiling point constraint equivalently activate as other constraints, its base number b is set smaller.

Table 4.1: Solvent property bounds and penalty function parameters for each property constraint

Solvent property	Lower bound	Upper bound	w	b
Molecular size (number of groups)	3	8	1	0.99
Biocompatibility	/	3.50	1	0.99
Normalized melting point	/	21.66	1	0.99
Normalized boiling point	4.19	/	1	0.97

4.4.2   Results and discussion

The design problem is encoded in C and run in Microsoft Visual C++ 2005 (Kruglinski et al., 1998). Compared to other optimization techniques, the GA-based optimization has a high potential of locating near-global designs in a moderate amount of computational time under adjusted parameters (Affenzeller et al., 2009; Sundaram and Venkatasubramanian, 1998). In order to evaluate the performance and robustness of the method, 10 consecutive optimizations were performed and the results are summarized in Table 4.2. As can be seen, two different solvent molecules are obtained from the 10 optimization runs. However, they have very similar structures (both are homologues with the $CHCl_2$ group). Additionally, small differences among the optimized solvent compositions can be found. In all runs, optimal solvents are obtained and remain unaltered after only a small number of generations. By contrast, solvent compositions evolve relatively slowly because of their limited effect on individual fitness. The fitness values of the optimal solutions are equivalent to the reaction equilibrium conversions in all cases because none of the obtained solvent molecules violate any of the defined property constraints. The difference between the lowest and highest reaction conversions obtained from the ten stochastically initialized optimizations is less than 0.01%. Considering the stochastic nature of

the algorithm and the very small deviation in the fitness values, the results are regarded as our final, best-case (very likely near-global) solutions. The CPU time for a typical run is about 28 minutes.

Table 4.2: Results of the 10 consecutive optimization runs

No. of run	Optimal solvent structure	Optimal solvent initial composition	Fitness value (reaction conversion)
1	$CH_3(CH_2)_2CHCl_2$	0.5524	0.918000
2	$CH_3(CH_2)_2CHCl_2$	0.5714	0.918019
3	$CH_3(CH_2)_2CHCl_2$	0.5619	0.918025
4	$CH_3(CH_2)_2CHCl_2$	0.5619	0.918025
5	$(CH_3)_2CHCHCl_2$	0.5524	0.918042
6	$(CH_3)_2CHCHCl_2$	0.5810	0.918043
7	$(CH_3)_2CHCHCl_2$	0.5714	0.918066
8	$(CH_3)_2CHCHCl_2$	0.5619	0.918068
9	$(CH_3)_2CHCHCl_2$	0.5619	0.918068
10	$(CH_3)_2CHCHCl_2$	0.5619	0.918068

The evolution of fitness value vs. the number of generations is shown in Figure 4.11. The data is taken from the 8th run found in Table 4.2 which represents the best obtained solution. In this run, the computation converges very early before it terminates at the 100th generation, thus we only show the evolution of fitness value during the first 50 generations. As can be seen, both the largest fitness value and the average fitness of individuals in a generation increase quite rapidly at the beginning. Afterwards, the change in fitness of the best individual quickly stagnates. As mentioned before, in order to avoid any premature convergence, a disturbance is created by increasing all genetic operation probabilities to 1.0 during the 14th to the 16th generation. Due to the introduction of a large number of new individuals, the average fitness value decreases significantly during this disturbance. After that, it increases once again and later fluctuates within a limited range. The fitness of the best individual remains unchanged from the 28th generation until the end.
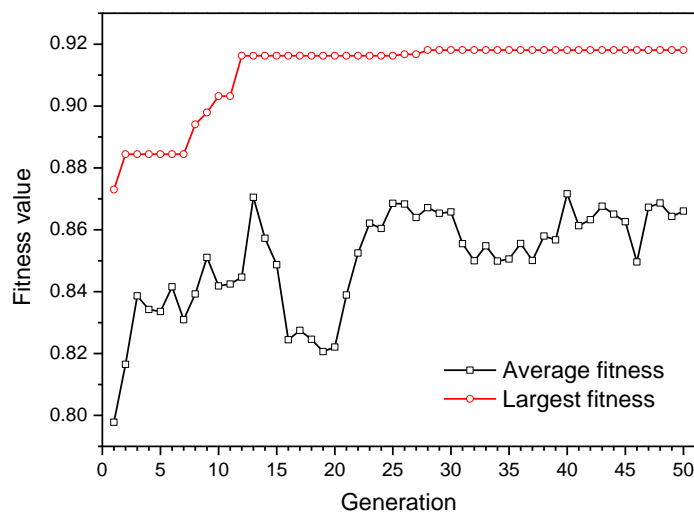
Figure 4.11: The evolution of fitness value vs. the number of generations

In GA-based molecular design, structural groups can be regarded as genes that constitute the molecules. Just as promising genes have more chances of being retained and unpromising genes are gradually eliminated in the natural selection process, the appearance frequency of a group in a generation behaves in a similar way. Figure 4.12 shows the evolution of average group weights in a generation. As can be seen, favorable groups (such as CH_3, CH, and $CHCl_2$) accumulate in the evolution. The weights of unfavorable groups (such as CH_3CO and OCH_2) generally decrease with increasing generations. Some group (such as CCl) weights do not change much at all during the evolution. These phenomena are consistent with our solvent design results.
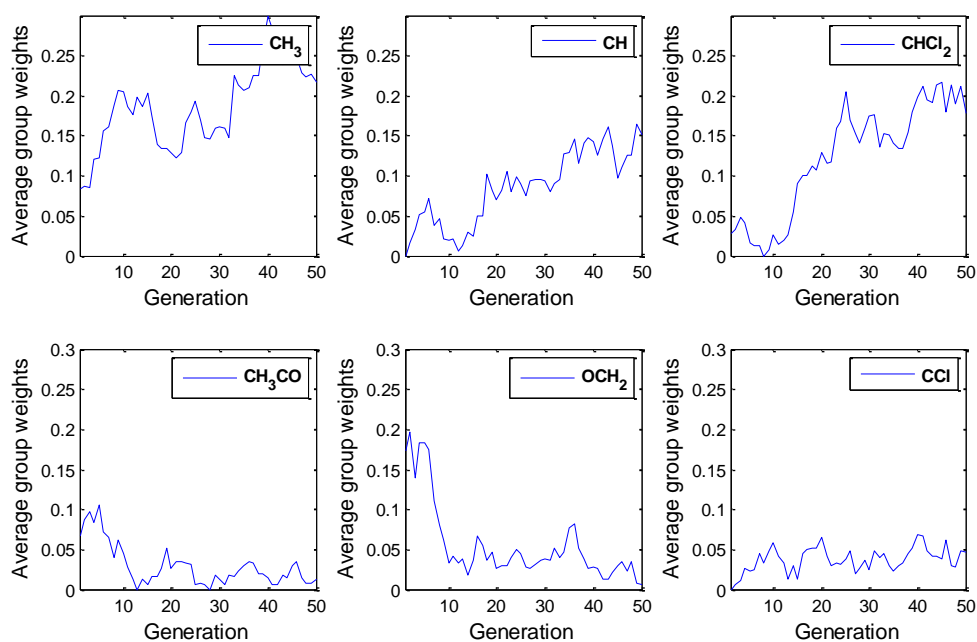

Figure 4.12: The evolution of average group weights in a generation

Because the developed solvent design method is purely based on the thermodynamic analysis of multiphasic reactive mixtures, the obtained results are always thermodynamically consistent. Nine representative solvents were investigated in Voutsas et al. (2002) regarding their effects on the equilibrium conversion of the esterification reaction. Isooctane has been found to be the best one with the highest conversion. Our optimally designed solvent 1,1-dichloro-2-methylpropane is predicted as having a slightly higher reaction performance than when making a similar calculation for isooctane. This finding suggests that the proposed design method has a high potential for quickly identifying optimal reaction solvents without the need for extensive experiments.

4.5 Summary and outlook

The rate-based dynamic method is extended to calculate the combined chemical and phase equilibria of liquid reaction mixtures, through which the reaction equilibrium conversion is determined. A genetic algorithm based CAMD method is proposed to design optimal solvents to maximize the reaction equilibrium conversion. The method is illustrated through application to an esterification reaction.

For simplification, only acyclic molecules are designed in this work. However, it is shown in Nachbar (2000) that tree structures can also represent cyclic and aromatic molecules. From this perspective, it is possible to extend the proposed method for the optimal design of cyclic molecules. The other issue worth noting is that currently the method cannot distinguish between structural isomers. Even though group connectivity is included in the dynamic tree structure, the employed UNIFAC model cannot make use of this connectivity information. For distinguishing between structural isomers, higher-level property models (e.g., quantum chemistry-based models) are required. The aforementioned two possible extensions on the proposed CAMD method deserve further investigations.

Part II

Integrated Solvent and Process Design

The chemical industry makes extensive use of solvents in reaction and separation processes in order to achieve a reduction of process costs while increasing the quality of products. For fulfilling these goals, both the solvent and the process system need to be optimally designed. As explained in Section 2.3.3, decomposed molecular and process design cannot reasonably capture the interdependent relationship between the selection of molecules and the operation of processes. In order to find a high-quality solution to a computer-aided solvent and process design problem, it is necessary to perform integrated solvent and process design.

Integrated solvent and process design problems are generally described as: Given a batch or continuous process requiring a solvent and a set of structural groups from which solvent molecules are built, find the optimal solvent and process operating conditions that would lead to a best process performance. This is a typical optimization problem where the design variables include discrete solvent structural variables and continuous process operational variables. The objective function is normally an appropriately defined process performance index, such as the total annual cost. As illustrated in Figure II.1, for calculating the objective function from given design variables, we need i) predictive property models that relate solvent structures to solvent properties and ii) reliable process models that relate the solvent properties and process operating conditions to the overall process performance.
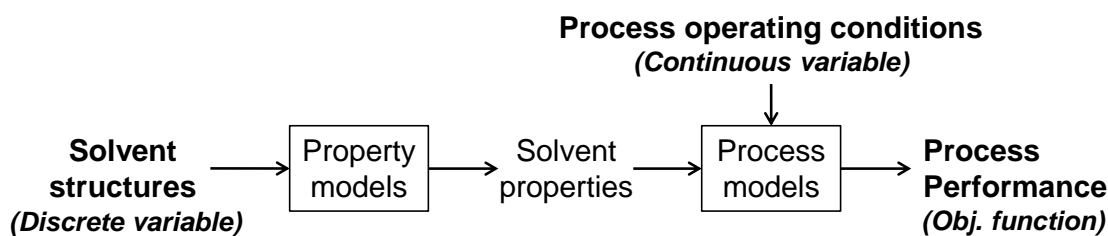

Figure II.1: Calculation of process performance based on property and process models

The generalized mathematical formulation of the integrated solvent and process design problem is given as follows:

$$\min_{x,y} F = f(x, y, q)$$

$$s.t. \ \ h(x, y, q) = 0$$

$$g(x, y, q) \leq 0$$

$$q = q(x, y)$$

$$c(y) = 0$$

$$d(y) \leq 0$$

$$x \in R^m, y \in N^r, q \in R^n$$

where F is the objective function, such as the process annual cost, to be minimized. x is a m-dimensional continuous vector of process variables, such as temperatures, compositions, flow rates, etc. y is a r-dimensional integer vector of solvent structural variables. It indicates the number of groups present in the solvent molecule. Both x and y are independent design variables being optimized. q is a n-dimensional continuous vector of dependent state variables that are determined by x and y. h $(x, y, q) = 0$ represent property and process models, such as activity coefficient equations, mass and heat balances, equipment sizing, etc. g $(x, y, q) \leq 0$ are specifications on process operating limits. c $(y) = 0$ are structural feasibility rules and d $(y) \leq 0$ denote structural complexity and solvent property constraints. Both of them contain molecular variables only.

Due to the high nonlinearity of the property and process models as well as the large mixed discrete-continuous design space, the above optimization problem is normally a complex MINLP problem. For solving such problem, advanced optimization algorithms are strongly required. Chapter 5 addresses an integrated reaction solvent and process design problem. The problem is simplified by employing shortcut process models and the simplified MINLP problem is successfully solved by a standard MINLP algorithm. In Chapter 6, a hybrid stochastic-deterministic algorithm is developed for solving complex integrated solvent and process design problems where rigorous process models are used. The reliability and efficiency of the hybrid optimization algorithm are demonstrated on an integrated separation solvent and process design problem. Figure II.2 provides an overview of the work in Part II of the dissertation.
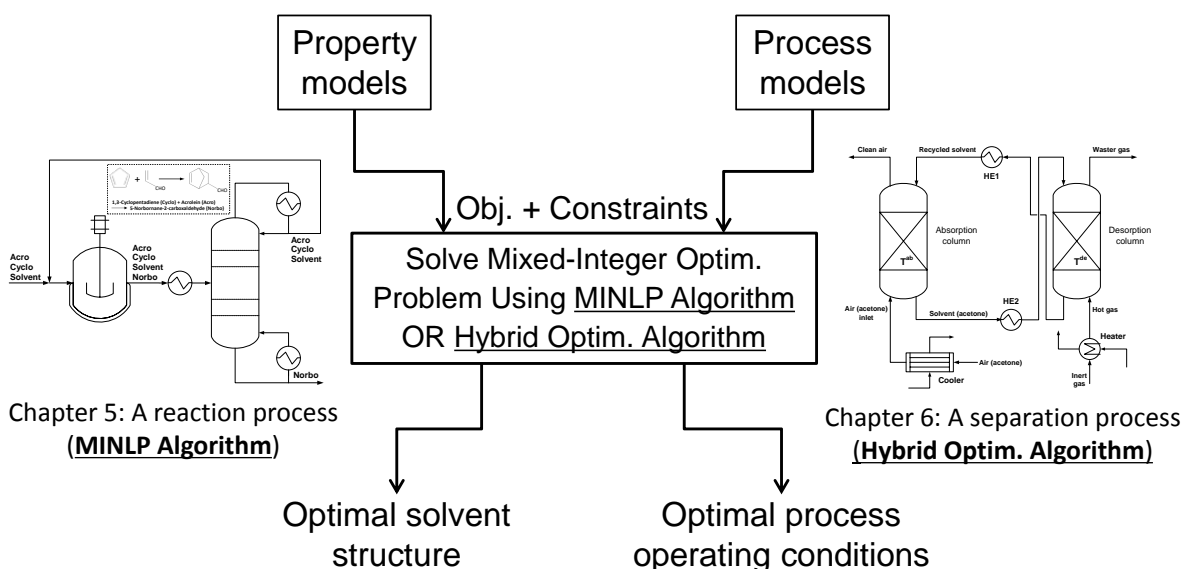

Figure II.2: Structural outline of the work in Part II of the dissertation

5. Integrated reaction solvent and process design

It is well known that a reaction solvent can have large effects on the efficiency of subsequent separation units where the product is separated from the solvent and unconverted reactants. In this chapter, the DA reaction investigated in Section 3.2.1 is used as the example reaction. However, instead of only maximizing the reaction performance, we now consider a continuous production process involving reaction and separation sections with recycle streams and optimize the overall performance of the process. The optimal reaction solvent and process operating conditions are identified from the formulation and solution of an MINLP-based integrated solvent and process design problem.

5.1 Application on a Diels-Alder reaction process

A simple flow sheet is constructed for the continuous DA reaction process (Figure 5.1). This process contains a continuous stirred tank reactor (CSTR), a heat exchanger, and a distillation column including a condenser and a reboiler. As depicted, the reactants acrolein (Acro) and 1,3-cyclopentadiene (Cyclo), together with a certain amount of solvent, are fed into the reactor. After the reaction, the mixture is heated and fed into the distillation column. The unconverted reactants and solvent are separated from the product 5-norbornane-2-carboxaldehyde (Norbo) and sent back into the reactor. Nearly pure product is collected from the bottom of the column.

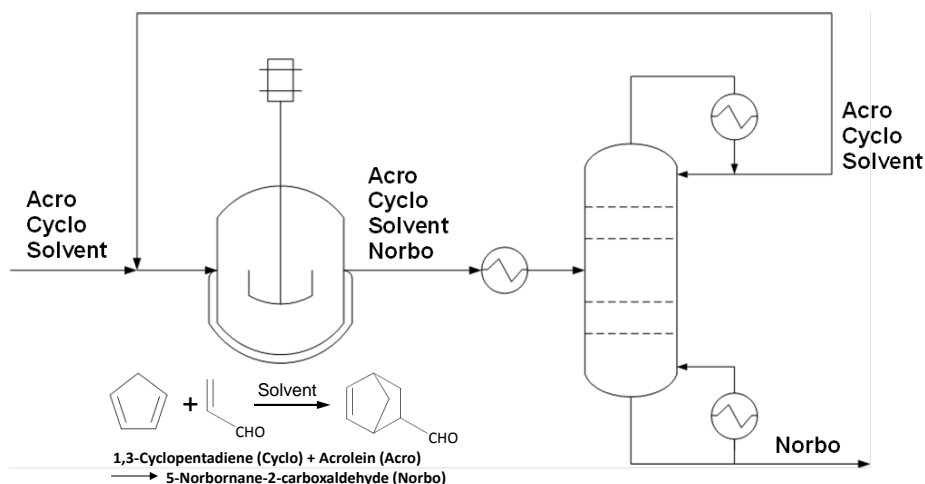**Figure 5.1:** Flow sheet diagram of the DA reaction process

The integrated reaction solvent and process design task is formulated as a MINLP optimization problem. Detailed property and process models that are used in the optimization are presented in Sections 5.1.1 and 5.1.2. The MINLP problem is summarized in Section 5.1.3 and the optimization results are shown and discussed in Section 5.1.4.

5.1.1 Solvent property models

Solvent effects on chemical processes are directly related to their physical properties. In order to develop an efficient chemical process, tradeoffs between different solvent properties need to be addressed based on their effects on the process performance. In this work, solvent effects on the reaction rate are quantified by the method introduced in Section 3.1. Solvent physical properties are estimated from public GC methods, given as Eq. (5.1 − 5.6). The sources of the GC methods are summarized in Table 5.1.

Boiling temperature (K):

$$T_b^S = 222.543 \ln\left(\sum_{j=1}^{N} n_j t_{b,j}\right) \tag{5.1}$$

Critical temperature (K):

$$T_c^S = 231.239 \ln\left(\sum_{j=1}^{N} n_j t_{c,j}\right) \tag{5.2}$$

Critical pressure (bar):

$$P_c^S = \left(0.108998 + \sum_{j=1}^{N} n_j p_{c,j}\right)^{-2} + 5.9827 \tag{5.3}$$

Standard enthalpy of vaporization (kJ/mol):

$$\Delta H_{vap}^S = \left(11.733 + \sum_{j=1}^{N} n_j \Delta h_{vap,j}\right) \times 1000 \tag{5.4}$$

Liquid molar volume (L/mol):

$$V_m^S = 0.01211 + \sum_{j=1}^{N} n_j v_{m,j} \tag{5.5}$$

Heat capacity (cal/(mol×K)):

$$C_p^S = \sum_{j=1}^{N} n_j a_j + \left(\sum_{j=1}^{N} n_j b_j\right) \cdot T + \left(\sum_{j=1}^{N} n_j c_j\right) \cdot T^2 + \left(\sum_{j=1}^{N} n_j d_j\right) \cdot T^3 \tag{5.6}$$

Table 5.1: A summary of the employed GC methods

Group contributions (GC) to solvent properties	Sources
GC to boiling point $t_{b,j}$, critical temperature $t_{c,j}$, critical pressure $p_{c,j}$, and standard enthalpy of vaporization $\Delta h_{vap,j}$	Marrero and Gani (2001)
GC to liquid molar volume $v_{m,j}$	Constantinou et al. (1995)
GC to heat capacity constants a_j, b_j, c_j, d_j	Rihani and Doraiswamy (1965)

5.1.2   Process and cost models

a) Reactor models

According to the experimental reaction condition given in Blankenburg et al. (1974), the component molar flow rates of the reactor inlet stream, $\dot{N}_{in,cyc}$, $\dot{N}_{in,acr}$, and $\dot{N}_{in,S}$, are set to 1 mol/s, 1 mol/s, and 2 mol/s, respectively. The reaction conversion not only decides the production rate, but also affects the reactor volume as well as the size and utility costs of the subsequent separation system. It must be carefully selected in order to optimally balance process revenue, reactor cost, and separation cost. In this work, the single-pass conversion of the reaction, X, is set as a design variable to be optimized. As a result, the component molar flow rates of the reactor outlet stream can be determined as follows.

$$\dot{N}_{out,cyc} = \dot{N}_{in,cyc}(1-X) \tag{5.7}$$

$$\dot{N}_{out,acr} = \dot{N}_{in,acr}(1-X) \tag{5.8}$$

$$\dot{N}_{out,nor} = \dot{N}_{in,cyc} X \tag{5.9}$$

$$\dot{N}_{out,S} = \dot{N}_{in,S} \tag{5.10}$$

The subscripts cyc, acr, nor, and S represent 1,3-cyclopentadiene, acrolein, 5-norbornane-2-carboxaldehyde, and the solvent, respectively. The concentration of compound i in the outlet of the CSTR can be calculated as

$$C_i = \dot{N}_{out,i} \Big/ \sum_{i \in COM} \dot{N}_{out,i} V_m^i \tag{5.11}$$

COM includes S, cyc, acr, and nor. Solvent molar volume V_m^S (L/mol) is estimated from Eq. (5.5). Molar volumes of the reactants and product V_m^i (i = cyc, acr, and nor) are given in the Supporting Information of Zhou et al. (2015a). The reaction was reported in Blankenburg et al. (1974) to be an irreversible second-order reaction with respect to the reactants. Therefore, the required reactor volume V_R (m^3) can be determined by

$$V_R = \dot{N}_{out,nor} \times 0.001 \Big/ \left(k C_{cyc} C_{acr} \right) \tag{5.12}$$

The solvent-dependent reaction rate constant k is determined by Eq. (3.1) and Eq. (3.26). The heat duty of the reactor cooling water can be evaluated by

$$Q_R = \Delta H_R^{303.15} \dot{N}_{in,cyc} X \tag{5.13}$$

where the estimated reaction enthalpy change is $\Delta H_R^{303.15} = -165.75$ kJ/mol.

b) Heat exchanger models

The composition of the feed stream of the distillation column can be calculated as follows.

$$\dot{N}_{F,i} = \dot{N}_{out,i} \tag{5.14}$$

$$x_{F,i} = \dot{N}_{F,i} \bigg/ \sum_{i \in COM} \dot{N}_{F,i} \tag{5.15}$$

The pressure of the feed stream p_F is set to 1.1 bar. The bubble point feed condition can be written as

$$P_{sat}^j(T_F) = p_F \bigg/ \sum_{i \in COM} \left(\alpha_{ij}^F \cdot x_{F,i} \right) \tag{5.16}$$

where the temperature-dependent relative volatility is calculated from the ratio of the vapor pressures of the two components.

$$\alpha_{ij}^F = P_{sat}^i(T_F) \big/ P_{sat}^j(T_F) \tag{5.17}$$

Methods for calculating the temperature dependences of vapor pressures of the solvent, reactants, and product are given in Appendix C. The heat duty of the heat exchanger can be evaluated after the feed temperature T_F is determined.

$$Q_H = \int_{T_0}^{T_F} (C_p^S \dot{N}_{F,S} + \sum_{i \in Species} C_p^i \dot{N}_{F,i}) dT \tag{5.18}$$

where Species includes cyc, acr, and nor, and T_0 is 303 K. Solvent heat capacity C_p^S is estimated from Eq. (5.6). Heat capacities of the reactants and product C_p^i are also expressed as functions of temperature with their heat capacity constants listed in the Supporting Information of Zhou et al. (2015a).

$$C_p^i = a_i + b_i T + c_i T^2 + d_i T^3 \tag{5.19}$$

c) Distillation column models

Due to the complex nonlinear structure of the process design problem combined with the large discrete molecular design space, the resulting MINLP problem could be very computationally demanding. For simplification, the distillation column is represented by a shortcut model including several assumptions such as equilibrium stages, ideal vapor and liquid phases, and constant relative volatilities throughout the column. The pressure at the top of the column p is set to 1 bar and the total pressure drop in the column Δp is assumed to be 0.2 bar. In order to meet the product purity requirement, the recovery of the solvent (light key component) in the distillate ξ_S is specified to 99.99%. As a key process operating condition, the recovery of the product (heavy key component) ξ_{nor} in the distillate is set as an optimization control variable. The recoveries of the reactants, ξ_{cyc} and ξ_{acr}, are considered to be 100% due to the sharp split assumption. Moreover, to avoid azeotrope formation and to insure a sufficiently large relative

volatility for the solvent and product pair, a minimum normal boiling point difference of 30 K between the solvent and the product is specified.

The molar compositions of the distillate and bottom streams are calculated as

$$\dot{N}_{D,i} = \dot{N}_{F,i} \cdot \xi_i \tag{5.20}$$

$$\dot{N}_{B,i} = \dot{N}_{F,i} - \dot{N}_{D,i} \tag{5.21}$$

$$x_{D,i} = \dot{N}_{D,i} \Big/ \sum_{i \in COM} \dot{N}_{D,i} \tag{5.22}$$

$$x_{B,i} = \dot{N}_{B,i} \Big/ \sum_{i \in COM} \dot{N}_{B,i} \tag{5.23}$$

Bubble point calculation at the bottom of the column

$$\alpha_{ij}^B = P_{sat}^i(T_{bub}) \big/ P_{sat}^j(T_{bub}) \tag{5.24}$$

$$P_{sat}^j(T_{bub}) = (p + \Delta p) \Big/ \sum_{i \in COM} \left(\alpha_{ij}^B \cdot x_{B,i} \right) \tag{5.25}$$

Dew point calculation at the top of the column

$$\alpha_{ij}^D = P_{sat}^i(T_{dew}) \big/ P_{sat}^j(T_{dew}) \tag{5.26}$$

$$P_{sat}^j(T_{dew}) = p \cdot \sum_{i \in COM} \left(\frac{x_{D,i}}{\alpha_{ij}^D} \right) \tag{5.27}$$

The average relative volatility of the solvent-product pair throughout the column is defined by

$$\alpha_{S,nor} = \sqrt{\alpha_{S,nor}^D \cdot \alpha_{S,nor}^B} \tag{5.28}$$

The Westerberg method (Biegler et al., 1997) is used to provide a rough estimation of the column size and reflux ratio. The arbitrary weights γ_N and γ_R are set to 0.8 in this work.

$$N_{lk} = 12.3 \Big/ \left((\alpha_{S,nor} - 1)^{2/3} \cdot (1 - \xi_S)^{1/6} \right) \tag{5.29}$$

$$N_{hk} = 12.3 \Big/ \left((\alpha_{S,nor} - 1)^{2/3} \cdot \xi_{nor}^{1/6} \right) \tag{5.30}$$

$$R_{lk} = 1.38 \Big/ \left((\alpha_{S,nor} - 1)^{0.9} \cdot (1 - \xi_S)^{0.1} \right) \tag{5.31}$$

$$R_{hk} = 1.38 \Big/ \left((\alpha_{S,nor} - 1)^{0.9} \cdot \xi_{nor}^{0.1} \right) \tag{5.32}$$

$$N_T = \gamma_N \max\{N_{lk}, N_{hk}\} + (1 - \gamma_N) \min\{N_{lk}, N_{hk}\} \tag{5.33}$$

$$R = \gamma_R \max\{R_{lk}, R_{hk}\} + (1 - \gamma_R)\min\{R_{lk}, R_{hk}\} \tag{5.34}$$

Enthalpy of vaporization of the stream mixture at the condenser and reboiler are expressed as molar weight sum of the enthalpies of vaporization of the individual compounds.

$$\Delta H_{vap}^D = \sum_{i \in COM} x_{D,i} \Delta H_{vap}^i(T_{dew}) \tag{5.35}$$

$$\Delta H_{vap}^B = \sum_{i \in COM} x_{B,i} \Delta H_{vap}^i(T_{bub}) \tag{5.36}$$

where the temperature dependence of the enthalpy of vaporization (Poling et al., 2001) is expressed by

$$\Delta H_{vap}^i(T) = \Delta H_{vap,298.15}^i \left(\frac{1 - T/T_c^i}{1 - 298.15/T_c^i} \right)^{0.375} \tag{5.37}$$

The standard enthalpy of vaporization and critical temperature of the solvent are estimated by Eq. (5.4) and Eq. (5.2), respectively. These two properties of the reactants and product are provided in the Supporting Information of Zhou et al. (2015a).

Finally, the heat duties of the condenser and the reboiler can be determined by

$$Q_{cond} = \Delta H_{vap}^D(R+1) \sum_{i \in COM} \dot{N}_{D,i} \tag{5.38}$$

$$Q_{reb} = \Delta H_{vap}^B(R+1) \sum_{i \in COM} \dot{N}_{D,i} \tag{5.39}$$

d) Cost models

The determination of the overall process economics requires the evaluation of the economic potential (EP), capital investment (CI), and utility cost (UC) of the process. The detailed calculation of these factors for the DA reaction process is given below with all the prices and cost model parameters provided in the Supporting Information of Zhou et al. (2015a).

(1) Economic potential ($/year)

The EP per year: $EP = 122 \times 60 \times 60 \times 24 \times 330 \times \dot{N}_{B,nor} \cdot GI$ (5.40)

(2) Capital investment ($/year)

The CI of the reactor: $CI_R = V_R \cdot \psi_R / PBT$ (5.41)

The CI of the distillation column consists of the cost for trays and the cost for the column vessel.

$$CI_{column} = ((N_T/\xi_T) \cdot \psi_T + ((N_T/\xi_T - 1) \times 0.6 + 6) \cdot \psi_V)/PBT \tag{5.42}$$

The heat transfer areas of the heat exchanger, condenser, and reboiler are given by

$$S_{heater} = Q_H \left/ \left(\frac{T_F - T_0}{\ln\left((423 - T_0)/(423 - T_F)\right)} \times 1420 \right) \right. \tag{5.43}$$

$$S_{reb} = Q_{reb} / \left(1420 \times (493 - T_{bub}) \right) \tag{5.44}$$

$$S_{cond} = Q_{cond} / \left(567.8 \times 20 / \ln\left((T_{dew} - 300)/(T_{dew} - 320)\right) \right) \tag{5.45}$$

Condensing steams of 423 K and 493 K are used as heating media in the heat exchanger and reboiler, respectively. The temperature of the cooling water in the condenser is assumed to increase from 300 to 320 K. The heat-transfer coefficients in the condensing steam heating and the room temperature water cooling processes are estimated as 1420 $W/(m^2 \cdot K)$ and 567.8 $W/(m^2 \cdot K)$, respectively.

With the calculated heat equipment sizes, their capital investments can be evaluated according to the bare module cost model (Guthrie, 1969), where u = heater, cond, reb denote heat exchanger, condenser, and reboiler, respectively.

$$BC_u = C_0 (S_u / S_0)^\alpha \tag{5.46}$$

$$CI_u = BC_u \times UF \times (MF + MPF - 1)/PBT \tag{5.47}$$

The total CI of the process is calculated as

$$CI_{tot} = CI_R + CI_{column} + CI_{heater} + CI_{cond} + CI_{reb} \tag{5.48}$$

(3) Utility cost ($/year)

Assuming that the temperature increase of the cooling water in the reactor and the condenser are 5 K and 20 K, respectively, UCs of the reactor and the condenser can be evaluated as follows.

$$UC_R = 330 \times 24 \times 60 \times 60 \times Q_R \cdot \psi_{CW} / (75.33 \times 5) \tag{5.49}$$

$$UC_{cond} = 330 \times 24 \times 60 \times 60 \times Q_{cond} \cdot \psi_{CW} / (75.33 \times 20) \tag{5.50}$$

The costs of hot steams in the heat exchanger and reboiler are calculated by

$$UC_{heater} = 330 \times 24 \times 60 \times 60 \times Q_H \cdot \psi_{HS} / 38012.4 \tag{5.51}$$

$$UC_{reb} = 330 \times 24 \times 60 \times 60 \times Q_{reb} \cdot \psi_{HS} / 33303.6 \tag{5.52}$$

The heat capacity of room temperature cooling water is 75.33 $J/(mol \cdot K)$. The enthalpies of vaporization of 423 and 493 K hot steams are 38012.4 and 33303.6 J/mol, respectively.

The total annual UC: $UC_{tot} = UC_R + UC_{heater} + UC_{cond} + UC_{reb}$ \tag{5.53}

5.1.3 MINLP optimization

A reduced set of 15 common groups (CH_3, CH_2, CH, C, OH, CH_3CO, CH_2CO, CHO, CH_3COO, CH_2COO, $HCOO$, OCH_3, OCH_2, OCH, and $COOH$) selected from the full set of groups listed in Appendix A is used to generate solvent molecules. Thus the total number of different groups in the group set N is 15. The minimum and maximum number of groups present in a molecule n_{min} and n_{max} are set to 2 and 5, respectively. The integrated solvent and process design task is formulated as a MINLP optimization problem. Integer variables n_j represent the number of group j present in the solvent molecule. Continuous variables include the reaction conversion X and the product recovery in the distillate stream ξ_{nor}. The objective is to maximize the process annual profit. The MINLP problem is summarized as follows.

Maximize: Total annual profit = $EP - CI_{tot} - UC_{tot}$

Variables: Integer n_j ($j = 1, 2, …, N$)

Reaction conversion X and product recovery ξ_{nor}

Subject to: Variable boundaries

$$0 \leq \xi_{nor} \leq 0.2$$
$$0.50 \leq X \leq 0.99$$
$$0 \leq n_j \leq n^{upp}(j) \ (j = 1, 2, …, N)$$

Solvent structural constraints

Chemical feasibility: Eq. (3.3 − 3.5)

Chemical complexity: Eq. (3.9 − 3.12)

Solvent property constraints

Reaction rate constant: Eq. (3.1) and Eq. (3.26)

Physical property estimation: Eq. (5.1 − 5.6)

Property boundaries: $330 \leq T_b^S \leq 416$; $\alpha_{S,nor} > 1$

Process models

Reactor: Eq. (5.7 − 5.13)

Heat exchanger: Eq. (5.14 − 5.19)

Distillation column: Eq. (5.20 − 5.39)

Vapor pressure calculation: Eq. (C.1 − C.7)

Cost models

Economic potential: Eq. (5.40)

Capital investment: Eq. (5.41 − 5.48)

Utility cost: Eq. (5.49 − 5.53)

5.1.4   Results and discussion

The solvent molecular structure, the reaction conversion X, and the product recovery ξ_{nor} were simultaneously optimized through the solution of the above MINLP problem using the KNITRO solver (Byrd et al., 2006) in the AMPL modelling environment (Fourer et al., 2002). For better illustration of the results, a reference case is optimized where acetic acid, the best experimentally determined reaction solvent, is fixed as the solvent. Because the solvent is fixed, the reference design case becomes a NLP problem. Table 5.2 shows the optimization results of the integrated solvent and process design as well as the reference design problems. Isopropanol is found to be the best solvent in the integrated design case. The corresponding optimal reaction conversion is 0.755 and product recovery is 0.0055.

Table 5.2: Optimization results of the integrated solvent and process design and the reference design problems for the DA reaction process

	Integrated solvent and process design (MINLP)	Reference case (NLP)
Solvent	Isopropanol	Acetic acid
Reaction conversion X	0.755	0.872
Product recovery ξ_{nor}	0.0055	0.0223
Annual profit (US \$/year)	27918.1	22776.4
EP (US \$/year)	65319.7	74118.8
CI_R (US \$/year)	10145.0	5750.3
CI_{heater} (US \$/year)	654.3	670.6
CI_{column} (US \$/year)	7662.7	17133.2
CI_{reb} (US \$/year)	705.2	712.7
CI_{cond} (US \$/year)	725.1	705.9
UC_R (US \$/year)	2340.9	2701.7
UC_{heater} (US \$/year)	1261.4	2325.4
UC_{reb} (US \$/year)	13399.3	20816.1
UC_{cond} (US \$/year)	507.7	526.5
$\log k\ (L/(mol \cdot s))$	-3.294	-2.551
$V_R\,(m^3)$	1.90	1.08
N_T (number of trays)	4	15

Reflux ratio R	0.128	0.920

When comparing the integrated design case to the reference case, it is clear that both the lower process economic potential EP and the higher reactor investment cost CI_R are resulted from the much lower reaction rate of isopropanol. However, although isopropanol shows relatively low reaction efficiency, it dramatically improves the energetic performance of the solvent-product separation. In contrast, despite the excellent reaction performance of acetic acid, it is not the best choice for the continuous process due to its extremely high energy consumption in the distillation column. This result highlights the importance of investigating trade-offs among different solvent properties in order to achieve an overall highest process performance. It can be concluded from the data in Table 5.2 that the integrated solvent and process design leads to an increase of the process annual profit by more than 20%, compared to the reference case.

It should be mentioned that due to the non-convexity of the MINLP problem and the utilization of local solvers, suboptimal solutions can be obtained. The probability of finding high-quality solutions is increased by solving the same optimization problem multiple times starting from different initializations. The solution presented in Table 5.2 is the best-case solution we have obtained.

5.2   Summary and outlook

This chapter proposes a method for integrated reaction solvent and process design. The best reaction solvent and optimal process operating conditions are simultaneously identified through the formulation and solution of an MINLP optimization problem whereby the economic performance of the entire process is maximized. The method is applicable beyond the example of the here considered DA reaction process. Its application is straightforward for general solvent-involved reaction processes once the reaction kinetic data are available for a small number of solvents.

For simplifying the design problem, a relatively small number of structural groups are considered and shortcut process models are employed. A larger solvent group set and more detailed process models would, of course, increase the reliability and applicability of the results. However, as the search space and complexity of the optimization problem increase, computational efficiency is likely to become a limiting factor. The extension of the design method to more complex solvent structures and more accurate process representations will be attainable, once more efficient solution algorithms and more powerful computer systems are available.

6. Integrated separation solvent and process design

Chapter 5 addresses an integrated reaction solvent and process design problem. In order to efficiently solve the problem using standard MINLP algorithms, the problem is simplified by assuming ideal mixture behavior and employing shortcut process models. However, it is clear that the ideal gas and liquid behaviors are normally not valid for most industrial cases. Additionally, shortcut models often cannot fully represent the characteristics of processes. Based on these considerations, efficient optimization algorithms or methods are strongly required for solving complex integrated solvent and process design problems where rigorous thermodynamic and process models are employed.

This chapter first proposes a new hybrid optimization algorithm. The algorithm is then used to solve a real-world integrated separation solvent and process design problem. A coupled absorption-desorption process is considered where the absorption solvent structure and the operating conditions of the absorption and desorption columns are simultaneously optimized. For better comparison, the problem is also solved by conventional MINLP algorithms. The results demonstrate the high reliability and robustness of the proposed hybrid algorithm.

6.1   Hybrid stochastic-deterministic algorithm

For large-scale complex integrated solvent and process design problems, global MINLP algorithms (Sahinidis, 1996; Misener and Floudas, 2013) are at the moment too expensive to be implemented. Local deterministic algorithms rely very much on initializations. Without good initial estimates, poor suboptimal or infeasible solutions are often obtained. In comparison with deterministic methods, stochastic optimization methods favor the search of global or near-global solutions under random initializations (Biegler, 2014; Rangaiah, 2010). They have been proven to be very efficient for solving discrete optimization problems (Rangaiah, 2010). However, one should note that stochastic optimizations are usually restricted to unconstrained or simple boundary-constrained problems. By contrast, deterministic algorithms can efficiently handle nonlinear constraints and are preferable methods for large-scale NLP problems. Moscato (1989) first introduced a memetic algorithm that combines population-based stochastic algorithms with local refinement strategies. Since then, many combined stochastic and deterministic algorithms have been proposed and applied to various optimization problems, including chemical process synthesis (Athier et al., 1997; Urselmann et al., 2011a; Skiborowski et al., 2015) and industrial-scale distillation and reactive distillation design (Gómez et al., 2006; Urselmann et al., 2011b). Studies have shown that optimization methods that combine advantages of stochastic and deterministic algorithms can considerably improve the optimization performance in terms of solution quality and computational cost (Lima et al., 2006; Molina et al., 2010).

The genetic algorithm (GA) is one of the most prominent evolutionary-based stochastic algorithms. It has been proven to be very efficient in solving optimization problems with large combinatorial and/or discontinuous search spaces (Affenzeller et al., 2009). Chapter 4 proposes a GA-based solvent design method. In this chapter, a hybrid optimization algorithm combining the GA developed in Chapter 4 with a deterministic NLP algorithm is proposed to solve complex integrated solvent and process design problems. In the hybrid stochastic-deterministic algorithm, the optimization of discrete molecular variables is performed by the GA and the continuous process variables are optimized by a gradient-based NLP solver at fixed solvent molecules proposed by the GA. The general structure of the algorithm is shown in Figure 6.1 with the major steps summarized below.
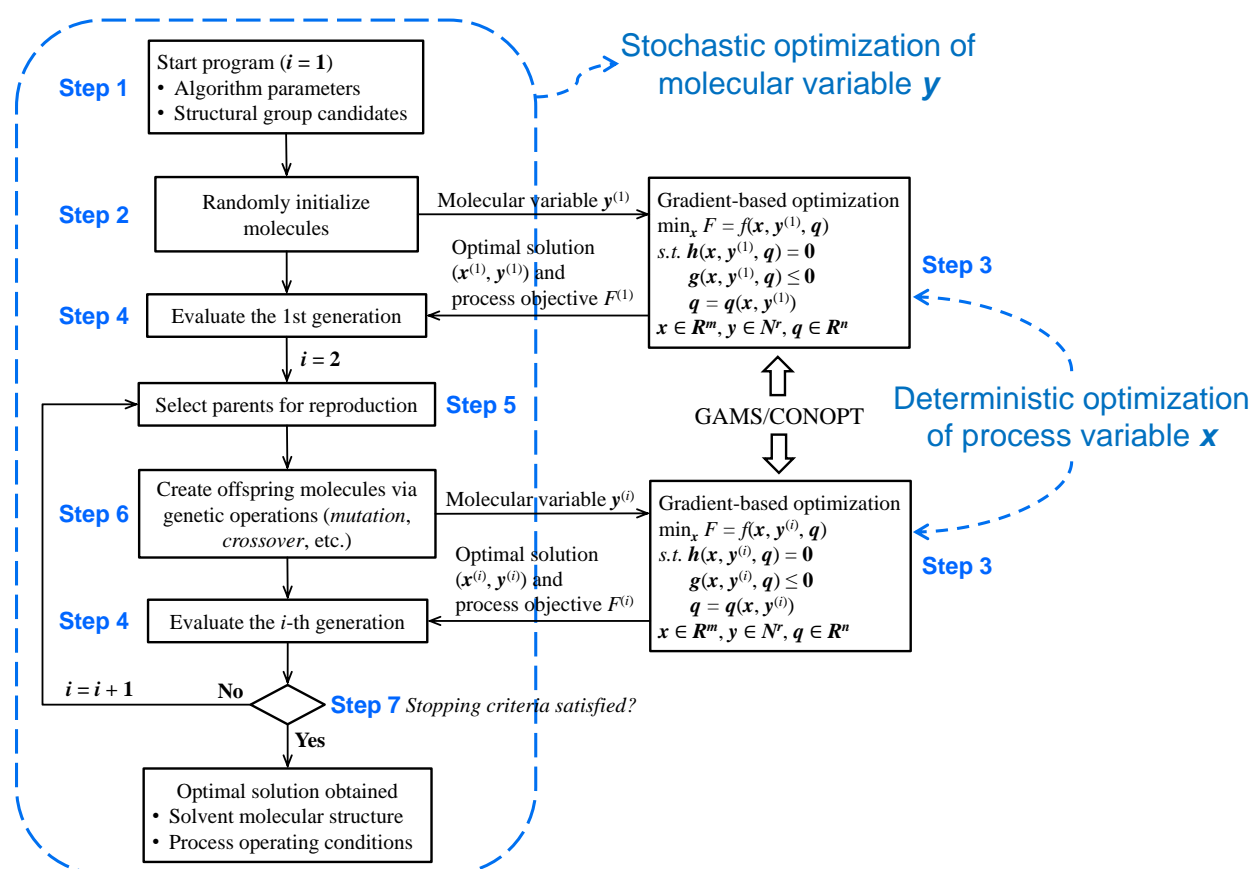
Figure 6.1: Schematic diagram of the hybrid stochastic-deterministic algorithm for integrated solvent and process design (Zhou et al., 2016b)

1. To start a program, first set GA parameters and specify a set of structural groups from which solvent molecules are generated.

2. Randomly initialize solvent molecules for the first generation using the dynamic tree structure (Zhou et al., 2016a).

3. Optimize process variables using the gradient-based CONOPT solver (Drud, 1994) at fixed molecular variables and return the optimal solution as well as process objective value. This procedure is performed for all the molecules in the generation.

4. Assign a fitness value to each molecule in the generation based on the corresponding process objective value.

5. Select parent molecules from the current generation based on the *roulette wheel selection* rule (Lipowski and Lipowska, 2012).

6. Create offspring molecules for the next generation via genetic operations (Zhou et al., 2016a) performed on the selected parents. Repeat Step 3 and Step 4.

7. The computation is terminated if predefined stopping criteria are satisfied (usually a maximum number of generations is specified). The best solution in the current generation represents the final solution to the design problem which includes an optimal solvent molecular structure and the corresponding best process operating conditions. If the criteria are not satisfied, $i = i + 1$ and return to Step 5.

The result of each calculation including the optimal solution ($\mathbf{x}^{(i)}$, $\mathbf{y}^{(i)}$) and process objective $F^{(i)}$ is recorded in a database, which provides two advantages. On the one hand, if a molecule that has been previously tested is created, the result is directly exported from the database without re-optimizing the process using the NLP solver. This strategy helps saving a lot of computational efforts. On the other hand, the construction of the database facilitates the generation of a list of top solutions after the entire computation terminates. These solutions can be more rigorously evaluated e.g., by experiments before a final decision is made.

6.2 Application on an absorption-desorption process

The proposed optimization algorithm is demonstrated on an absorption-desorption (AD) process which consists of an absorption column to separate acetone from air, a desorption column for recovering the absorption solvent, two internal heat exchangers, one cooler, and one heater (see Figure 6.2). Both absorption and desorption columns are operated at atmospheric pressure. The operating temperatures (T^{ab} and T^{de}) are considered as key process variables to be optimized together with the solvent structure. Ideal gas phase behavior is assumed due to the low operating pressure. The UNIFAC model is used to predict the non-ideality of the components in the liquid phases. The dissolution of air in the solvent and the vaporization of the solvent are neglected. A rate-based mass transfer approach is employed to determine the packing heights of the two columns.
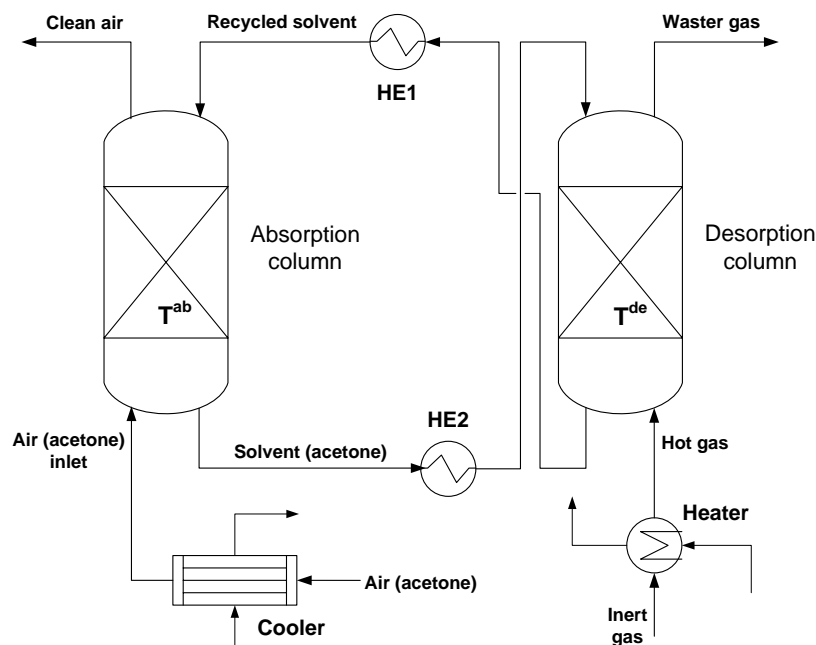
Figure 6.2: Flow sheet of the AD process

The selected UNIFAC groups from which solvent molecules are built are: CH_3, CH_2, CH, C, OH, CH_3CO, CH_2CO, CHO, CH_3COO, CH_2COO, HCOO, OCH_3, OCH_2, OCH, and COOH. Structural feasibility constraints are omitted because the employed molecular encoding method (Zhou et al., 2016a) already guarantees structurally feasible molecules. Taking into account the limitation and accuracy of first-order GC methods (see Section 6.2.1), the designed molecules should have no more than 10 groups and at most two functional groups (Giovanoglou et al., 2003). In order to rationalize the assumption of non-volatility of the solvent, the lower bound of solvent boiling point is set to 370 K. In this work, each molecule generated by the GA is tested against these constraints and those violating the constraints are immediately discarded. Solvent molecules are continuously created and tested until a pre-defined number (i.e., the population size of a generation) of molecules are obtained.

In order to obtain high-quality solutions in a reasonable amount of computational time, GA parameters should be properly selected. The selection of GA parameters is task-specific. The population size and maximum number of generations are normally selected according to the size of the design space. In this case study, the maximum number of generations is set to 30 and each generation includes 11 molecule individuals. Increasing the probabilities of genetic operations facilitates the generation of new individuals during the evolution and therefore increases the possibility of finding high-quality solutions. However, this action can slow down the convergence of the GA computation. Considering the tradeoff between the solution quality and computational cost, the probabilities of performing mutation, crossover, insertion, and deletion operations are set to 0.3, 0.3, 0.6, and 0.6, respectively. The probabilities of the insertion and

deletion operations are set higher than those of mutation and crossover to favor the generation of molecules with different sizes. In order to ensure that the best individual in a generation does not deteriorate with the increasing of generation, the best molecule in one generation is directly passed into the next generation without any modifications. In GAs, each individual solution is evaluated and assigned with a fitness value that tells how desirable the solution is. In this case study, the fitness function is defined as the total annual cost (TAC) of the AD process. The following provides all the equations for determining the process TAC.

6.2.1   Physical property models

a) Pure component properties

Physical properties of solvent (S) and acetone (A) are estimated by first-order GC methods where the required information is the number and type of structural groups present in the molecule.

Critical pressure (Scilipoti et al., 2014) is determined by

$$P_c = \frac{\sum_j n_j \Delta MW_j}{\left(\sum_j n_j \Delta P_j + 0.34\right)^2} \tag{6.1}$$

where n_j is the number of group j present in the molecule, ΔMW_j is the contribution of group j to the molecular weight MW in g/mol, and ΔP_j is the contribution of group j to the critical pressure P_c in atm.

Critical volume (Scilipoti et al., 2014) can be calculated as

$$V_c = 3.3127 \left(\sum_j n_j \Delta V_j\right)^{0.9542} \tag{6.2}$$

where ΔV_j is the contribution of group j to the critical volume V_c in cm^3/mol.

Molar volume at the normal boiling temperature (Scilipoti et al., 2014) can be determined from the critical volume.

$$V = 0.285 V_c^{1.048} \tag{6.3}$$

The ratio of normal boiling temperature to critical temperature (Scilipoti et al., 2014)

$$\frac{T_b}{T_c} = 1 - \frac{\left(\sum_j n_j \Delta MW_j\right)^{0.0268}}{1 + \sum_j n_j \Delta T_j} + \frac{\sum_j n_j \Delta A_j}{0.122 + 0.1219\left(\sum_j n_j \Delta MW_j\right)^{1.3769}} \tag{6.4}$$

where ΔT_j represents the contribution of group j to the ratio of normal boiling temperature to critical temperature T_b/T_c and ΔA_j denotes the association contribution of group j.

Normal boiling temperature (Scilipoti et al., 2014) can be determined by

$$T_b = V_c P_c \left(\frac{T_b}{T_c}\right) \left[0.002876 \ln P_c \left(\frac{\frac{T_b}{T_c}}{1 - \frac{T_b}{T_c}}\right) + 0.02603\right] \tag{6.5}$$

Saturated vapor pressure (in atm) is estimated from the Clapeyron equation where T is the temperature in K.

$$P^{sat}(T) = P_c \exp\left(\left(1 - \frac{T_c}{T}\right)\left(\frac{\frac{T_b}{T_c}}{1 - \frac{T_b}{T_c}}\right)\left(\ln\frac{P_c}{1.01325}\right)\right) \tag{6.6}$$

Viscosity (Scilipoti et al., 2014) is estimated by

$$\mu = \frac{\sum_j n_j \Delta\mu_j}{\left(P^{sat}\right)^{0.2 + \sum_j n_j \Delta N_j}} \tag{6.7}$$

where $\Delta\mu_j$ and ΔN_j are the contributions of group j to the viscosity μ in mPa$\times$s.

Heat capacity (Rihani and Doraiswamy, 1965) is calculated as

$$C_p = \sum_j n_j a_j + \left(\sum_j n_j b_j\right)\cdot T + \left(\sum_j n_j c_j\right)\cdot T^2 + \left(\sum_j n_j d_j\right)\cdot T^3 \tag{6.8}$$

where a_j, b_j, c_j, and d_j are the contributions of group j to the heat capacity C_p in cal/(mol$\times$K).

Normal melting temperature (Constantinou and Gani, 1994) can be determined by

$$T_m = 102.425 \ln\left(\sum_j n_j tm_j\right) \tag{6.9}$$

where tm_j is the contribution of group j to the normal melting temperature T_m in K.

b) Mixture properties

According to Poling et al. (2001), the infinite dilution diffusion coefficient of acetone (A) in the solvent (S) can be estimated by Eq. (6.10) where ϕ is the dimensionless association factor, set to 1.0 in this work.

$$D_{AS}^{\circ} = \frac{7.4 \times 10^{-8} \left(\phi_S MW_S\right)^{0.5} T}{\mu_S V_A^{0.6}} \tag{6.10}$$

The equation for calculating the infinite dilution diffusion coefficient of S in A, D_{SA}^o, can be derived by simply exchanging the indices of A and S in Eq. (6.10).

Diffusion coefficient (in cm^2/s) of the acetone and solvent mixture at arbitrary compositions

$$D_{AS} = \left(D_{AS}^{\circ} x_S + D_{SA}^{\circ} x_A\right) \tag{6.11}$$

where x represents mole fraction in the liquid phase.

According to Cussler (2009), the liquid-phase mass transfer coefficient in packed columns can be estimated by

$$\frac{k_L d_p}{D_{AS}} = 25 \left(\frac{d_p v_0}{v_{AS}}\right)^{0.45} \left(\frac{v_{AS}}{D_{AS}}\right)^{0.5} \tag{6.12}$$

where:

$$v_{AS} = \frac{\mu_{AS}}{\rho_{AS}} \tag{6.13}$$

$$\ln \mu_{AS} = x_A \ln \mu_A + x_S \ln \mu_S \tag{6.14}$$

$$\rho_{AS} = x_A \left(MW_A / V_A\right) + x_S \left(MW_S / V_S\right) \tag{6.15}$$

In the above equations, d_p represents the packing size, 5.08 cm for the 2-inch saddle used in this work, k_L is the liquid-film mass transfer coefficient in cm/s, v is the kinematic viscosity ($0.01 \times cm^2$/s), and v_0 is the superficial flow velocity in cm/s.

Superficial flow velocity

$$v_0 = \frac{\sum\limits_{i=A,S} N_i^L \times \sum\limits_{i=A,S} x_i V_i}{\frac{1}{4} \pi d^2} \tag{6.16}$$

where d denotes the column diameter that is set to 30.0 cm.

The overall mass transfer coefficient K_y is finally calculated from

$$\frac{1}{K_y a} = \frac{1}{k_y a} + \frac{m_A}{k_x a}$$ (6.17)

where

$$k_x = k_L \bigg/ \sum_{i=A,S} x_i V_i$$ (6.18)

k_y is the local mass transfer coefficient in gas phases which is set to 1.70×10^7 mol/(cm^2×s) for the investigated air system. a is the surface area per volume, 1.05 cm^2/cm^3 for the used saddle packing. m is the vapor-liquid equilibrium constant defined in Eq. (6.30), and k_x denotes the local mass transfer coefficient in liquid phases. K_y values in the absorption and desorption columns are determined individually according to Eq. (6.10 – 6.18).

6.2.2   Process and cost models

Mass balances in the absorption and desorption columns are written as

$$0 = \frac{dN_A^L}{dz^{ab}} - \frac{dN_A^G}{dz^{ab}}$$ (6.19)

$$0 = \frac{dN_A^L}{dz^{de}} - \frac{dN_A^G}{dz^{de}}$$ (6.20)

where N denotes molar flow rate in mol/s, dz (cm) is the differential packing height of the column. The indices ab and de represent the absorption and desorption columns, respectively. G and L denote gas and liquid phases, respectively.

Inert gas and nonvolatile solvent assumptions lead to

$$N_S^G = N_{air}^L = 0$$ (6.21)

$$\frac{dN_{air}^G}{dz^{ab}} = \frac{dN_S^L}{dz^{ab}} = 0$$ (6.22)

$$\frac{dN_{air}^G}{dz^{de}} = \frac{dN_S^L}{dz^{de}} = 0$$ (6.23)

The flow rates of acetone in the gas and liquid phases are expressed by

$$N_A^G = \frac{N_{air}^G y_A}{1 - y_A}$$ (6.24)

$$N_A^L = \frac{N_S^L x_A}{1 - x_A}$$ (6.25)

where x and y indicate the mole fraction in liquid and gas phases, respectively. Eqs. (6.21), (6.24), and (6.25) holds for the entire columns including inlet and outlet streams.

Connectivity constraints for the recycle streams

$$N_i^L(ab,out) = N_i^L(de,in) \quad (i = A, S) \tag{6.26}$$

$$N_i^L(ab,in) = N_i^L(de,out) \quad (i = A, S) \tag{6.27}$$

where in and out represent inlet and outlet steams, respectively.

Process specifications are the following

$$
\begin{aligned}
&N_{air}^G(ab,in) = 10 \; mol / s \\
&y_A(ab,in) = 0.03 \\
&y_A(ab,out) = 0.0015 \\
&N_S^L(ab,in) = 4 \; mol / s \\
&x_A(ab,in) = 0.005 \\
&N_{air}^G(de,in) = 5 \; mol / s \\
&y_A(de,in) = 0
\end{aligned}
\tag{6.28}
$$

Eq. (6.29) is used to determine the packing heights of the absorption and desorption columns (i.e., Z^{ab} and Z^{de}) with the VLE condition given in Eq. (6.30). Finite difference methods (FDM) are used to solve the differential equations. Specifically, the entire solute-concentration range (from $y_{A,in}$ to $y_{A,out}$) is discretized into 30 regions and for each region, the differential equations are discretized and solved as algebraic equations.

$$-\frac{d\left(\dfrac{N_{air}^G y_A}{1 - y_A}\right)}{dz} = K_y a \left(y_A - y_A^{eq}\right)\left(\frac{1}{4}\pi d^2\right) \tag{6.29}$$

where the equilibrium composition of acetone in the gas phase is given by:

$$y_A^{eq} = m_A x_A = \frac{\gamma_A(T)P_A^{sat}(T)}{P_{tot}} x_A \tag{6.30}$$

The temperature and solvent dependent activity coefficient of acetone γ_A is calculated by the reformulated UNIFAC model (Buxton et al., 1999). In the model, the activity coefficient of component i is given by:

$$\ln(\gamma_i) = \ln(\gamma_i^C) + \ln(\gamma_i^R) \tag{6.31}$$

Combinatorial part

$$\ln\left(\gamma_i^C\right) = \ln(R_i) - \ln\left(\sum_{ii} x_{ii} R_{ii}\right) - 5Q_i \ln(R_i) - 5Q_i \ln\left(\sum_{ii} x_{ii} Q_{ii}\right)$$

$$+ 5Q_i \ln(Q_i) + 5Q_i \ln\left(\sum_{ii} x_{ii} R_{ii}\right) - 5Q_i + 1 + C_i \tag{6.32}$$

$$C_i = \left(5\sum_{ii} x_{ii} Q_{ii} - 1\right) \frac{R_i}{\sum_{ii} x_{ii} R_{ii}} \tag{6.33}$$

Residual part

$$\ln\left(\gamma_i^R\right) = R1_i - R2_i \tag{6.34}$$

$$R1_i = Q_i - \sum_j n_{i,j} q_j \ln(R3_j) + Q_i \ln\left(\sum_{ii} x_{ii} Q_{ii}\right) - \sum_j \frac{R4_{i,j}}{R3_j} \tag{6.35}$$

$$R2_i = Q_i \ln(Q_i) - \sum_j n_{i,j} q_j \ln\left(\sum_{mj} q_{mj} n_{i,mj} \psi_{mj,j}\right) \tag{6.36}$$

$$R3_j = \sum_{mj} q_{mj} \sum_{ii} n_{ii,mj} x_{ii} \psi_{mj,j} \tag{6.37}$$

$$R4_{i,j} = \sum_{mj} n_{i,mj} q_{mj} q_j \sum_{ii} n_{ii,j} x_{ii} \psi_{mj,j} \tag{6.38}$$

In the above equations, j and mj are group indices; i and ii are component indices. Van der Waals volume R_i and surface area Q_i for component i are estimated by

$$R_i = \sum_j n_{i,j} r_j \tag{6.39}$$

$$Q_i = \sum_j n_{i,j} q_j \tag{6.40}$$

r_j and q_j are UNIFAC volume and surface area parameters of group j, respectively. $n_{i,j}$ represents the number of group j in component i. In this case study, there are only two components (acetone and the solvent) present in the liquid phase. $n_{A,j}$ is known for the acetone molecule and $n_{S,j}$ is the molecular variable of solvent to be optimized.

Interaction parameters between group mj and group j

$$\psi_{mj,j} = \exp\left(-a_{mj,j}/T\right) \tag{6.41}$$

The r_j, q_j, and $a_{mj,j}$ values can be found in Gmehling et al. (1982).

In order to ensure that the designed solvent is liquid in both absorption and desorption columns, the following inequality constraints are defined.

$$T_{m,S} < T^{ab}, \; T_{m,S} < T^{de} \tag{6.42}$$

$$T_{b,S} > T^{ab}, \; T_{b,S} > T^{de} \tag{6.43}$$

The TAC ($/year) of the process includes the annual utility cost (UC) and the annual capital investment (CI).

Cooling duty:

$$Q_G^{Cooling} = N_A^G(ab,in)\int_{T^{am}}^{T^{ab}} C_{p,A}dT + N_{air}^G(ab,in)C_{p,air}\left(T^{ab}-T^{am}\right) < 0 \tag{6.44}$$

$$Q_L^{Cooling} = \sum_{i=A,S}\left(N_i^L(de,out)\int_{T^{de}}^{T^{ab}} C_{p,i}dT \right) < 0 \tag{6.45}$$

$$Q_{total}^{Cooling} = Q_G^{Cooling} + Q_L^{Cooling} \tag{6.46}$$

Heating duty:

$$Q_G^{Heating} = N_A^G(de,in)\int_{T^{am}}^{T^{de}} C_{p,A}dT + N_{air}^G(de,in)C_{p,air}\left(T^{de}-T^{am}\right) > 0 \tag{6.47}$$

$$Q_L^{Heating} = \sum_{i=A,S}\left(N_i^L(ab,out)\int_{T^{ab}}^{T^{de}} C_{p,i}dT \right) > 0 \tag{6.48}$$

$$Q_{total}^{Heating} = Q_G^{Heating} + Q_L^{Heating} \tag{6.49}$$

where $Q^{Cooling}$ and $Q^{Heating}$ are the cooling and heating duties, respectively. The subscripts G and L denote gas and liquid phases, respectively. $C_{p,air}$ is the heat capacity of air with a constant value of 29.19 J/(mol×K) and T^{am} represents the ambient temperature that is set to 305.15 K.

The utility cost majorly consists of refrigeration electricity cost UC^C and heating steam cost UC^H (Towler and Sinnott, 2012).

$$UC_G^C = 330 \times 24 \times 60 \times 60 \times \left|Q_G^{Cooling}\right| \times \left(\frac{T^{am}-T^{ab}}{\zeta \times T^{ab}} \right) \times \psi_{EL} \tag{6.50}$$

$$UC_L^C = 330 \times 24 \times 60 \times 60 \times \left|Q_L^{Cooling}\right| \times \left(\frac{T^{de}-T^{ab}}{\zeta \times T^{ab}} \right) \times \psi_{EL} \tag{6.51}$$

$$UC^C = UC_G^C + UC_L^C \tag{6.52}$$

$$UC^H = 330 \times 24 \times 60 \times 60 \times Q_{total}^{Heating} \times \psi_{HS} \Big/ \Delta H_{vap}^{water} \tag{6.53}$$

ζ is the cooling cycle efficiency, set to 0.80. ψ_{EL} and ψ_{HS} are the electricity price (0.06 $/kwh) and heating steam price (2.57×10^{-4} $/mol), respectively. 250 °C high-pressure steam is used as the heat source. Its enthalpy of vaporization ΔH_{vap}^{water} is 1715.8 kJ/kg.

Total annual utility cost

$$UC^{total} = UC^{C} + UC^{H} \tag{6.54}$$

According to Loh et al. (2002), the annual capital investment of the absorption and desorption columns, CI^{ab} and CI^{de}, can be estimated by

$$CI^{ab} = (C_{shell}^{ab} + C_{packing}^{ab})/PBT \tag{6.55}$$

$$C_{shell}^{ab} = \psi_{S0} + \psi_{S} \times Z^{ab} \tag{6.56}$$

$$C_{packing}^{ab} = \left(\frac{1}{4}\pi d^{2}\right) \times Z^{ab} \times \psi_{P} \tag{6.57}$$

$$CI^{de} = (C_{shell}^{de} + C_{packing}^{de})/PBT \tag{6.58}$$

$$C_{shell}^{de} = \psi_{S0} + \psi_{S} \times Z^{de} \tag{6.59}$$

$$C_{packing}^{de} = \left(\frac{1}{4}\pi d^{2}\right) \times Z^{de} \times \psi_{P} \tag{6.60}$$

where C_{shell} and $C_{packing}$ represent the cost of shell and packing of the column, respectively. *PBT* is the payback time, set to 8 years in this work. ψ_{S0} and ψ_{S} are two parameters of the linearized shell cost model. They are 5100 $ and 6.56 $/cm, respectively. ψ_{P} is the packing price with a value of 7.42×10^{-4} $/cm^{3}.

Total annual capital investment

$$CI^{total} = CI^{ab} + CI^{de} \tag{6.61}$$

Finally,

$$TAC = UC^{total} + CI^{total} \tag{6.62}$$

6.2.3 Results and discussion

The GA is encoded in C and run in Microsoft Visual C++ 2005 (Kruglinski et al., 1998). The process optimization problem is solved by the CONOPT solver (Drud, 1994) in the GAMS modelling system (Rosenthal, 2006). In order to evaluate the performance and robustness of the hybrid algorithm, 10 optimization runs were consecutively performed with the results summarized in Table 6.1. 9 of the 10 runs result in the same optimum (Solution 1) with

CH$_3$COOH as the best solvent. In the remaining one run, another solution (Solution 2) with CH$_3$CH$_2$COOH as the optimal solvent is found. The CPU time for each run is about 20 minutes. In order to more directly verify the reliability of the hybrid optimization method, all the solvents in the design space (the total number is 1696) were enumerated and evaluated. Solution 1 and Solution 2 have been proven to be the best and the second best solutions, respectively. This high probability of finding the best solutions from random initializations demonstrates the high reliability and robustness of the method.

Table 6.1: Results of 10 consecutive optimization runs

	Solution 1	Solution 2
Optimal solvent	CH$_3$COOH	CH$_3$CH$_2$COOH
T^{ab} (K)	303.54	304.17
T^{de} (K)	325.38	326.28
Z^{ab} (cm)	199.89	241.12
Z^{de} (cm)	311.93	382.62
UC^{C} ($/year)	261.28	362.78
UC^{H} ($/year)	2264.75	2846.80
CI^{total} ($/year)	1728.36	1827.49
TAC ($/year)	4254.39	5037.07

For better comparison, the problem has also been handled by deterministic MINLP algorithms, including the global optimization solver BARON and local solvers DICOPT and SBB (Brooke et al., 1998). For DICOPT and SBB, the problem was solved multiple times starting from different initial estimates. The results show that the problem cannot be successfully settled by BARON within a reasonable amount of time. The performances of DICOPT and SBB are similar. Both of them rely much on good initializations. Over 80% of the runs failed to converge to a feasible solution and only about 5% of them succeeded to find Solution 1 (Table 6.1) as the optimal solution. Details about the solved MINLP problem are given in Table 6.2.

Table 6.2: Computational details of the solved MINLP problems (CONOPT for NLP subproblems and CPLEX for MILP subproblems)

Solver	DICOPT
Number of continuous variables	1198
Number of discrete variables	15
Number of equations	1190

Number of NLPs	6
NLP CPU time / MILP CPU time (s)	231.2 / 4.0
Total CPU time (s)	235.8

As described before, the result of each calculation including the optimal solution and the corresponding process TAC value is stored in a database. A list of top solutions can be obtained by sorting all solutions in the database according to their TAC values after an entire computation is completed. Table 6.3 shows the top five solutions obtained from a random optimization run. Taking into account the deviations in the employed property predictive models, the generation of multiple promising solutions is desirable since the solutions can be further evaluated by higher-level property models or experiments before making a final selection.

Table 6.3: Top five solutions obtained for the integrated solvent and process design problem

Ranking	Optimal solvent	T^{ab} (K)	T^{de} (K)	TAC ($/year)
1		Solution 1, Table 6.1		
2		Solution 2, Table 6.1		
3	$CH_3CH(CHO)_2$	295.51	319.28	5291.23
4	$CHO(CH_2)_2CHO$	295.54	319.31	5394.91
5	$CH_3CH(OH)CHO$	282.72	307.30	5490.98

6.3 Summary and outlook

A hybrid stochastic-deterministic optimization method is proposed for solving complex integrated solvent and process design problems. It is a combination of a genetic algorithm that optimizes the discrete molecular variables and a gradient-based deterministic algorithm that optimizes the continuous process variables. The reliability and efficiency of the method has been demonstrated on a coupled absorption-desorption process where the solvent molecular structure as well as the operating conditions of the absorption and desorption columns are simultaneously optimized. The results indicate that while conventional MINLP algorithms rely much on well-selected initial values, the hybrid optimization algorithm can steadily and reliably solve the problem under random initializations.

7. Conclusions and perspectives

7.1 Summary of major achievements

This research focuses on the area of multi-scale product and process design. As representative and important examples, the molecular design of reaction solvents as well as the integrated solvent and process design are primarily studied in this dissertation. The main contributions are summarized below.

In Chapter 3, we propose a QSPR model using a new type of COSMO-based solvent descriptor to correlate the effect of solvents on chemical reaction rates. Based on the parameterized QSPR model and a developed group contribution method that is used to estimate the solvent descriptors, optimal solvents having the highest reaction rates are identified from the formulation and solution of a CAMD optimization problem. We have demonstrated the reliability and wide applicability of the method on both simple and complex reactions.

In Chapter 4, we propose a GA-based CAMD method for designing solvents to maximize reaction equilibrium conversion. A novel molecular encoding method is introduced within the GA to facilitate the generation and evaluation of structurally feasible solvent molecules. The application to a selected esterification reaction shows that the method is a valuable tool for quickly identifying promising solvents that can break the chemical equilibrium limitation allowing for higher product yields.

In Chapter 5, instead of focusing on chemical reactions, continuous production processes involving reaction and separation sections with recycle streams are considered. The optimal reaction solvent and process operating conditions are identified from the solution of an MINLP-formulated integrated solvent and process design problem where the overall process performance is maximized. To the best of my knowledge, this is one of the first attempts to integrate reaction solvent design into a process-wide optimization framework.

In Chapter 6, we propose a hybrid stochastic-deterministic optimization method for solving complex integrated solvent and process design problems where rigorous thermodynamic and process models are employed. The high reliability and efficiency of the method are demonstrated on a coupled absorption-desorption process where the absorption solvent structure and the operating conditions of the absorption and desorption columns are simultaneously optimized.

7.2 Limitations and future directions

Despite several important achievements, a few limitations should be pointed out. In this work, the objective of solvent design is to maximize either the reaction performance or the process performance. However, one should note that when selecting solvents, their availabilities and

impacts on health, safety, and environment are also important factors to consider. How to efficiently incorporate these criteria into a solvent design framework deserves serious attention. Other limitations and future directions are discussed in the following sections.

7.2.1 Computational issue

Optimization lies at the heart of molecular and process design. Except the first case study in Chapter 3, all the design tasks addressed in this work are inherently nonconvex MINLP problems. Given the large computational cost of global optimization, local MINLP algorithms are used to solve the second case study in Chapter 3 and the problem in Chapter 5. This means suboptimal solutions can be obtained for both problems. In order to increase the probability of finding high-quality solutions, we solve the optimization program multiple times starting from different initial values and provide the best solutions we have obtained. Despite these efforts, global optimality of the solutions cannot be guaranteed. On the other hand, due to the stochastic nature of the algorithm, the methods proposed in Chapter 4 and Chapter 6 are able to find global or near-global optima from random initializations. However, these solutions are still not theoretically guaranteed to be the global solution. With these considerations, the development of deterministic global MINLP algorithms with an acceptable computational cost is always significant.

7.2.2 Model reliability

In this work, first-order GC models are used to predict several physical properties of solvent. Despite their popularity and effectiveness, limitations in these models are also obvious. Firstly, the models have not taken into account the connectivity between groups. As a result, they cannot distinguish between structural isomers. Secondly, the additive assumption in the model requires the contributions of structural groups to be independent of each other. These two limitations make the high reliability and accuracy of first-order GC models limited only to those molecules with simple structures and small or medium sizes.

For designing large complex molecules with high reliability, two methods are suggested. The first is to replace the first-order GC models with more sophisticated and accurate higher-order GC models (e.g., Marrero and Gani, 2001). However, one should note that when higher-order groups are included, the computational complexity will be significantly increased due to the much larger number of design variables and equations. The other method is to generate a list of top solutions instead of only one optimal solution and later introduce a post-design step to further screen and more rigorously evaluate the top solutions by using higher-order GC models or experimental data if available. When using stochastic optimization to solve solvent design or integrated solvent and process design problem, the result of each evaluated solvent can be stored in a database. After completing an optimization procedure, a list of top solutions can be directly generated from sorting all the solutions in the database according to their objective function

values. When using deterministic optimization to solve the problem, the integer cut method (Folić et al., 2007) can be used to generate a list of top solutions.

Most CAMD procedures use GC models to predict molecular properties. However, as an alternative to the GC models, QSPR models based on signature molecular descriptors (SMDs) have received increasing attention. Currently, one of the most popular and widely used SMDs is the topological index (TI), which is obtained from the two-dimensional topologic representation of molecular structures. Due to the inclusion of atom connectivity information, TIs provide a higher level of molecular representation compared to the simple group partitioning and group number counting. Therefore, in principle, TI-based QSPR models can be more accurate than simple GC models for predicting molecular properties. In fact, numerous TI-based models have been developed to estimate solvent physical properties (e.g., in Patel et al., 2009). However, unfortunately there is a lack of TI-based thermodynamic model for predicting activity coefficients in liquid phases, which is an essential property for selecting solvents. For this reason, the direct application of TI-based property models for solvent design is uncommon at the moment. Nevertheless, it deserves further investigation.

7.2.3   Extension of methods

a) Ionic liquid solvents and solvent mixtures

This work only focuses on organic solvent design. However, ionic liquids (ILs), as a new type of solvent, have received tremendous attention and wide applications during the last few decades (Plechkova and Seddon, 2008). Compared to conventional organic solvents, ILs have some unique properties and advantages, such as powerful dissolving and electrical conductivity abilities, low volatility, thermal stability, etc. Moreover, IL properties can be tuned by modifying the cation structure or changing the cation-anion combination, which makes ILs "designable solvents". Since the proposed methods are not limited to certain solvent types, they can be extended to IL design as long as reliable IL property models are available.

In addition to pure solvents, solvent blends are also widely used in industry. The advantage of using solvent blends is that their properties can be well tuned by changing the composition of the mixture. Although mixture design is not an area as much studied as pure-component design, a few significant contributions such as Karunanithi et al. (2005) can still be found. In general, mixture design problems are addressed by adding certain additional constraints relevant to the mixture properties to the MILP or MINLP formulated pure-component design problem. This work proposes methods for the optimal design of pure solvents. The extension of the methods to solvent blend design is obviously a worthwhile direction to pursue in future studies.

b) Integrated solvent and process synthesis

Integrated solvent and process design is performed, however, under fixed process configurations. For processes whose configurations are not fixed, it is necessary to perform integrated solvent

and process synthesis to capture the interaction between the selection of solvents and process alternatives. Compared to the design problem, the synthesis problem is much more complex due to the introduction of binary variables indicating the existence of process units and additional equations for the alternative units. A possible way to solve this problem is to incorporate the CAMD of solvents into a superstructure-based process synthesis framework by using the generalized disjunctive programming (GDP) method.

Appendix

Appendix A. Table A1

Table A1: Sixty structural groups and single-group solvents with their IDs, valences, maximum numbers, and contributions to the six solvent descriptors

Group ID	Group j	Valence $v(j)$	Maximum group number $n^{\mathrm{upp}}(j)$	s_{1j}	s_{2j}	s_{3j}	s_{4j}	s_{5j}	s_{6j}
1	CH_3	1	$n_{max}y_1 + y_4 + y_6$	0.00089	0.02073	0.53888	2.06187	-0.17281	-0.02667
2	CH_2	2	$n_{max}y_1$	-0.00004	0.00742	1.05649	0.91999	-0.00238	-0.00132
3	CH	3	$3y_1$	-0.00208	0.01217	1.14222	-0.18643	0.14520	0.02145
4	C	4	y_1	-0.00437	0.01606	1.51306	-1.85052	0.30961	0.07360
5	$CH_2{=}CH$	1	$y_1 + y_7 + y_4 + y_6$	0.00419	0.11012	0.99885	2.94047	-0.10216	-0.05282
6	$CH{=}CH$	2	$y_1 + y_7 + y_6$	0.00028	0.10202	1.54385	1.85037	0.04173	-0.01827
7	$CH{=}C$	3	y_1	-0.00059	-0.60012	3.68092	-0.35402	0.25616	0.00906
8	$C{=}C$	4	y_1	-0.00146	-1.57226	5.73254	-2.39786	0.47058	0.03639
9	$CH{\equiv}C$	1	y_1	0.00125	0.54523	0.51504	2.55271	-0.00825	-0.04230
10	ACH	2	$6y_3 + 8y_2$	0.00042	0.01990	0.34061	1.25012	-0.06168	-0.01246
11	AC	3	$y_7 + 2y_2$	0.00001	-0.06217	0.98538	-0.25030	0.10503	0.01567
12	$ACCH_3$	2	$6y_3 + 8y_2$	0.00023	0.03093	1.54454	1.86466	-0.06579	-0.01173
13	$ACCH_2$	3	y_6	0.00358	0.01361	2.45084	0.24363	0.10191	-0.00404
14	ACCH	4	y_4	-0.00176	0.00379	2.69615	-1.08616	0.26908	0.04291
15	OH	1	$2y_1$	0.01484	0.71461	-0.31120	0.31695	0.77063	0.08152
16	ACOH	2	$6y_3 + 8y_2$	0.21121	0.66711	-0.27753	1.26076	0.61421	-0.01135
17	CH_3CO	1	$y_1 + y_7 + y_4 + y_6$	0.00121	0.11035	2.57475	0.77126	1.31332	-0.02939

Group ID	Group j	Valence $v(j)$	Maximum group number $n^{upp}(j)$	s_{1j}	s_{2j}	s_{3j}	s_{4j}	s_{5j}	s_{6j}
18	CH_2CO	2	$y_1 + y_7 + y_6$	0.00056	0.07364	3.11906	-0.47464	1.43224	-0.01007
19	CHO	1	$y_1 + y_7 + y_4 + y_6$	0.00121	0.11534	1.38480	0.13605	1.19788	-0.04322
20	CH_3COO	1	$y_1 + y_7 + y_4 + y_6$	0.00121	0.11534	3.61839	0.72511	1.57978	-0.04302
21	CH_2COO	2	$y_1 + y_7 + y_6$	0.00026	0.10573	3.87689	-0.18063	1.62852	-0.01871
22	HCOO	1	$y_1 + y_7 + y_4 + y_6$	0.00115	0.29929	1.66505	0.58384	1.44054	-0.04561
23	OCH_3	1	$y_1 + y_7 + y_4 + y_6$	-0.00610	0.00842	1.61665	0.79532	0.87103	-0.03756
24	OCH_2	2	$y_1 + y_7 + y_6$	-0.00008	0.08996	2.55219	-0.17182	0.75078	0.03014
25	OCH	3	y_1	0.00054	0.05580	2.67201	-1.11185	0.79676	0.16094
26	CH_2NH_2	1	$2y_1 + y_7 + y_4 + y_6$	0.00121	0.49071	1.39382	1.34315	0.22805	0.34375
27	CH_3NH	1	y_1	-0.00006	0.71858	1.29259	1.83777	0.11208	-0.02630
28	CH_2NH	2	$y_1 + y_7 + y_6$	0.00032	0.23948	2.07790	0.64838	0.29887	0.27948
29	$ACNH_2$	2	$6y_3 + 8y_2$	-0.00005	1.24791	0.12337	1.10092	0.35031	0.01823
30	CH_2CN	1	$y_1 + y_7 + y_4 + y_6$	0.00115	0.19507	1.97855	1.56929	1.14896	-0.04561
31	COOH	1	$y_1 + y_7 + y_4 + y_6$	0.26792	0.70732	0.53942	0.72350	1.59226	-0.04357
32	CH_2Cl	1	$2y_1 + y_7 + y_4 + y_6$	0.00096	0.20956	1.00841	3.42696	-0.19105	-0.03755
33	CHCl	2	y_1	0.00028	0.10202	1.65035	1.84147	0.01193	-0.01827
34	CCl_2	2	y_1	0.00106	1.26480	-0.67746	5.75529	-0.19605	-0.03539
35	CCl_3	1	$2y_1 + y_7 + y_4 + y_6$	0.00113	0.18487	1.54257	6.44233	-0.21430	-0.04627
36	ACCl	2	$6y_3 + 8y_2$	0.00013	0.07639	0.58193	2.74455	-0.07234	-0.01136
37	$ACNO_2$	2	$6y_3 + 8y_2$	0.00004	0.12734	1.79831	1.47803	0.72343	-0.01099
38	ACCN	2	$6y_3 + 8y_2$	-0.00005	0.18321	1.73137	0.97682	1.03356	-0.01062
39	ACCHO	2	$6y_3 + 8y_2$	-0.00005	0.05471	2.65267	1.24612	0.44596	-0.01062

Group ID	Group j	Valence $v(j)$	Maximum group number $n^{upp}(j)$	s_{1j}	s_{2j}	s_{3j}	s_{4j}	s_{5j}	s_{6j}
40	CH_2NO_2	1	$2y_1 + y_7 + y_4 + y_6$	0.00115	0.48784	1.55762	2.63991	0.70929	-0.04561
41	$CHNO_2$	2	$y_1 + y_7 + y_6$	0.00024	0.13509	2.64094	1.11861	0.79805	-0.01960
42	CH_2SH	1	$y_1 + y_7 + y_4 + y_6$	0.00113	0.23727	1.55512	2.73973	0.47355	-0.04627
43	I	1	$2y_1 + y_7 + y_4 + y_6$	0.00098	0.31142	0.28793	3.42427	-0.19957	-0.03852
44	Br	1	$2y_1 + y_7 + y_4 + y_6$	0.00122	0.29019	-0.07726	3.01428	-0.18491	-0.03482
45	ACF	2	$6y_3 + 8y_2$	0.00033	0.02723	0.42266	1.84768	-0.06490	-0.01211
46	CF_3	1	$2y_1 + y_7 + y_4 + y_6$	0.16827	0.40553	-1.61744	5.88581	-0.34510	-0.15314
47	$CONH_2$	1	$y_1 + y_7 + y_4 + y_6$	0.01222	1.76786	-1.14500	2.61975	1.40994	0.04246
48	CH_2S	2	$y_1 + y_7 + y_6$	0.00028	0.10202	2.73840	0.81752	0.77933	-0.01827
49	CH_3OH	0	y_1	0.02102	0.87691	-0.09780	2.24890	0.61929	0.11971
50	H_2O	0	y_1	0.02952	1.75981	-3.01045	1.61070	0.63294	0.31571
51	CH_3CN	0	y_1	0.00202	0.45276	0.94750	2.98415	0.98014	-0.07294
52	HCOOH	0	y_1	0.41207	0.94666	-1.07100	2.75785	1.28849	-0.07294
53	CH_2Cl_2	0	y_1	0.00202	1.26231	-0.74140	6.81825	-0.38711	-0.07294
54	$CHCl_3$	0	y_1	0.00202	0.97646	-0.15620	8.42280	-0.38711	-0.07294
55	CCl_4	0	y_1	0.00202	0.15091	1.39700	9.36285	-0.38711	-0.07294
56	CH_3NO_2	0	y_1	0.00202	0.93386	0.25205	4.20715	0.54659	-0.07294
57	DMSO	0	y_1	0.00202	0.33316	3.81845	2.46050	0.91024	0.67446
58	DMF	0	y_1	0.00202	0.15091	4.45645	2.61090	1.35759	0.04316
59	NMP	0	y_1	0.00202	0.15091	6.16875	3.14725	1.34054	0.13306
60	THF	0	y_1	0.00202	0.15091	4.01005	3.41960	0.57469	0.05256

Appendix B. Kinetic experiments and rate constant regression

The competitive DA reaction (Figure 3.5) was carried out in a 100 ml stainless steel reactor, equipped with an agitator and a heating jacket (see Figure B1). The kinetic experiments were performed in a nitrogen atmosphere to keep a constant pressure (9.0 bar). In a typical run, about 3.0 ml of methyl acrylate is added into a thermo-stated (100 °C) solution composed of about 10.0 ml isoprene and 67.0 ml solvent. The resulting mixture is stirred and the reaction is considered to start. Samples are taken out every 0.5 h in the first two hours and every 1 h afterwards. The samples are analyzed using GC 6890N from Agilent equipped with a HP5MS (Part-Nr. 19091S-333) column connected with another DB-5MS (Part-Nr. 122-5561) column. The concentration of methyl acrylate (C_A) is determined from the internal standard method using toluene as the internal standard compound for the cyclohexane and 1-butanol solvents and using benzene for the other solvents. The para/meta selectivity (C_C/C_D) is quantified from the ratio of the product chromatographic peak areas while the relative response factor for the two products is set to 1.0, according to Sabat et al. (1994). All the chemicals were purchased from the Sigma-Aldrich company (purity $\geq$ 99.5%) and used without further purification.
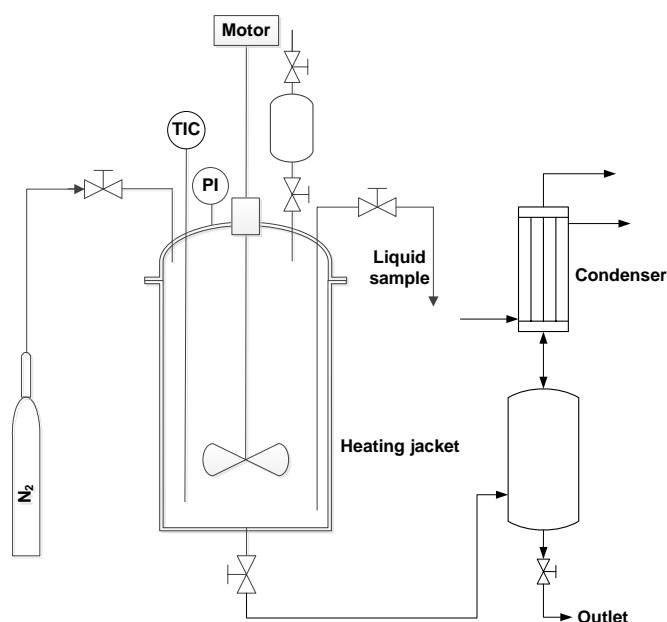
Figure B1: Schematic diagram of the reactor

It has been reported that both the parallel reactions have straightforward single-step mechanism and second-order kinetics (Sheehan and Sharratt, 1998). For each solvent, the total reaction rate constant, $k_1 + k_2$, was regressed from the experimental time-dependent concentration of methyl acrylate based on the second-order kinetic expression. Figure B2 compares the experimental methyl acrylate concentrations with the concentrations predicted by the regressed kinetic models.

The maximum average deviation between the experimental and predicted concentrations is 2.29% for the DMF (dimethylformamide) solvent.
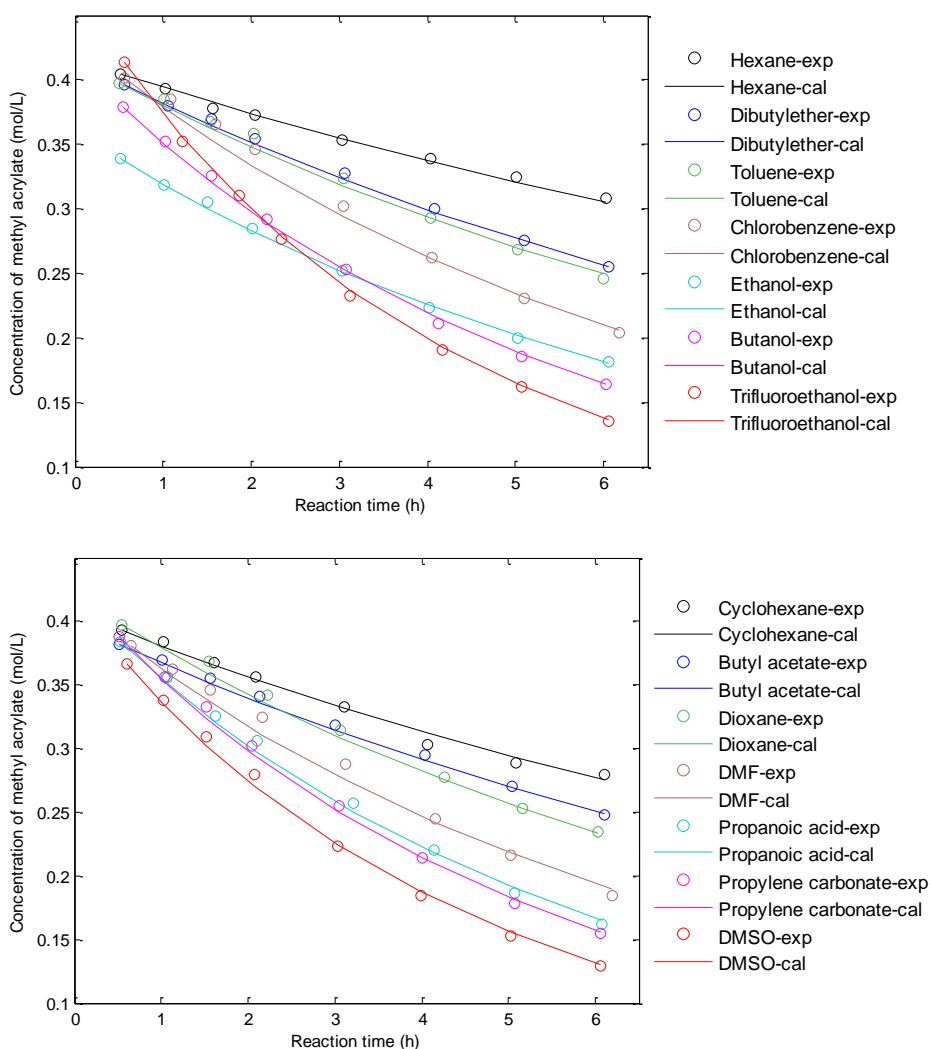
Figure B2: Experimental and calculated methyl acrylate concentrations in 14 solvents

From the regressed total reaction rate constant and the measured selectivity values, the rate constants of the two parallel reactions, k_1 and k_2, are determined and presented in Table 3.5 for all the investigated solvents.

Appendix C. Vapor pressure calculation

a) Solvent vapor pressure is calculated from the Clapeyron equation.

$$T_r^S = T/T_c^S \tag{C.1}$$

$$T_{br}^S = T_b^S/T_c^S \tag{C.2}$$

$$h = T_{br}^S \frac{\ln\left(P_c^S/1.01325\right)}{1-T_{br}^S} \tag{C.3}$$

$$\ln P_{vpr}^S = h\left(1-\frac{1}{T_r^S}\right) \tag{C.4}$$

$$P_{sat}^S(T) = P_{vpr}^S \cdot P_c^S \tag{C.5}$$

b) Vapor pressures of the reactants and product are estimated from the Nannoolal-Rarey equation given in Nannoolal et al. (2008).

$$T_{rb}^i = T/T_b^i \tag{C.6}$$

$$\log_{10}\left(\frac{P_{sat}^i(T)}{1\,atm}\right) = \left(4.1012 + dB_i\right)\left(\frac{T_{rb}^i-1}{T_{rb}^i-(1/8)}\right), \ (i = \mathrm{cyc, acr, and\ nor}) \tag{C.7}$$

The normal boiling point T_b and equation parameter dB of the reaction species are provided in the Supporting Information of Zhou et al. (2015a).

Bibliography

1. Abildskov J, van Leeuwen MB, Boeriu CG, van den Broek LAM. Computer-aided solvent screening for biocatalysis. J Mol Catal B: Enzym. 2013, 85, 200−213.

2. Abraham MH, Doherty RM, Kamlet MJ, Harris JM, Taft RW. Linear solvation energy relationships. Part 37. An analysis of contributions of dipolarity-polarisability, nucleophilic assistance, electrophilic assistance, and cavity terms to solvent effects on t-butyl halide solvolysis rates. J Chem Soc Perkin Trans. 1987, 2, 913−920.

3. Achenie LEK, Gani R, Venkatasubramanian V. Computer-Aided Chemical Engineering. Vol. 12. Computer Aided Molecular Design: Theory and Practice. Amsterdam: Elsevier, 2002.

4. Affenzeller M, Wagner S, Winkler S, Beham A. Genetic Algorithms and Genetic Programming: Modern Concepts and Practical Applications. Chapman and Hall: CRC Press, 2009.

5. Athier G, Floquet P, Pibouleau L, Domenech S. Process optimization by simulated annealing and NLP procedures. Application to heat exchanger network synthesis. Comput Chem Eng. 1997, 21, S475−S480.

6. Bardow A, Steur K, Gross J. Continuous-molecular targeting for integrated solvent and process design. Ind Eng Chem Res. 2010, 49, 2834−2840.

7. Bausa J, Marquardt W. Quick and reliable phase stability test in VLLE flash calculations by homotopy continuation. Comput Chem Eng. 2000, 24, 2447−2456.

8. Biegler LT, Grossmann IE, Westerberg AW. Systematic Methods of Chemical Process Design. Englewood Cliffs, NJ: Prentice Hall, 1997.

9. Biegler LT. Recent advances in chemical process optimization. Chem Ing Tech. 2014, 86, 943−952.

10. Blankenburg B, Fiedler H, Hampel M, Hauthal HG, Just G, Kahlert K, Korn J, Müller KH, Pritzkow W, Reinhold Y, Röllig M, Sauer E, Schnurpfeil D, Zimmermann G. DIELS-ALDER-Reaktionen. II. Über die Anwendung linearer Freier-Energie-Beziehungen auf DIELS-ALDER-Reaktionen. J Prakt Chemie. 1974, 316, 804−816.

11. Brignole EA, Bottini S, Gani R. A strategy for the design and selection of solvents for separation processes. Fluid Phase Equilib. 1986, 29, 125−132.

12. Brooke A, Kendrick D, Meeraus A, Raman R. GAMS: the Solver Manuals. GAMS Development Corporation. Washington D.C., 1998.

13. Burger J, Papaioannou V, Gopinath S, Jackson G, Galindo A, Adjiman CS. A hierarchical method to integrated solvent and process design of physical CO2 absorption using the SAFT-Mie approach. AIChE J. 2015, 61, 3249−3269.

14. Buxton A, Livingston AG, Pistikopoulos EN. Optimal design of solvent blends for environmental impact minimization. AIChE J. 1999, 45, 817−843.

15. Byrd RH, Nocedal J, Waltz RA. KNITRO: An integrated package for nonlinear optimization, a chapter from the book Large-Scale Nonlinear Optimization. Berlin/Heidelberg, Germany: Springer, 2006.

16. Campbell DS, Hogg DR. Electrophilic additions to alkenes. Part IV. Kinetics of the reaction of 2, 4-dinitrobenzenesulphenyl bromide with cyclohexene in benzene and in chloroform solution. J Chem Soc B. 1967, 889−892.

17. Cativiela C, Garcia JI, Mayoral JA, Salvatella L. Modelling of solvent effects on the Diels-Alder reaction. Chem Soc Rev. 1996, 25, 209−218.

18. Chen B, Lei Z, Li Q, Li C. Application of CAMD in separating hydrocarbons by extractive distillation. AIChE J. 2005, 51, 3114−3121.

19. Cheng HC, Wang FS. Trade-off optimal design of a biocompatible solvent for an extractive fermentation process. Chem Eng Sci. 2007, 62, 4316−4324.

20. Chiappe C, Malvaldi M, Pomelli CS. The solvent effect on the Diels–Alder reaction in ionic liquids: multiparameter linear solvation energy relationships and theoretical analysis. Green Chem. 2010, 12, 1330−1339.

21. Chipperfield JR. Non-aqueous solvents. Oxford University Press, 1999.

22. Clifford A, Clifford T. Fundamentals of supercritical fluids. Oxford University Press, 1999.

23. Constantinou L, Gani R, O'Connell JP. Estimation of the acentric factor and the liquid molar volume at 298 K using a new group contribution method. Fluid Phase Equilib. 1995, 103, 11−22.

24. Constantinou L, Gani R. New group contribution method for estimating properties of pure compounds. AIChE J. 1994, 40, 1697−1710.

25. Constantinou L, Bagherpour K, Gani R, Klein JA, Wu DT. Computer aided product design: problem formulations, methodology and applications. Comput Chem Eng. 1996, 20, 685−702.

26. Cussler EL. Diffusion: Mass Transfer in Fluid Systems. Cambridge University Press, 2009.

27. Dimroth O. On intramolecular rearrangement, Part 5. The influence of solvent on reaction rate and equilibrium. Justus Liebigs Ann Chem. 1910, 377, 127−163.

28. Dontsova NE, Nesterov VN, Shestopalov AM. Effect of solvent nature on the regioselectivity of the reactions of pyridinium ylides with E-1, 2-di(alkylsulfonyl)-1, 2-dichloroethene. From the reaction of 1, 3-dipolar cycloaddition to the reaction of nucleophilic addition-elimination (AdN-E1, 5). Tetrahedron 2013, 69, 5016−5021.

29. Drud AS. CONOPT − a large-scale GRG code. ORSA J Comput. 1994, 6, 207−216.

30. Eden MR, Jorgensen SB, Gani R, El-Halwagi MM. A novel framework for simultaneous separation process and product design. Chem Eng Process. 2004, 43, 595−608.

31. Eljack FT, Eden MR, Kazantzi V, Qin X, El-Halwagi MM. Simultaneous process and molecular design − A property based approach. AIChE J. 2007, 53, 1232−1239.

32. Fainberg AH, Winstein S. Correlation of solvolysis rates. III. 1 t-Butyl chloride in a wide range of solvent mixtures. J Am Chem Soc. 1956, 78, 2770−2777.

33. Folić M, Adjiman CS, Pistikopoulos EN. Computer-aided solvent design for reactions: maximizing product formation. Ind Eng Chem Res. 2008, 47, 5190−5202.

34. Folić M, Adjiman CS, Pistikopoulos EN. Design of solvents for optimal reaction rate constants. AIChE J. 2007, 53, 1240−1256.

35. Fourer R, Gay DM, Kernighan BW. AMPL: A Modeling Language for Mathematical Programming. Duxbury Press, 2002.

36. Fowler FW, Katritzky AR, Rutherford RJD. The correlation of solvent effects on physical and chemical properties. J Chem Soc B. 1971, 460−469.

37. Fredenslund A, Gmehling J, Rasmussen P. Vapor-liquid Equilibria Using UNIFAC: A Group Contribution Method. Amsterdam: Elsevier, 1977.

38. Frisch MJ, Trucks GW, Schlegel HB, et al. Gaussian 03, Revision C.02; Gaussian, Inc.: Wallingford, 2004.

39. Gani R, Gomez PA, Folic M, Jimenez-Gonzalez C, Constable DJC. Solvents in organic synthesis: Replacement and multi-step reaction systems. Comput Chem Eng. 2008, 32, 2420−2444.

40. Gani R. Solvent Selection through ICAS-ProCAMD. Copenhagen, 2010.

41. Gani R, Brignole EA. Molecular design of solvents for liquid extraction based on UNIFAC. Fluid Phase Equilib. 1983, 13, 331−340.

42. Gani R, Jiménez-González C, Constable DJ. Method for selection of solvents for promotion of organic reactions. Comput Chem Eng. 2005, 29, 1661−1676.

43. Gani R, Nielsen B, Fredenslund A. A group contribution approach to computer-aided molecular design. AIChE J. 1991, 37, 1318−1332.

44. Giovanoglou A, Barlatier J, Adjiman CS, Pistikopoulos EN, Cordiner JL. Optimal solvent design for batch separation based on economic performance. AIChE J. 2003, 49, 3095−3109.

45. Gmehling J, Rasmussen P, Fredenslund A. Vapor-liquid equilibriums by UNIFAC group contribution. Revision and extension. 2. Ind Eng Chem Process Des Dev. 1982, 21, 118−127.

46. Gómez JM, Reneaume JM, Roques M, Meyer M, Meyer X. A mixed integer nonlinear programming formulation for optimal design of a catalytic distillation column based on a generic nonequilibrium model. Ind Eng Chem Res. 2006, 45, 1373−1388.

47. Green KA, Zhou S, Luks KD. The fractal response of robust solution techniques to the stationary point problem. Fluid Phase Equilib. 1993, 84, 49−78.

48. Grossmann IE, Westerberg AW. Research challenges in process systems engineering. AIChE J. 2000, 46, 1700−1703.

49. Grunwald E, Winstein S. The correlation of solvolysis rates. J Am Chem Soc. 1948, 70, 846−854.

50. Guthrie KM. Data and techniques for preliminary capital cost estimating. Chem Eng. 1969, 76, 114.

51. Chum HL, Koch VR, Miller LL, Osteryoung RA. Electrochemical scrutiny of organometallic iron complexes and hexamethylbenzene in a room temperature molten salt. J Am Chem Soc. 1975, 97, 3264−3265.

52. Harper PM, Gani R, Kolar P, Ishikawa T. Computer-aided molecular design with combined molecular modeling and group contribution. Fluid Phase Equilib. 1999, 160, 337−347.

53. Harper PM, Gani R. A multi-step and multi-level approach for computer aided molecular design. Comput Chem Eng. 2000, 24, 677−683.

54. Herring RH, Eden MR. Evolutionary algorithm for de novo molecular design with multi-dimensional constraints. Comput Chem Eng. 2015, 83, 267−277.

55. Hildebrand JH, Scott RL. Solutions of nonelectrolytes. Annu Rev Phys Chem. 1950, 1, 75−92.

56. Holland JH. Adaptation in Natural and Artificial Systems. Ann Arbor: The University of Michigan Press, 1975.

57. Hughes ED, Ingold CK. Mechanism of substitution at a saturated carbon atom. Part IV. A discussion of constitutional and solvent effects on the mechanism, kinetics, velocity, and orientation of substitution. J Chem Soc. 1935, 244−255.

58. Jessop PG, Subramaniam B. Gas-expanded liquids. Chem Rev. 2007, 107, 2666−2694.

59. Jiménez-González C, Poechlauer P, Broxterman QB, et al. Key green engineering research areas for sustainable manufacturing: A perspective from pharmaceutical and fine chemicals manufacturers. Org Process Res Dev. 2011, 15, 900−911.

60. Jurs PC. Quantitative structure-property relationships. Volume 4 in Handbook of Chemoinformatics: From Data to Knowledge. 2008, 1314−1335.

61. Kamlet MJ, Abboud JLM, Abraham MH, Taft RW. Linear solvation energy relationships. 23. A comprehensive collection of the solvatochromic parameters, π, α, and β, and some methods for simplifying the generalized solvatochromic equation. J Org Chem. 1983, 48, 2877−2887.

62. Kamlet MJ, Abboud JL, Taft RW. The solvatochromic comparison method. 6. The π-scale of solvent polarities. J Am Chem Soc. 1977, 99, 6027−6038.

63. Kamlet MJ, Taft RW. The solvatochromic comparison method. 1. The β-scale of solvent hydrogen-bond acceptor (HBA) basicities. J Am Chem Soc. 1976, 98, 377−383.

64. Karelson M. Molecular Descriptors in QSAR/QSPR. Wiley Interscience. New York, 2000.

65. Karunanithi AT, Achenie LEK, Gani R. A computer-aided molecular design framework for crystallization solvent design. Chem Eng Sci. 2006, 61, 1247−1260.

66. Karunanithi AT, Achenie LEK, Gani R. A new decomposition-based computer-aided molecular/mixture design methodology for the design of optimal solvents and solvent mixtures. Ind Eng Chem Res. 2005, 44, 4785−4797.

67. Katritzky AR, Kuanar M, Slavov S, Hall CD, Karelson M, Kahn I, Dobchev DA. Quantitative correlation of physical and chemical properties with chemical structure: utility for prediction. Chem Rev. 2010, 110, 5714−5789.

68. Kim KJ, Diwekar UM. Integrated solvent selection and recycling for continuous processes. Ind Eng Chem Res. 2002, 41, 4479−4488.

69. Klamt A, Eckert F, Arlt W. COSMO-RS: an alternative to simulation for calculating thermodynamic properties of liquid mixtures. Annu Rev Chem Biomol Eng. 2010, 1, 101−122.

70. Klamt A, Schüürmann G. COSMO: A new approach to dielectric screening in solvents with explicit expressions for the screening energy and its gradient. J Chem Soc Perkin Trans. 1993, 5, 799−805.

71. Kossack S, Kraemer K, Gani R, Marquardt W. A systematic synthesis framework for extractive distillation processes. Chem Eng Res Des. 2008, 86, 781−792.

72. Kruglinski DJ, Wingo S, Sheperd GW. Programming Microsoft Visual C++. Redmond: Microsoft Press, 1998.

73. Lek-utaiwan P, Suphanit B, Douglas PL, Mongkolsiri N. Design of extractive distillation for the separation of close-boiling mixtures: Solvent selection and column optimization. Comput Chem Eng. 2011, 35, 1088−1100.

74. Lima RM, Salcedo RL, Barbosa D. SIMOP: Efficient reactive distillation optimization using stochastic optimizers. Chem Eng Sci. 2006, 61, 1718−1739.

75. Lipowski A, Lipowska D. Roulette-wheel selection via stochastic acceptance. Physica A. 2012, 391, 2193−2196.

76. Loh HP, Lyons J, White CW. Process Equipment Cost Estimation, Final Report. National Energy Technology Laboratory, Pittsburgh, 2002.

77. Lowrey AH, Cramer CJ, Urban JJ, Famini GR. Quantum chemical descriptors for linear solvation energy relationships. Comput Chem. 1995, 19, 209−215.

78. Macchietto S, Odele O, Omatsone O. Design on optimal solvents for liquid-liquid extraction and gas absorption processes. Chem Eng Res Des. 1990, 68, 429−433.

79. Maranas CD. Optimal molecular design under property prediction uncertainty. AIChE J. 1997, 43, 1250−1264.

80. Marcoulaki EC, Kokossis AC. On the development of novel chemicals using a systematic optimisation approach. Part II. Solvent design. Chem Eng Sci. 2000, 55, 2547−2561.

81. Marrero J, Gani R. Group-contribution based estimation of pure component properties. Fluid Phase Equilib. 2001, 183-184, 183−208.

82. Martin TM, Young DM. Prediction of the acute toxicity (96-h LC50) of organic compounds to the fathead minnow (Pimephales promelas) using a group contribution method. Chem Res Toxicol. 2001, 14, 1378−1385.

83. McDonald CM, Floudas CA. GLOPEQ: A new computational tool for the phase and chemical equilibrium problem. Comput Chem Eng. 1997, 21, 1−23.

84. Michalewicz Z, Schoenauer M. Evolutionary algorithms for constrained parameter optimization problems. Evol Comput. 1996, 4, 1−32.

85. Michelsen ML. The isothermal flash problem. Part I. Stability. Fluid Phase Equilib. 1982, 9, 1−19.

86. Misener R, Floudas CA. GloMIQO: Global mixed-integer quadratic optimizer. J Global Optim. 2013, 57, 3−50.

87. Molina D, Lozano M, García-Martínez C, Herrera F. Memetic algorithms for continuous optimisation based on local search chains. Evolut Comput. 2010, 18, 27−63.

88. Moscato P. On evolution, search, optimization, genetic algorithms and martial arts: Towards memetic algorithms. Caltech concurrent computation program, C3P Report, 1989.

89. Müller D, Marquardt W. Dynamic multiple-phase flash simulation: Global stability analysis versus quick phase determination. Comput Chem Eng. 1997, 21, S817−S822.

90. Nachbar RB. Molecular evolution: automated manipulation of hierarchical chemical topology and its application to average molecular structures. Genet Program Evol M. 2000, 1, 57−94.

91. Nannoolal Y, Rarey J, Ramjugernath D. Estimation of pure component properties: Part 3. Estimation of the vapor pressure of non-electrolyte organic compounds via group contributions and group interactions. Fluid Phase Equilib. 2008, 269, 117−133.

92. Ng LY, Chong FK, Chemmangattuvalappil NG. Challenges and opportunities in computer-aided molecular design. Comput Chem Eng. 2015, 81, 115−129.

93. Nobuoka K, Kitaoka S, Yanagisako A, Maki Y, Harran T, Ishikawa Y. Stereoselectivity of the Diels-Alder reaction in ionic liquids with cyano moieties: effect of the charge delocalization of anions on the relation of solvent-solvent and solute-solvent interactions. RSC Adv. 2013, 3, 19632−19638.

94. Odele O, Macchietto S. Computer aided molecular design: A novel method for optimal solvent selection. Fluid Phase Equilib. 1993, 82, 47−54.

95. Papadopoulos AI, Linke P. Efficient integration of optimal solvent and process design using molecular clustering. Chem Eng Sci. 2006, 61, 6316−6336.

96. Papadopoulos AI, Linke P. Integrated solvent and process selection for separation and reactive separation systems. Chem Eng Process. 2009, 48, 1047−1060.

97. Papadopoulos AI, Linke P. Multiobjective molecular design for integrated process-solvent systems synthesis. AIChE J. 2005, 52, 1057−1070.

98. Papadopoulos AI, Stijepovic M, Linke P. On the systematic design and selection of optimal working fluids for organic rankine cycles. Appl Therm Eng. 2010, 30, 760−769.

99. Patel SJ, Ng D, Mannan MS. QSPR flash point prediction of solvents using topological indices for application in computer aided molecular design. Ind Eng Chem Res. 2009, 48, 7378−7387.

100. Pereira FE, Keskes E, Galindo A, Jackson G, Adjiman CS. Integrated solvent and process design using a SAFT-VR thermodynamic description: High-pressure separation of carbon dioxide and methane. Comput Chem Eng. 2011, 35, 474−491.

101. Pham HN, Doherty MF. Design and synthesis of heterogeneous azeotropic distillations I. Heterogeneous phase diagrams. Chem Eng Sci. 1990, 45, 1823−1836.

102. Pistikopoulos EN, Georgiadis MC, Dua V, Adjiman CS, Galindo A. Process Systems Engineering. Volume 6. Molecular Systems Engineering. Weinheim: Wiley-VCH, 2010.

103. Plechkova NV, Seddon KR. Applications of ionic liquids in the chemical industry. Chem Soc Rev. 2008, 37, 123−150.

104. Poling BE, Prausnitz JM, O'Connell JP. The Properties of Gases and Liquids, 5th ed. New York: McGraw-Hill, 2001.

105. Pollet P, Eckert CA, Liotta CL. Switchable solvents. Chem Sci. 2011, 2, 609−614.

106. Pretel EJ, López PA, Bottini SB, Brignole EA. Computer-aided molecular design of solvents for separation processes. AIChE J. 1994, 40, 1349−1360.

107. Rangaiah GP. Stochastic Global Optimization: Techniques and Applications in Chemical Engineering. World Scientific, 2010.

108. Reichardt C, Welton T. Solvents and Solvent Effects in Organic Chemistry. John Wiley & Sons, 2011.

109. Rihani DN, Doraiswamy LK. Estimation of heat capacity of organic compounds from group contributions. Ind Eng Chem Fund. 1965, 4, 17−21.

110. Rosenthal RE. GAMS-A Users' Guide. GAMS Development Corporation, Washington D.C., 2006.

111. Roughton BC, Christian B, White J, Camarda KV, Gani R. Simultaneous design of ionic liquid entrainers and energy efficient azeotropic separation processes. Comput Chem Eng. 2012, 42, 248−262.

112. Ruiz-Lopez MF, Assfeld X, Garcia JI, Mayoral JA, Salvatella L. Solvent effects on the mechanism and selectivities of asymmetric Diels-Alder reactions. J Am Chem Soc. 1993, 115, 8780−8787.

113. Sabat M, Reynolds KA, Finn MG. An Exo-selective Diels-Alder reaction of a bimetallic carbene complex: a case of steric control. Organometallics 1994, 13, 2084−2087.

114. Sahinidis NV, Tawarmalani M. Applications of global optimization to process and molecular design. Comput Chem Eng. 2000, 24, 2157−2169.

115. Sahinidis NV. BARON: A general purpose global optimization software package. J Global Optim. 1996, 8, 201−205.

116. Samant KD, Ng KM. Synthesis of extractive reaction processes. AIChE J. 1998, 44, 1363−1381.

117. Samudra AP, Sahinidis NV. Optimization-based framework for computer-aided molecular design. AIChE J. 2013, 59, 3686−3701.

118. Schäfer A, Klamt A, Sattel D, Lohrenz JC, Eckert F. COSMO Implementation in TURBOMOLE: Extension of an efficient quantum chemical code towards liquid systems. Phys Chem Chem Phys. 2000, 2, 2187−2193.

119. Scilipoti J, Cismondi M, Brignole EA. Prediction of physical properties for molecular design of solvents. Fluid Phase Equilib. 2014, 362, 74−80.

120. Selim KB, Martel A, Laurent MY, Lhoste J, Py S, Dujardin G. Enantioselective ruthenium-catalyzed 1, 3-dipolar cycloadditions between C-carboalkoxy ketonitrones and methacrolein: solvent effect on reaction selectivity and its rational. J Org Chem. 2014, 79, 3414−3426.

121. Shang Q, Yan F, Xia S, Wang Q, Ma P. Predicting the surface tensions of ionic liquids by the quantitative structure property relationship method using a topological index. Chem Eng Sci. 2013, 101, 266−270.

122. Sheehan ME, Sharratt PN. Molecular dynamics methodology for the study of the solvent effects on a concentrated Diels-Alder reaction and the separation of the post-reaction mixture. Comput Chem Eng. 1998, 22, S27−S33.

123. Sheldon TJ, Adjiman CS, Cordiner JL. Pure component properties from group contribution: hydrogen-bond basicity, hydrogen-bond acidity, Hildebrand solubility parameter, macroscopic surface tension, dipole moment, refractive index and dielectric constant. Fluid Phase Equilib. 2005, 231, 27−37.

124. Shelley MD, El-Halwagi MM. Component-less design of recovery and allocation systems: a functionality-based clustering approach. Comput Chem Eng. 2000, 24, 2081−2091.

125. Skiborowski M, Rautenberg M, Marquardt W. A hybrid evolutionary–deterministic optimization approach for conceptual design. Ind Eng Chem Res. 2015, 54, 10054−10072.

126. Stanescu I, Achenie LE. A theoretical study of solvent effects on Kolbe−Schmitt reaction kinetics. Chem Eng Sci. 2006, 61, 6199−6212.

127. Steyer F, Flockerzi D, Sundmacher K. Equilibrium and rate-based approaches to liquid-liquid phase splitting calculations. Comput Chem Eng. 2005, 30, 277−284.

128. Struebing H, Ganase Z, Karamertzanis PG, S, Siougkrou E, Haycock P, Piccione PM, Armstrong A, Galindo A, Adjiman CS. Computer-aided molecular design of solvents for accelerated reaction kinetics. Nat Chem. 2013, 5, 952−957.

129. Sundaram A, Venkatasubramanian V. Parametric sensitivity and search-space characterization studies of genetic algorithms for computer-aided polymer design. J Chem Inf Comput Sci. 1998, 38, 1177−1191.

130. Taft RW, Kamlet MJ. The solvatochromic comparison method. 2. The α-scale of solvent hydrogen-bond donor (HBD) acidities. J Am Chem Soc. 1976, 98, 2886−2894.

131. Towler G, Sinnott RK. Chemical Engineering Design: Principles, Practice and Economics of Plant and Process Design. Elsevier, 2012.

132. Urselmann M, Barkmann S, Sand G, Engell S. A memetic algorithm for global optimization in chemical process synthesis problems. IEEE T Evolut Comput. 2011a, 15, 659−683.

133. Urselmann M, Barkmann S, Sand G, Engell S. Optimization-based design of reactive distillation columns using a memetic algorithm. Comput Chem Eng. 2011b, 35, 787−805.

134. Vaidyanathan R, El-Halwagi M. Computer-aided design of high performance polymers. J Elastom Plast. 1994, 26, 277−293.

135. van Dyk B, Nieuwoudt I. Design of solvents for extractive distillation. Ind Eng Chem Res. 2000, 39, 1423−1429.

136. Venkatasubramanian V, Chan K, Caruthers JM. Computer-aided molecular design using genetic algorithms. Comput Chem Eng. 1994, 18, 833−844.

137. Venkatasubramanian V, Chan K, Caruthers JM. Evolutionary design of molecules with desired properties using the genetic algorithm. J Chem Inf Comput Sci. 1995, 35, 188−195.

138. Voutsas EC, Stamatis H, Kolisis FN, Tassios D. Solvent effects on equilibrium position and initial rate of lipase-catalyzed esterification reactions in organic solvents: experimental results and prediction capabilities. Biocatal Biotransfor. 2002, 20, 101−109.

139. Walden P. Molecular weights and electrical conductivity of several fused salts. Bull Acad Imper Sci. 1914, 8, 405−422.

140. Wang Y, Achenie LEK. Computer aided solvent design for extractive fermentation. Fluid Phase Equilib. 2002, 201, 1−18.

141. Wasylkiewicz SK, Ung S. Global phase stability analysis for heterogeneous reactive mixtures and calculation of reactive liquid-liquid and vapor-liquid-liquid equilibria. Fluid Phase Equilib. 2000, 175, 253−272.

142. Welton T. Room-temperature ionic liquids. Solvents for synthesis and catalysis. Chem Rev. 1999, 99, 2071−2084.

143. Winstein S, Fainberg AH. Correlation of solvolysis rates. Solvent effects on enthalpy and entropy of activation for solvolysis of t-butyl chloride. J Am Chem Soc. 1957, 79, 5937−5950.

144. Winstein S, Grunwald E, Jones HW. The correlation of solvolysis rates and the classification of solvolysis reactions into mechanistic categories. J Am Chem Soc. 1951, 73, 2700−2707.

145. Wislicenus W. Ueber die isomerie der formylphenylessigester. Justus Liebigs Annalen der Chemie. 1896, 291, 147−216.

146. Xu W, Diwekar UM. Improved genetic algorithms for deterministic optimization and optimization under uncertainty. Part II. Solvent selection under uncertainty. Ind Eng Chem Res. 2005, 44, 7138−7146.

147. Ye K. PhD Thesis: Process Design Based on CO2-Expanded Liquids as Solvents. Otto-von-Guericke University Magdeburg, 2014.

148. Zhou T, Lyu Z, Qi Z, Sundmacher K. Robust design of optimal solvents for chemical reactions — A combined experimental and computational strategy. Chem Eng Sci. 2015b, 137, 613−625.

149. Zhou T, McBride K, Zhang X, Qi Z, Sundmacher K. Integrated solvent and process design exemplified for a Diels-Alder reaction. AIChE J. 2015a, 61, 147−158.

150. Zhou T, Qi Z, Sundmacher K. Model-based method for the screening of solvents for chemical reactions. Chem Eng Sci. 2014, 115, 177−185.

151. Zhou T, Wang J, McBride K, Sundmacher K. Optimal design of solvents for extractive reaction processes. AIChE J. 2016a, 62, 3238−3249.

152. Zhou T, Zhou Y, Sundmacher K. A hybrid stochastic-deterministic optimization approach for integrated solvent and process design. Chem Eng Sci. 2016b, doi:10.1016/j.ces.2016.03.011.

153. Zinser A, Rihko-Struckmann L, Sundmacher K. Dynamic method for computation of chemical and phase equilibria. Comput Chem Eng. 2016, 89, 1−10.

List of Figures

List of Tables

Curriculum Vitae

1. Personal Details

Name: Teng Zhou

Date of Birth: 31 January 1988

Nationality: Chinese

Address: Sandtorstr. 1, Magdeburg, Germany

Phone: +49 391 6110 406

E-mail: zhout@mpi-magdeburg.mpg.de

2. Research Area and Expertise

- Ionic liquids for reactions and separations
- Process simulation, design, and optimization
- Stochastic and deterministic mathematical programming
- Computer-aided molecular design, integrated molecular and process design

Future Interests

- Chemical product design (incl. catalyst and material design)
- Multi-scale process modeling and optimization
- Large-scale energy systems engineering

3. Education

2005 – 2009   *B.Eng. in Chemical Engineering*
                 Nanjing University of Technology, Nanjing, China

2009 – 2012   *M.Sc. in Chemical Engineering*
                 East China University of Science and Technology, Shanghai, China

2012 – 2016   *Ph.D. in Process Systems Engineering*
                 Max Planck Institute for Dynamics of Complex Technical Systems, Germany

4. Selected Honors and Awards

Chinese Government Award for Outstanding Self-financed Students Abroad	Dec. 2016
Elsevier Outstanding Reviewer	May 2015
CAST Directors' Award, American Institute of Chemical Engineers (AIChE)	Nov. 2014
Outstanding Master's Thesis Award, Shanghai Municipal Education Commission	Apr. 2013
Best Paper Award, East China University of Science and Technology	Dec. 2012
Distinguished Graduate Award, Nanjing University of Technology	Jun. 2009
University Scholarship (Several Times), Nanjing University of Technology	2005−2009

5. Journal Publications

[1] Zhang J, Peng D, Song Z, **Zhou T**, Cheng H, Chen L, Qi Z. COSMO-descriptor based computer-aided ionic liquid design for separation processes. Part I: Modified group contribution methodology for predicting surface charge density profile of ionic liquids. Chemical Engineering Science. 2016, accepted and in press.

[2] Zhang J, Qin L, Peng D, **Zhou T**, Cheng H, Chen L, Qi Z. COSMO-descriptor based computer-aided ionic liquid design for separation processes. Part II: Task-specific design for extraction processes. Chemical Engineering Science. 2016, accepted and in press.

[3] **Zhou T**, Wang J, McBride K, Sundmacher K. Optimal design of solvents for extractive reaction processes. AIChE Journal. 2016, 62, 3238−3249.

[4] **Zhou T**, Zhou Y, Sundmacher K. A hybrid stochastic-deterministic optimization approach for integrated solvent and process design. Chemical Engineering Science. 2016, doi:10.1016/j.ces.2016.03.011.

[5] **Zhou T**, Lyu Z, Qi Z, Sundmacher K. Robust design of optimal solvents for chemical reactions − A combined experimental and computational strategy. Chemical Engineering Science. 2015, 137, 613−625.

[6] **Zhou T**, McBride K, Zhang X, Qi Z, Sundmacher K. Integrated solvent and process design exemplified for a Diels-Alder reaction. AIChE Journal. 2015, 61, 147−158.

[7] Song Z, **Zhou T**, Zhang J, Cheng H, Chen L, Qi Z. Screening of ionic liquids for solvent-sensitive extraction − with deep desulfurization as an example. Chemical Engineering Science. 2015, 129, 69−77.

[8] **Zhou T**, Qi Z, Sundmacher K. Model-based method for the screening of solvents for chemical reactions. Chemical Engineering Science. 2014, 115, 177−185.

[9] Lyu Z, **Zhou T**, Chen L, Ye Y, Sundmacher K, Qi Z. Simulation based ionic liquid screening for benzene-cyclohexane extractive separation. Chemical Engineering Science. 2014, 113, 45−53.

[10] **Zhou T**, Wang Z, Ye Y, Chen L, Xu J, Qi Z. Deep separation of benzene from cyclohexane by liquid extraction using ionic liquids as the solvent. Industrial & Engineering Chemistry Research. 2012, 51, 5559−5564.

[11] **Zhou T**, Chen L, Ye Y, Chen L, Qi Z, Freund H, Sundmacher K. An overview of mutual solubility of ionic liquids and water predicted by COSMO-RS. Industrial & Engineering Chemistry Research. 2012, 51, 6256−6264.

[12] **Zhou T**, Wang Z, Chen L, Ye Y, Qi Z, Freund H, Sundmacher K. Evaluation of the ionic liquids 1-alkyl-3-methylimidazolium hexafluorophosphate as a solvent for the extraction of

benzene from cyclohexane: (Liquid + liquid) equilibria. Journal of Chemical Thermodynamics. 2012, 48, 145−149.

[13] Chen L, **Zhou T**, Chen L, Ye Y, Qi Z, Freund H, Sundmacher K. Selective oxidation of cyclohexanol to cyclohexanone in the ionic liquid 1-octyl-3-methylimidazolium chloride. Chemical Communications. 2011, 47, 9354−9356.

6. Invited Talks, Seminars, and Conferences

Invited Talks

1. Fast screening and molecular design of solvents for chemical reactions based on COSMO and COSMO-RS derived theoretical descriptors. 4th COSMO-RS symposium, 16 – 18 Mar. 2015, Bonn, Germany

2. Engineering of molecules for better chemical processes. International Max Planck Research School (IMPRS) Seminar − Tandem Talk, 14 Mar. 2016, Magdeburg, Germany

Conferences

3. Integrated solvent and process design exemplified for a Diels-Alder reaction. AIChE Annual Meeting, 16 – 21 Nov. 2014, Atlanta, USA

4. Robust design of optimal solvents for chemical reactions − A combined experimental and computer-aided strategy. PSE2015, 31 May – 04 June 2015, Copenhagen, Denmark

5. Computer-aided solvent design for extractive reaction processes. ECCE10, 27 Sept. − 01 Oct. 2015, Nice, France

6. Computer Aided Molecular Design (CAMD): Integration of molecular decisions into process systems design. SCPPE 2016, 31 May – 03 June 2016, Nanjing, China

7. Other Activities

✓ Assistant to the Executive Editor (Prof. Kai Sundmacher) of *Chemical Engineering Science*, 2013 – 2015

✓ Assistant lecturer for the graduate course "*Advanced Process Systems Engineering*" in the 2014, 2015, and 2016 academic years

✓ Research supervision on 5 master theses

8. Attended Advanced Courses

✓ 3rd International Max Planck Research School (IMPRS) Summer School on "*Multi-scale Modeling and Simulation*". 02 – 06 Sept. 2013, Magdeburg, Germany

✓ Advanced Course on "*Conceptual Design, Optimization Modeling and Integrated Process Operations*". Carnegie Mellon University, 07 – 14 May 2014, Pittsburg, USA

✓ 4th IMPRS Summer School on "*Process Systems Engineering*". 31 Aug. – 04 Sept. 2015, Magdeburg, Germany